

25th RAU

ANNUAL USERS

MEETING LNLS/CNPEM

September 16th and 17th, 2015

<http://pages.cnpem.br/rau/>



CNPEM

Ministério da
Ciência, Tecnologia
e Inovação



Support:



Sponsors:



Organizers:

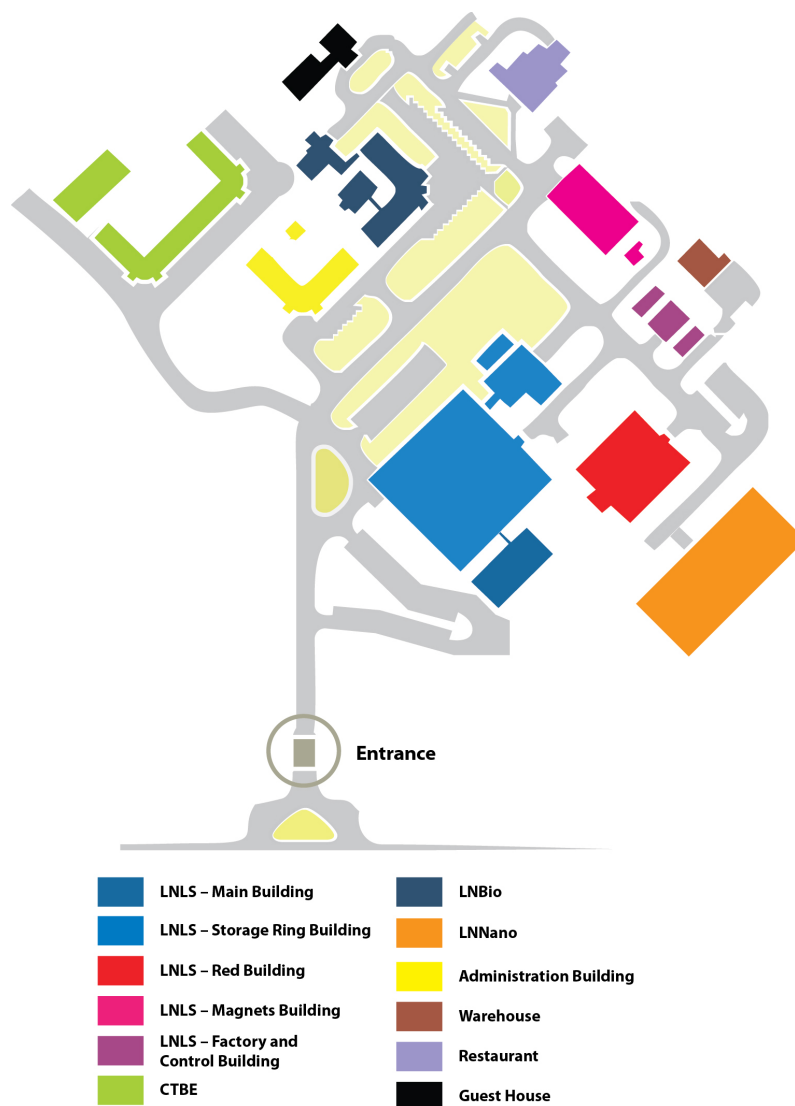


CNPEM

Ministério da
Ciência, Tecnologia
e Inovação



CNPEM – Campus Map



SUMMARY

Presentation	13
Organizers Scientific Committee	14
Program	15
Abstracts	17
The use of synchrotron radiation in Astrobiology: Lithopanspermia studies and the Biosun project	18
Presenter: Abrevaya X. C.	
Abrevaya, X. C.; Galante, D.; Nóbrega, F.; Tribelli, P.; Rodrigues, F.; Araujo, G.; Gallo, T.; Ribas I.; Sanz-Forcada, J.; Rodler, F.; Porto de Mello G.F.; Leitzinger, M; Odert, P.; Hanslmeier, A.; Horvath, J.	
Application of X-Ray Phase Contrast Microtomography Using Brazilian Synchrotron Light Laboratory to Improve the Visualization of External and Internal Structures of <i>Rhodnius prolixus</i> head	19
Presenter: De Almeida A. P.	
Sena G., Almeida A., Nogueira L., Braz D., Gonzalez M., Azambuja P., Barroso R.	
VUV excitation and SEM analysis in nanofluoride produced by microwave hydrothermal synthesis	20
Presenter: Andrade A. B.	
Andrade A. B., Valerio M. E. G.	
Bentonite: Al – Si k xanes characterization for this clay treated at two temperature	21
Presenter: Andrini L.	
Andrini L.; Toja R. M.; Gauna M. R.; Requejo F. G.; Rendtorff N.	
Small-angle x-ray scattering investigation of asphaltene structures in crude oils	22
Presenter: Balestrin L. B. da S.	
Balestrin L. B. da S., Padula L., Sabadini E., Cardoso M. B. and Loh W.	
Ultrafast charge transfer dynamics and morphological investigation in thermal annealed donor-acceptor copolymer and fullerene: F8T2 and F8T2: PCBM films	23
Presenter: Basabe Y. G.	
Garcia-Basabe Y., Yamamoto N. A. D., Roman L. S., and Rocco M. L.	
Hybrid nanostructured sulfonated poly (ether ether ketone) / zirconium oxide based membranes comprising protic ionic liquid for PEMFC application	24
Presenter: Batalha J. A. F. L.	
Batalha J. A. F. L.; Dahmouche K.; Gomes A. de S.	
Structural and Optical Studies of Nanoparticles of CaF₂	25
Presenter: Bezerra C. dos S. Bezerra C. dos S.; Valerio M. E. G.	

Arsenic speciation in geological samples using X-ray absorption spectroscopy	26
Presenter: Bia G. L. Bia G. L.; García M. G.; Borgnino L. C	
Nanostructured Ga doped ZnO thin films prepared by sol-gel spin-coating	27
Presenter: Bojorge C. D. Bojorge C.; Cánepa H.; Heredia E.; De Reça N. E. W.	
Photoionization studies on Thionitrites	28
Presenter: Canneva A.	
X-ray absorption spectroscopy characterization of Zn_{1-x}CoxO thin films applied as ozone gas sensors	29
Presenter: Catto A. C. Catto A. C., Zanatta A. R. and Mastelaro V. R.	
Iron altered oxidation energy due to Yttrium doping in Fe₃O₄ spinel ferrites	30
Presenter: Coelho L. N. Coelho L. N.; Silva A. F.; Parise M.; P. C. Morais	
XAFS characterization of Sr_{1-x}CuxTiO₃ and SrTi_{1-x}CuxO₃ perovskites applied to water-gas shift reaction	31
Presenter: Coletta V. C. Coletta V. C.; Marcos F. C. F.; Nogueira F. G. E.; Bernardi M. I. B.; Assaf E. M.; Gonçalves R. V.; Mastelaro V. R.	
Structural characterization of kraft lignin under different pH	32
Presenter: Dias O. A. T. Dias O. A. T., Negrão D. R., Gandin C. A., Leão A. L., Neto M. de O.	
Photoionization dynamic of O-methyl dithiocarbonate (dimethyl xanthate), CH₃OC(S)SCH₃, on the sulfur 2p absorption edge	33
Erben M. F., Cánneva A., Pirani L. S. R., Cavasso-Filho R. L., Védova C. O. D.	
Core-shell aggregates formed by polyion-surfactant complex salts: study of the internal liquid crystalline structures and stability	34
Presenter: Ferreira G. A. Ferreira G. A., Carneiro N. M., Vitorazi L., Loh W.	
Analysis of the concentration of heavy metals in the polychaete using the TXRF technique on sandy beaches of the coast of São Paulo	35
Presenter: Freitas M. C. S. Freitas M. C. S., Yokoyama L. Q., Ignacio B. L., De Jesus. F. O., Mársico E. T., Ribeiro R. de O. R., Barbosa R. de F.	

Present and future developments for UV-VUV science at LNLS	36
Presenter: Galante D. Galante D.; Ambrosio C.; Sobolewski S.; Teixeira V.; Araujo W.	
Degradation of carotenoid of poly-resistant bacterium Deinococcus radiodurans on simulated environments with applications in astrobiology	37
Presenter: Gallo T. M. Gallo T. M.; Rodrigues F.; Simões F. V.; Galante D.	
Grazing-incidence X-ray scattering studies of myelin membranes at air/water interface	38
Presenter: Gasperini A. A. M. Gasperini A. A. M.; Puentes-Martinez X. E.; Pusterla J. M.; Oliveira R.; Cavalcanti L. P.	
Magnetic moment of Fe₃O₄ films with thicknesses near the unit-cell size	39
Presenter: Gomes G. F. de M. Gomes G. F. M. Bueno T. E. P., Parreiras D. E., Abreu G. J. P., De Siervo A., Cezar J. C., Pfannes H.-D. and Paniago R.	
X-ray crystallographic structure of a transcriptional activator of virulence factor in enterococcus faecalis, ELRR.	40
Presenter: De Groote M. C. R. De Groote, M. C. R.; Camargo, I.; Repoila, F.; Serror, P.; Horjales, E.	
Electronic Structure of SrTi_{1-x}Ru_xO₃	41
Presenter: Guedes E. B. Guedes E. B.; Abbate M.; Abud F.; Jardim R. F.; Mossaneck R. J. O.	
Structure, activity and reaction mechanism of NahK and its complex with NahL	42
Presenter: Guimarães S. L. Guimarães S. L., Coitinho J. B., Costa D. M. A., De Araújo S. S., Whitman C. P., Nagem R. A. P.	
Au / Ag nanowires atomic distribution revealed by XAFS	43
Presenter: Herrera F. C. Herrera, F. C.; Giovanetti L. J.; Gutiérrez-Wing, C.; Requejo F. G.	
Python as a tool for analyze X-ray small angle scattering data	44
Presenter: Huck-Iriart C. Huck-Iriart C.; Giovanetti L. J.	
Real Time Monitoring Nanoparticles Distance and Structure upon Different Variables.	45
Presenter: Ibañez F. J. Ibañez F. J., Dalfovo M. C., Stanic V., Requejo F. G., Giovanetti L. J., Iriart C. H.	

Spectroscopic Techniques on the Study of Biosignatures: Degradation of the Heme Group under Environmental Stress	46
Presenter: Junior J. C. S. Junior J. C. S.; Rodrigues F.; Puglieri T.; Galante D.	
X-ray back-diffraction pointing to a target soft inelastic X-ray scattering spectrometer	47
Presenter: Kakuno E. M. Kakuno E. M., Hönnicke M. G., Conley R., Cusatis C., Zhou J., Bouet N, Marques J. B., Vicentin F. C. .	
Influence of the nanoparticle concentration on the magnetic and structural properties in Fe₃O₄-PVA nanocomposites	48
Presenter: Londoño O. M. Moscoso-Londoño O.; Tancredi P.; Muraca D.; Knobel M.; Wolff U.; Damm C; Neu V.; Rellinghaus B. ⁴ ; Socolovsky L. M. ¹	
Solving the structure of bimetallic particles with EXAFS	49
Presenter: López J. M. R. Ramallo-López J. M.; Mizrahi M.; Giovanetti L. G.; Krylova G.; Béron F.; Pirota K.; Shevchenko E.; Requejo F. G.	
XANES and micro-XRF spectroscopies for chemical characterization of fossil samples	50
Presenter: Maldanis L. Maldanis L.; Perez C. A.; Lima F. A.; Rodrigues F.; Galante D.; Xavier-Neto J.	
Trace elements alterations in mammary cells exposed to doses used in mammograms – an investigation using TXRF	51
Presenter: Mantuano A. Mantuano A.; Mota C. L.; Pickler A.; Machado S. C. F.; Salata C.; De Almeida C. E.; Braz D.; Barroso R. C.	
Core level and valence band electronic structure of Sr₂FeMoO₆	52
Presenter: Martins H. P. Martins H. P.; Prado F.; Caneiro A.; Mossanek R. J. O.; Abbate M.	
Study of a highly crystalline Y₂O₃ sample by Rietveld and Pair Distribution Function Analysis	53
Presenter: Martinez, L. G. Martinez, L. G.; Ichikawa, R. U.; Turrillas, X	
Temperature and high-pressure dependent X-ray absorption of SmNiO₃ at the Ni K- and Sm-L₃ edges	54
Presenter: Massa N. E. Massa N. E., Ramos A. Y., Tolentino H. C. N., Neto N. S., Junior J. F., Martínez-Lope M. J. and Alonso J. A.	

Short-range order study around Iron atoms: Crystallization Process in glassy samples followed by X-ray absorption spectroscopy	55
Presenter: Mastelaro V. Mastelaro V. R.; Bayer P. S.; Zanotto E. D.	
In situ XPD study of structural changes in iron-cerium mixed oxides under reducing conditions	56
Presenter: Mazan M. O. Mazan M.; Martins T.; Prado R.; Larrondo S.	
In situ SR μXRF analysis of Pb in plants used for phytoextraction of soil pollutants	57
Presenter: Mera M. F. Mera M. F., Rubio M., Pérez C. A.4, Germanier A., Cazón S., Carranza L.	
Application of XANES spectroscopy to investigate Sb species in corroded bullets crust material oriented to evaluate the potential toxic effects in the environment	58
Presenter: Mera M. F. Mera M. F., Rubio M., Pérez C. A., Vicentin F. C., Germanier A.	
Amine-alcohol-silicate hybrid matrix as efficient adsorbents for water cleaning	59
Presenter: Molina E. F. Moura A. L. A., De Oliveira L. K., Ciuffi K. J. and Molina E. F.	
Spectroscopic characterization of the interface semiconductor/active layer in sensors based on DNA	60
Presenter: De Moraes M. O. S. Silva-Moraes M. O., Brito W. R., Mota A. J., Assis I. M., Wilson D., Passos R. R., Galante D., Garcia-Basabe Y., Rocco M. L. M., Casarini J. R.	
In-situ and in-operando studies of cobalt doped titanates by XRD, XAS and electrochemical impedance spectroscopy simulating working conditions as SOFC anodes and cathodes	61
Presenter: Napolitano F. R. Napolitano F.; Soldati A.; Geck J.; Giebeler L.; Fernández-Zuvich A.; Saleta M.; Caneiro A.; Serquis A.; Mogni L.	
Structural characterization of fragmented kraft lignin by biological processes by SAXS	62
Presenter: Negrão D. R. Negrão D. R., Brenelli L. B., Gandin C. A., Dias. A. T., Leão A. L., Neto M. de O., Squina F. M., Monteiro R. T. R	
Iterative Reconstruction of Tomographic Images Using Accelerated Projection/Backprojection Techniques	63
Presenter: Neto E. S. H. Neto E. S. H.	

Small angle X-ray scattering applied to Glycoside hydrolases from families GH5 and GH6	64
Presenter: Neto M. de O. Neto M. de O.; Gandin C. A.; Gonçalves T.; Pimentel A. C.; Alvarez T. M.; Squina F. M.	
In situ study of austenite decomposition during thermal cycles and under application of stress in ferrous alloys	65
Presenter: Nishikawa A. S. Nishikawa A. S.; Echeverri E. A. A.; Centeno D. M. A.; Huallpa E. A.; Tschiptschin A. P.; Goldenstein H.	
Synchrotron small angle X-ray scattering Investigation of niobium oxyhydroxide nanostructured	66
Presenter: Pereira I. M. Pereira I. M., De Souza S. D., Oliveira L. C. A., De Souza A. R., Rodrigues A. P. H., Boaventura T. P., Oréfica R. L., Patrício P. S. O.	
Investigation of the Morphology Exhibited by Multilayered Films of Collagen and Cellulose Nanowhiskers by Small-angle X-ray Scattering	67
Presenter: Pereira I. M. Pereira I. M., De Souza S. D., Patricio P. S. de O.	
Use of oyster Crassostrea rhizophorae as biomonitor in analysis of heavy metals pollution in the marine environment under influence of the ports of Santos and São Sebastião.	68
Presenter: Pezzatti R. R. Pezzatti R. R., Yokoyama L. Q., Ignacio B. L., De Jesus E. F. O., Mársico E. T., Ribeiro R. de O. R., Barbosa R. de F.	
Refinement of single crystal structures by X-ray multiple diffraction.	69
Presenter: Remédios C. M. R. Remédios C. M. R.; Morelhão S. L.	
Thermal transformations metakaolin – spinel type aluminosilicate: Al and Si k-xanes characterization	70
Presenter: Requejo F. G. Requejo F. G.; Andrini L.; Rendtorff N.	
Study of Eu³⁺/Eu²⁺ reduction in BaAl₂O₄: Eu prepared in different gas atmospheres	71
Presenter: Rezende M. V. dos S. Rezende M. V. dos S. a, Valerio M. E.G., Jackson R. A.	
Ionization and fragmentation of the acetaldehyde (CH₃CHO) molecule by 20-330 eV photons	72
Presenter: Ribeiro L. C.	

Ribeiro L. C.; Santos M. de J.; Dos Santos A. M.; Arruda M. S.; Mendes L. A. V.; Dos Santos A. C. F.; Marinho R. dos R. T.; Prudente F. V.

Heavy metals measurement in sandy beaches: influence of the benthic fauna associated **73**

Presenter: Ribeiro R. M. M.

Ribeiro R. M. M., Yokoyama L. Q., Jesus E. F. O., Ribeiro R. O. R., Mársico E. T., Gennari R. F., Barbosa R. F.

Exploratory Methodology for Retrieving Oxidation State Information from X-ray Resonant Raman Scattering Spectrometry **74**

Presenter: Robledo J. I.

Robledo J. I.; Sánchez H. J.; Leani J. J.; Pérez C. A.

The effect of annealing on the electronic structure, morphology and charge transport in polymer: fullerene blends for photovoltaics **75**

Presenter: Rocco M. L.

Rocco M. L. M., Garcia-Basabe Y., Marchiori C. F. N., De Moura C. E. V., Rocha A. B., Roman L. S.

Iron oxide nanoparticles coated with different Silica thicknesses: SAXS analysis of size, shape and agglomeration and its relationship with magnetic properties. **76**

Presenter: Rojas P. C. R.

Rivas P.; Tancredi P.; Moscoso-Londoño O.; Socolovsky L. M.

Electronic Studies on Coordination Metal Complexes with Xanthates Ligands: S, Ni and Mn K-edge XANES **77**

Presenter: Romano R. M.

Juncal L. C.; Condorí E. A. O.; Védova C. O. D.; Romano R. M.

Atomic Pair Distribution Function at LNLS: A New Tool for Material Science **78**

Presenter: Saleta M. E.

Saleta M. E.; Mastelaro V. R.; Granada E.

Multivariate SAXS Profiles Analysis Applied to Synthesis of Heterogeneous Titania Photocatalysts by Sol-Gel Method **79**

Presenter: Dos Santos J. H. Z.

Dos Santos J.H.Z., Moreno Y.P.

The importance of the active site molecular interactions to the oligomerization and reactivity of the typical 2-Cys Prx **80**

Presenter: Dos Santos M. C.

Dos Santos M. C.; Junior C. A. T.; Netto L. E. S.; De Oliveira M. A.

Microemulsions for application as corrosion inhibition: a SAXS approach **81**

Presenter: Sarmiento V. H. V.

Sarmiento V. H. V.; Gonçalves H. B.; Huck-Iriart C.; Costa E. V.

Phase Contrast X-ray Imaging of Human Peripheral Nerves	82
Presenter: Scopel J. F.	
Scopel J. F.; Queiroz L. S.; O'Down F. P.; Junior M. C. F.; Nucci A.; Hönnicke M. G.	
Structural 3D Characterization of Silica, Zirconia and Titania Monoliths and Columns for Capillary Liquid Chromatography	83
Presenter: Da Silva C. G. A.	
Da Silva C. G. A., Archilha N. L., Collins C. H., Bottoli C. B. G.	
Near edge structure at the lithium K-edge in LiH by inelastic X-ray scattering	84
Presenter: Stutz G. E.	
Stutz G. E., Mellone O.A. P., Ceppi S.A., Larochette PP.A.	
Characterization of nanostructured A_{1-x}Sr_xFe_{0.8}Cu_{0.2}O_{3-d} perovskites (A=La, Ba) as IT-SOFC cathodes.	85
Presenter: Suescun L.	
Suescun L.; Vázquez S.; Davyt S.; Faccio R.; Basbus J.; Napolitano F.; Soldati A. L.; Serquis A.	
Study of Ag@Fe₃O₄ nano-heterostructures by synchrotron radiation techniques	86
Presenter: Tancredi P.	
Tancredi P.; Moscoso-Londoño O.; Muraca D.; Pirota K.; Knobel M.; Wolff U.; Damm C.; Neu V.; Rellinghaus B.; Socolovsky L.M.	
Investigation of band structure of insulators using vacuum ultraviolet spectroscopy	87
Presenter: Teixeira V. de C.	
Teixeira V. de C.; Valerio M. E. G.	
XANES study of the oxidation state of Cu, Ni and Ce cations in the Cu-Ni/ce{Ce_{0.9}Zr_{0.1}O₂} cermet in reducing atmospheres	88
Presenter: Toscani. M.	
Toscani L. M.; Zimicz M. G.; Martins T.; Lamas D. G.; Larrondo S. A.	
Photofragmentation of a perfluorocarboxylic acid using synchrotron radiation: Study of CF₃CF₂C(O)OH	89
Presenter: Védova. O. D.	
Védova C. O. D.; Martínez Y. B.; Bava Y. B.; Filho R. C.; Romano R. M.	
Phosphorus speciation during the production of phosphate fertilizers using a metallurgical acid residue	90
Presenter: Vergütz L.	
Vergütz L.; Santos W. O.; Filho L. F. S. S.; Hesterberg D. R. L.; Mattiello E. M.	

Identification of the substrate binding sites in Actinobacteria sulfotransferase Cpz8	91
Presenter: Vieira B. D.	
Vieira B. D.; Fernandes A. Z. N.; Kaysser L.; Gust B.; Trivella D. B. B.	
Surface nanomodification of polypropylene	92
Presenter: Waldman W. R.	
Waldman W. R., Galante D., Fitaroni L. B., Cruz S. A.	
Extreme UV and Selective Inner-Shell Fragmentation Studies of Novel Polymeric Resist Materials	93
Presenter: Weibel D. E.	
Chagas G.; Satyanarayana V. S. V.; Kessler F.; Belmonte G. K.; Gonsalves K. E. ; Weibel D. E.	
Purification, Crystallization and Preliminary Analysis of the X-Ray Diffraction Data from an Epoxide Hydrolase identified in Streptomyces sp.	94
Presenter: Wilson C.	
Wilson, C.; Santos, J. C.; González, G. D. T.; Oliveira, L. G.; Dias, M. V. B.	
Physical Simulation and Advanced Characterization of Structural Materials	95
Presenter: Wu L.	
Wu L.	
Micelle and mesoporous silica formation with different cethylammonium surfactants	96
Presenter: Zapelini I. W.	
Zapelini I. W., Campos A. F. P., Modesto P. P., Ferreira A. R. O., Alkimim I. P., Araujo J. A., Silva L. L., Cardoso D.	
Fragment based drug discovery targeting proteins associated with virulence and resistance to antibiotics in Mycobacterium tuberculosis	97
Presenter: Zuniga G. A. L.	
Libreros-Zuniga G.A; Dias M.V.B	
An investigation of the Morphology exhibited by HDPE composites after being subjected at very high rates of loading	98
Presenter: Zylberberg M. P.	
Zylberberg M. P.; Saldanha A. L. M.; Patricio P. S. de O.; Pereira I. M.	

PRESENTATION

Dear participant,

The Users Committee welcomes all the participants of **the 25th Annual Users Meeting of the Brazilian Synchrotron Light Laboratory (RAU/LNLS)**.

This year's meeting highlights two important dates: the celebration of both the **25th Annual Users Meeting** as well as **the International Year of Light and Light-based Technologies (IYL2015)**. The history of RAU started even before the LNLS has become an important international facility open to users since 1996. The laboratory's scientific community has grown fast since then, consisting of more than 1600 researchers from all over the world nowadays.

The importance of LNLS to the global scientific scenario has led to the conception of a new 4th generation machine – Sirius – which will be available to users in the year 2019. This breakthrough situates Brazil as one of the leading countries in synchrotron-based technologies. As preconized by Richard Feynman in 1959, “there is plenty of room at the bottom” and the opportunities provided by the new source will, literally, shed some light on the most challenging today's problems.

The chairperson would like to thank all the scientific committee for its efforts in the indication of the invited speakers as well as on the evaluation of the oral and poster presentations. We also thank the LNLS directors and all the local committee for the valuable support on the meeting organization.

Fabio Furlan Ferreira

On behalf of the LNLS Users Committee

ORGANIZERS | SCIENTIFIC COMMITTEE

1. Dr. Alexandre Malta Rossi – Vice-President (CBPF)
2. Prof. Dr. Edenir Pereira Filho (UFSCar)
3. Prof. Dr. Fabio Furlan Ferreira (Chair) – President (UFABC)
4. Prof. Dr. João Henrique dos Santos (UFRGS)
5. Prof. Dr. Manoel Gustavo Petrucelli Homem (UFSCar)
6. Prof. Dr. Marcelo Alves (USP)
7. Prof. Dr. Mario de Oliveira Neto (UNESP)
8. Prof. Dr. Valmor Roberto Mastelaro (USP)

LOCAL COMMITTEE

1. Adriana Paracencio (LNLS – CNPEM)
2. Dora Marques (Communication – CNPEM)
3. Fábio Reis Fonseca (Communication – CNPEM)
4. Gabriela Campeão (LNLS – CNPEM)
5. Graziela Pereira Esteves (LNLS – CNPEM)
6. Ildéria Marques dos Santos (Communication – CNPEM)
7. Marcelo Ramos (LNLS – CNPEM)
8. Meire Picoli (LNLS – CNPEM)
9. Luciana Noronha (Communication – CNPEM)
10. Pamela Machado (Communication – CNPEM)
11. Priscila Moya (LNLS – CNPEM)
12. Tatiane Cortes (Communication – CNPEM)
13. Renan Picoreti (LNLS – CNPEM)
14. Vilmara Congílio (LNLS – CNPEM)

PROGRAM

16th September 2015	
08:00 - 08:30	Reception/Registrations
08:30 - 08:50	Opening Carlos Américo Pacheco (Director-General of CNPEM) and Antonio José Roque da Silva (Director of the Brazilian Synchrotron Light Laboratory, LNLS)
08:50 - 09:30	RAU 25 years Retrospective – José Antônio Brum
09:30 - 10:30	Plenary 1 <i>Pushing the XAS frontiers: XANES approaches for chemical speciation and structure characterization and cutting-edge features of Balder beam-line at the MAX IV synchrotron radiation facility</i> Ingmar Persson – Swedish University of Agricultural Sciences
10:30 - 11:00	Coffee Break
11:00 - 12:40	Thematic Session ↗
12:40 - 14:00	Lunch
14:00 - 15:00	Plenary 2 <i>Relaxation dynamics of isolated atoms and molecules in the tender x-ray domain (1-12 keV)</i> Marc Simon – CNRS
15:00 - 16:00	Plenary 3 <i>Application of Synchrotron Radiation for Chemical Industry</i> Wolfgang Hoeffken – BASF
16:00 - 16:30	Coffee Break
16:30 - 17:30	Panel discussion: Committee & LNLS with the users
17:30 - 19:30	Posters Session

17th September 2015

08:00 - 08:30	Reception/Registrations
08:30 - 09:30	Plenary 4 <i>Looking inside materials using synchrotron X-ray diffraction</i> Jon Wright – ESFR
09:30 - 10:30	Oral Communication 1 ↗
10:30 - 11:00	Coffee Break
11:00 - 12:40	Oral Communication 2 ↗
12:40 - 14:00	Lunch
14:00 - 15:00	Sirius: Status and Perspectives Antonio José Roque da Silva
15:00 - 15:10	Closing

25th RAU

ANNUAL USERS

MEETING LNLS/CNPEM

September 16th and 17th, 2015

ABSTRACTS

The use of synchrotron radiation in Astrobiology: Lithopanspermia studies and the Biosun project

Presenter: Abrevaya X. C.

Abrevaya, X. C.^{1,2}; Galante, D.³; Nóbrega, F.⁴; Tribelli, P.⁵; Rodrigues, F.⁶; Araujo, G.⁷; Gallo, T.³; Ribas I.⁸; Sanz-Forcada, J.⁹; Rodler, F.^{10, 11}; Porto de Mello G.F.¹²; Leitzinger, M.¹³; Odert, P.¹³; Hanslmeier, A.¹³; Horvath, J.²

¹ Instituto de Astronomía y Física del Espacio (IAFE), UBA – CONICET, Buenos Aires, Argentina; ² Research Unit in Astrobiology, IAG – USP, São Paulo, Brazil; ³ Brazilian Synchrotron Light Laboratory (LNLS/CNPEM), Campinas – SP, Brazil; ⁴ Instituto Oceanográfico, USP, São Paulo, Brazil; ⁵ Depto de Química Biológica, FCEyN – UBA, IQUIBICEN – CONICET, Buenos Aires, Argentina; ⁶ Instituto de Química, USP, São Paulo, Brazil; ⁷ Programa de Pós-Graduação em Biotecnologia, ICB/USP, São Paulo, Brazil; ⁸ Institut de Ciències de l'Espai, Barcelona, Spain; ⁹ Centro de Astrobiología, Madrid, Spain; ¹⁰ Max-Planck-Institut für Astronomie, Heidelberg, Germany; ¹¹ Harvard-Smithsonian Center for Astrophysics, Cambridge, USA; ¹² Observatorio do Valongo, UFRJ, Rio de Janeiro, Brazil; ¹³ Institut für Physik, IGAM, Universität Graz, Graz, Austria
abrevaya@iafe.uba.ar

Panspermia theory assumes that microscopic life forms (e.g.: microorganisms) could survive long interplanetary travels (Arrhenius, 1903; Hoyle and Wickramasinghe, 1979). This has been matter of debate since a long time ago, opening the possibility of an extraterrestrial origin of life on the Earth. One of the open issues is that it is still not known if these life forms could survive these travels because they would be exposed to multiple extreme conditions (e.g.: radiation, vacuum). Abrevaya et al (2011) showed the capacity of some species of microorganisms to survive several doses of VUV radiation and vacuum as those related to the conditions of low Earth orbit (L.E.O.). In a new round of experiments performed at the TGM beamline (LNLS, Campinas, Brazil) we tested the survival of the microorganisms considering Lithopanspermia (interplanetary transfer of life through meteorites) in the context of the BioSun project (Abrevaya et al., 2013). The Martian meteorite “Nakhla” was chosen as model for these studies because it contains halite inclusions (NaCl evaporitic minerals). This is connected to the fact that microorganisms known as haloarchaea were found entrapped inside ancient halites (250 Mya) on Earth (e.g.:McGenity et al., 2000); therefore these organisms were proposed as possible inhabitants of Mars and possible candidates for the interplanetary transfer of life (Stan-Lotter et al., 2004). As the project is focused in the radiation environment of the young Sun, for the simulation experiments we selected as main parameters low pressure (vacuum) and VUV radiation as those we could found in L.E.O. around 3.8 Gyr ago. Two species of haloarchaea and the radioresistant bacteria *D. radiodurans* were entrapped inside halites and irradiated with VUV (57.5 –124 nm) with different doses up to 40000 J/m² (eq. to 10 days in L.E.O.). We showed that the survival of of the microorganisms is strongly dependent on the specie and that halites could not offer enough protection.

Abrevaya XC, Paulino-Lima IG, Galante D, et al. 2011. *Astrobiology*, 11, 1034-1040. Abrevaya XC, Hanslmeier A, Leitzinger M, et al., 2014. The BIOSUN project: an astrobiological approach to study the origin of life. *REVMEXAA* 44: 144-145. Arrhenius, S. 1903. *Umschau* 7:481–485. Hoyle F. and Wickramasinghe NC.1979. *Diseases from Space*. Harper and Row, New York. McGenity TJ, Gemmill RT, Grant WD, Stan-Lotter H. 2000. *Environ. Microbiol.* 2:243–250 Stan-Lotter H, Radax C, McGenity TJ, et al. 2004. From intraterrestrials to extraterrestrials - viable haloarchaea in ancient salt deposits. *Halophilic Microorganisms*, edited by A.Ventosa, Springer Verlag, Berlin, Heidelberg, New York, pp.89-102.

Application of X-Ray Phase Contrast Microtomography Using Brazilian Synchrotron Light Laboratory to Improve the Visualization of External and Internal Structures of *Rhodnius prolixus* head

Presenter: De Almeida A. P.

Sena G.¹, Almeida A.², Nogueira L.³, Braz D.¹, Gonzalez M.⁴, Azambuja P.⁵, Barroso R.³

¹COPPE/Federal University of Rio de Janeiro, ²State University Centre of West Zone, ³Lab of Applied Phys to Biomed and Environmental Sci/Physics Institute/State University of Rio de Janeiro, ⁴Fluminense Federal University, ⁵Oswaldo Cruz Institute, Brazil.
apalmeid@gmail.com

Phase Contrast Microtomography (PhC- μ CT) using synchrotron radiation is a non-destructive technique that allows the microanatomical investigations of *Rhodnius prolixus* head, one of the most important insect vectors of *Trypanosoma cruzi* the etiologic agent of Chagas' disease, which accounts for about 12,000 deaths per year. The control of insect vector is the most efficient method to prevent this disease and this work is part of a series of articles [1-3] that uses PhC- μ CT for the study of *R. prolixus* morphology. This technique provides anatomical details that could not be seen with others techniques. In this work, nymphs of *Rhodnius prolixus* were taken from the Laboratory of Biochemistry and Physiology of Insects, Oswaldo Cruz Foundation (FIOCRUZ), Brazil. The micro tomographic images were obtained using the new experimental setup which was recently made available at the Brazilian Synchrotron Light Laboratory (LNLS) with a 2 μ m resolution, and the results showed internal and external structures of *Rhodnius prolixus* head. Understanding the behavior of internal and external structures of *Rhodnius prolixus* head can help to understand the mechanism of blood digestion by *Rhodnius prolixus* and its interaction with the agent of Chagas' disease, *Trypanosoma cruzi*, the parasite that grows within the insect's digestive system. PhC- μ CT is clearly one of the best imaging techniques for insect research and has allowed a better documentation of the detailed external and internal morphology of *Rhodnius prolixus* without dissecting.

[1] - A. P. Almeida, D. Braz, *Radiat Phys Chem* 95 243-246 (2014). [2] - A. P. Almeida, D. Braz, *JINST* 8 C07004 (2012). [3] - G. Sena, A. P. Almeida, *J. Phys.: Conf. Ser.* 499 012018 (2014). [4] - C. B. Mello, D. Mendonça-Lopes, *Mem. Inst. Oswaldo Cruz* 103 8 (2008).

VUV excitation and SEM analysis in nanofluoride produced by microwave hydrothermal synthesis

Presenter: Andrade A. B.

Andrade A. B.¹, Valerio M. E. G.¹

Federal University of Sergipe¹
abandrade1@gmail.com

Different nanoparticles (NP's) size of barium fluoride (BaF₂) has been studied by x-ray powder diffraction (XRPD) and Rietveld refinement method analysis, scanning electron microscopy (SEM), X-ray photoelectron spectroscopy (XPS) and vacuum ultraviolet excitation measures. We show in this study that BaF₂ nanoparticles produced by hydrothermal microwave method (HTMW), displayed a structural lattice strain which depend of the NP's size. From Rietveld refinement method, were observed that lattice parameters to nanoparticles are smaller than crystal bulk. These refined lattice parameters increase as function of the median size distribution of the BaF₂ NP's. Vacuum ultraviolet excitation spectra were performed at Brazilian Synchrotron Light laboratory (LNLS) in the Toroidal grating monochromator (TGM) beamline for all samples, and was possible observe a distinct initial and final region energy to self-trapped exciton (STE) formation energy around 9.4-9.6 eV. The width band gap was observed in 10.5 eV to all samples, without shift. These results suggest that the binding energy of the self-trapped exciton depends on particle size and that the lattice strain can be induced by lattice compression as function of the nanoparticle size effect.

Bentonite: Al – Si k xanes characterization for this clay treated at two temperature

Presenter: Andrini L.

Andrini L.*; Toja R. M.; Gauna M. R.; Requejo F. G.; Rendtorff N.

INIFTA (FCE-UNLP, CCT La Plata-CONICET); FCE-UNLP; CETMIC (FCE-UNLP, CIC, CCT La Plata-CONICET); INIFTA (FCE-UNLP, CCT La Plata-CONICET, CONICET); CETMIC (FCE-UNLP, CIC, CCT La Plata-CONICET)
andrini@inifta.unlp.edu.ar

Bentonite is an absorbent aluminium phyllosilicate (Smatitec 2:1 group) and Montmorillonite is the best known member of the this group [1]. Bentonites are highly valued for their sorptive properties, which stem from their high surface area and their tendency to absorb water in the interlayer sites [2] which are most extensively used are Na-Bentonite and Ca-Bentonite [3] as it are called in the industry. We studied by Al – Si K XANES a predominantly Na-Bentonite before and after thermal treatment at 800°C and 1050°C to correlate the information obtained with this technique with that obtained by conventional X-ray Diffraction, and clarify and assign the structural changes. The results from the Si K XANES spectra show no major structural changes attributed to the Si sites, but there are significant changes in the Si 3p-holes density which increases due to thermal treatment. The results from the Al K XANES spectra show significant structural changes. The shoulder associated at AlO₄ disappear with the thermal treatment and the first main peak has a broadening for higher temperature. The same goes for the second main peak but more intensely. This is assignable to splits Al 3p-levels due to the effects of crystal ligand field in Al morphological reconfiguration.

[1] P.F. Luckhum, S. Rossi, *Adv. Colloid Interfuce Sci.* 82 (1999) 43-92. [2] G.E. Christids, P.W. Scott, A.C. Dunham, *Appl. Clay. Sci.* 12 (1997) 329-347. [3] H.H. Murray, *Clay Minerals* 34 (1999) 39-49.

Small-angle x-ray scattering investigation of asphaltene structures in crude oils

Presenter: Balestrin L. B. da S.

Balestrin L. B. da S., Padula L., Sabadini E., Cardoso M. B. and Loh W.

IQ/UNICAMP, IQ/UNICAMP, IQ/UNICAMP, LNLS/CNPEM, IQ/UNICAMP
lia.bsb@gmail.com

Crude oil asphaltenes represent a solubility class, not specific molecules. Crude oil asphaltenes consists of a complex mixture of several distinct molecules whose properties and structures are strongly related to the fractionation method for their isolation and to the geologic source from which they are extracted. [1] A representative asphaltene molecule is described as possessing an aromatic core of several rings, surrounded by alkyl chains. [2] Several problems related with petroleum are associated with asphaltenes stability during many operations. [3] The deposition of solids is reported at various places in the crude oil systems, thereby limiting oil production rates. [1] Crude oil asphaltenes behave, in some cases, like classical colloids. [1-3] They have been studied with a colloidal approach by numerous techniques, at various length scales. [2] They display surface-active properties and a self-assembling tendency. Overall, most of the results seem to agree that there are different levels of aggregation producing structures with varied sizes. However, there are few evidences supporting that this pattern is also present in crude oil samples (as opposed to simpler model systems). This work reports studies employing SAXS measurements on Brazilian crude oil samples with different asphaltene contents. These samples were analyzed by SAXS using synchrotron source (at the Brazilian Synchrotron Laboratory). In all cases, the SAXS curves confirmed that different levels of aggregation are presented: the first one at the nanometer scale, followed by at least two other higher levels of organization. Other experiments were performed with crude oils in the presence of diluent (toluene) or flocculant (heptane). The preliminary results suggest that the second level is affected by heptane even well below the precipitation onset, but less affected by toluene.

[1] Loh, W., Mohamed, R. S., dos Santos, R. G., Crude Oil Asphaltenes: Colloidal Aspects, Encyclopedia of Surface and Colloid Science, 1:1, 1-18 (2007); [2] Eyssautier, J., Levitz, P., Espinat, D., Jestin, J., Gummel, J., Grillo, I., Barré, L., Insight into Asphaltene Nanoaggregate Structure Inferred by Small Angle Neutron and X-ray Scattering, J. Phys. Chem. B, 115, 6827–6837 (2011); [3] Giavarini, C., Mastrofini, D., Scarsella, M., Macrostructure and Rheological Properties of Chemically Modified Residues and Bitumens, Energy & Fuels, 14, 495-502 (2000).

Ultrafast charge transfer dynamics and morphological investigation in thermal annealed donor-acceptor copolymer and fullerene: F8T2 and F8T2:PCBM films

Presenter: Basabe Y. G.

Garcia-Basabe Y.*, Yamamoto N. A. D.¹, Roman L. S.¹, and Rocco M. L.*

Institute of Chemistry, Federal University of Rio de Janeiro, Rio de Janeiro, 21941-909, Brazil¹ Department of Physics, Federal University of Paraná, Curitiba, 81531-990, Brazil
yunier@iq.ufrj.br

Synopsis Ultrafast charge delocalization dynamics on internal donor-acceptor polymer poly(9,9-dioctylfluorenyl-co-bithiophene) (F8T2) and its blend with the fullerene derivate [6,6]-Phenyl C₆₁ butyric acid methyl ester (PCBM) was studied by the resonant Auger spectroscopy (RAS) measured around sulfur *K*-edge using the synchrotron-based core-hole clock approach. The RAS spectra were measured at the SXS beamline at the Brazilian Synchrotron Light Source (LNLS) using an ultrahigh vacuum chamber with a base pressure of 10⁻⁸ mbar and hemispherical electron energy analyzer. The effect of thermal annealing on the charge transfer delocalization times (τ_{CT}) was also investigated recording RAS spectra while detuning the photon energy around S-1s absorption edge. Poor charge delocalization was observed for as-cast polymeric films at photon energies corresponding to the S 1s $\rightarrow\pi^*$ transition, which may suggest a weak π -electronic coupling due to weak polymer crystallinity and chain stacking. Atomic Force Microscopy (AFM) topography for as cast F8T2:PCBM shows a top position of PCBM units relative to the polymer, homogeneously distributed in film surface. This configuration improves the charge delocalization through S 1s $\rightarrow\pi^*$ molecular orbital for as cast blended film, suggesting a strong π -electronic coupling. A new rearrangement of F8T2:PCBM film was found after thermal annealing, leading to a more efficient electron transfer channel through σ^* molecular orbitals.

Hybrid nanostructured sulfonated poly (ether ether ketone) / zirconium oxide based membranes comprising protic ionic liquid for PEMFC application

Presenter: Batalha J. A. F. L.

Dahmouche K.²; Gomes A. de S.¹

¹ IMA/UFRJ; ² UFRJ Campus Xerém
jabatalha@ima.ufrj.br

In view of the lack of fossil fuels in a near future, and aiming, not only to diminish the environmental impacts caused by its gas emissions from combustion, but also better quality of life for the population, alternative energy sources are being each time more studied, which is the case of fuel cells, normally fed by hydrogen. Among the many types of fuel cells, the solid, non-corrosive, non-toxic polymer electrolyte one stands out. The great challenge of this technology nowadays is that its operation occurs in temperatures higher than 100 °C, the limit for Nafion®, reference material for electrolytes. Many efforts are being effected towards this possibility, such as synthesis of composites with inorganic fillers. However, the most promising studies face the employment of ionic liquids, especially the protic ones, as integral replacement to water in the operation of this kind of fuel cell. With this being said, the greatest challenge to the development of this technology is to retain the ionic liquid within membranes, without great decrease in conductivity properties. In this work, hybrid membranes based on sulfonated poly(ether ether ketone) (sPEEK) and zirconium oxide, incorporated via sol-gel, comprising diethylmethylamine triflate ([dema][TfOH]) were explored. The membranes presented good mechanical and chemical stabilities, as well as thermal stability over 300 °C. SAXS curves indicated the possible formation of ionic domains. Moreover, other analysis such as ionic conductivity, DMTA and XRD were also executed.

PADILHA, J.C.; BASSO, J.; TRINDADE, L.G.; MARTINI, E.M.A.; SOUZA, M.O.; SOUZA, R.F. Ionic liquids in proton exchange membrane fuel cells: efficient systems for energy generation. *Journal of Power Sources*, v. 195, n. 19, p. 6483-6485, abr. 2010. Disponível em: . Acesso em: 24 out. 2011. PEIGHAMBARDOUST, S.J.; ROWSHANZAMIR, S.; AMJADI, M. Review of the proton exchange membranes for fuel cell applications. *International Journal of Hydrogen Energy*, Rio de Janeiro, v. 35, p. 9349-9384, jun. 2010 PERLES, C.E. Propriedades físico-químicas relacionadas ao desenvolvimento de membranas de Nafion® para aplicações em células a combustível do tipo PEMFC. *Polímeros: Ciência e Tecnologia*, Rio de Janeiro, v. 18, n. 4, p. 281-288, jun. 2008 PRADO, L.A.S.A.; PONCE, M.L.; FUNARI, S.S.; SCHULTE, K.; GARAMUS, V.M.; WILLUMEIT, R.; NUNES, S.P. SAXS/WAXS characterization of proton-conducting membranes containing phosphomolybdic acid. *Journal of Non-crystalline Solids*, v. 351, n. 27-29, p. 2194-2199, jul. 2005. Disponível em: . Acesso em: 7 fev. 2013. MORI, K.; HASHIMOTO, S.; YUZURI, T.; SAKAKIBARA, K. Structural and spectroscopic characteristics of a proton-conductive ionic liquid diethylmethylammonium trifluoromethanesulfonate [dema][TfOH]. *Bulletin of Chemical Society of Japan*, v. 83, n. 4, p. 328-334, mar. 2010. Disponível em: . Acesso em: 6 dez. 2012. NAKAMOTO, H.; WATANABE, M. Brønsted acid-base ionic liquids for fuel cell electrolytes. *Chemical Communications*, Rio de Janeiro, n. 24, p. 2539-2541, mar. 2007.

Structural and Optical Studies of Nanoparticles of CaF₂

Presenter: Bezerra C. dos S.

Bezerra C. dos S.; Valerio M. E. G.

Universidade Federal de Sergipe
cdsantos20@gmail.com

The development of scintillators materials is an experimental field that has attracted attention from researchers in last years and one interesting class of materials are the fluoride matrices doped with rare earth ions that have attracted interest also due to applications in lasers. Compared with the oxide matrices fluorides have advantages such as high transparency in a wide wavelength region from the VUV to IR and low energy phonons. In this work, the CaF₂ pure and doped with erbium were produced by microwave-assisted hydrothermal synthesis, which is a promising method to produce nanostructured powders in a simple, low cost and fast way. The samples were produced using chelating agent (EDA-Ethylenediamine) and synthesized at low temperature and a short time period. The crystalline phases of the samples were identified by X-ray diffraction (XRD) and the morphology of the particles was determined by scanning electron microscopy (FEG-SEM). The results shown that the microwave-assisted hydrothermal synthesis is efficient for production of the CaF₂ nanoparticles and the use of the chelating agent in the production of the samples influences the average particles size. The study of the chemical composition in the surface was performed by X-ray Photoelectron Spectroscopy (XPS) and indicated the presence of greater amounts of hydroxyl groups and oxygen ions in the samples produced with EDA. Radioluminescence (RL) measurements showed that the CaF₂ presents an intrinsic luminescence with an emission band at approximately 300 nm. Optical study was conducted to understand the formation of band structure and to determine the band gap of the materials. The excitation spectra in the VUV region were measurements in Brazilian Synchrotron Light Laboratory (LNLS) and the results shown evidences that the formation energy of the exciton and band gap energy are smaller than the ones for the single crystal.

Arsenic speciation in geological samples using X-ray absorption spectroscopy

Presenter: Bia G. L.

Bia G. L.; García M. G.; Borgnino L. C.

Centro de Investigaciones en Ciencias de la Tierra
gonzaloluis.bia@gmail.com

The Chaco Pampean plain is one of the largest regions in the world (1,000,000 Km²) affected by the presence of high concentrations of As in groundwater (Nicolli et al. 2012). The primary source of As is associated with the presence of volcanic ash spread in the loessic sediments that blanket the entire region. Bia et al. (2015) identified by XPS the presence of As (III)-S and As (V)-O nanocoatings, deposited on the surface of volcanic glass particles. The As contained in these coatings is easily released in contact with water, but a higher proportion of As remain within the aluminosilicate glass structure as an impurity. The aim of this work is to determine the oxidation state of arsenic, its local chemical coordination (to a radius of ~4 Å around As) and the relative proportion of the As species in volcanic Andean ashes and loess sediments. To carry out this study, volcanic ash samples of recent eruptions (Hudson, 1991 Chaitén, 2008 and Puyehue, 2011) and samples of loess were analyzed by X-ray absorption fine structure spectroscopy (XAFS), using the facilities of the Brazilian Synchrotron Light Laboratory (LNLS, Brazil). XANES analysis allowed to discriminate three oxidation states of arsenic in the studied samples: As⁵⁺ is the dominant oxidation state in loess sediments while in volcanic ash samples just the oxidation states As⁻¹ and As³⁺ were identified. The proposed EXAFS models fit well with the experimental data, suggesting that in loess sediments, As⁵⁺ could be in the form of arsenate ions adsorbed onto ferric oxyhydroxides, or precipitated as scorodite (FeAsO₄•2H₂O). In volcanic ashes, the species As⁻¹ identified is likely associated with arsenopyrite (FeAsS) or arsenical pyrite (FeS₂-2xAs_x), while As³⁺ is likely related to As atoms present as impurities within the glass structure.

Nicolli, H.B., Bundschuh, J., Blanco, M. del C., Tujchneider, O.C., Panarello, H.O., Dapeña, C. & Rusansky, J.E. 2012. Arsenic and associated trace-elements in groundwater from the Chaco-Pampean plain, Argentina: Results from 100 years of research. Science of the Total Environment 429, 36-56. Bia, G, Borgnino, L. Gaiero, D., García, M.G. 2015. Arsenic-bearing phases in South Andean Volcanic ashes: Implications for As mobility in Aquatic environments. Chemical Geology 393-394, 26-35.

Nanostructured Ga doped ZnO thin films prepared by sol-gel spin-coating

Presenter: Bojorge C. D.

Bojorge C.¹; Cánepa H.¹; Heredia E.¹; De Reca N. E. W.¹

¹ CINSO, UNIDEF (CITEDEF-CONICET), J.B. de La Salle 4397, (1603) Villa Martelli, Pcia. de Buenos Aires, Argentina
cbojorge@citedef.gob.ar

ZnO based films have been actively studied because of their applications as solar cells, gas sensors, piezoelectric transducers, ultrasonic oscillators and for different optoelectronic applications. Besides their interesting optical, electrical and piezoelectrical properties, this material exhibits a high chemical and mechanical stability. ZnO presents novel properties and potential applications in optoelectronic fields because its nonlinear optical properties, excitonic emission at room temperature and quantum size effect. In the present work we studied pure and Ga-doped ZnO thin films prepared by the sol-gel spin coating technique by grazing incidence small-angle X-ray scattering (GISAXS) and X-ray reflectivity (XR) methods. We also compare the present spin coating pore distribution results with those obtained in previous works.

Photoionization studies on Thionitrites

Presenter: Canneva A.

Nitric oxide (NO) has been recognized as a fundamental molecule in biology and medicine. Among them, S-nitrosothiols, RSNO, have been shown to store, transport, and release NO within the mammalian body(1). It has been suggested that the formation and decay of low molecular weight RSNOs, such as S-nitrosoglutathione and S-nitrosocysteine, also represent a mechanism for the storage or transport of NO.(2) The determination of the electronic properties of simple thionitrites is an important task, because they serve as a model compounds for more complex species, especially in connection with the previously described biological importance. The main objective was the determination of their molecular and electronic properties. Thus, depending on their chemical stability, different approaches have been applied, including Gas Electron Diffraction and vibrational spectroscopy techniques. Moreover, the gas phase He(I) photoelectron spectrum (PES) of t-BuSNO has been measured. Here, we present the results of studies on the shallow-core electronic levels of thionitrites species (CH₃)₂CHSNO and (CH₃)₃CSNO. The dissociation process that dominates the RS–NO photolysis is mostly influenced by the electronic distribution around the sulfur atom as we conclude of the analysis to the sulfur 2p level, which could be studied by using the TGM beamline.

(1) Stamler, J. S.; Jaraki, O.; Osborne, J.; Simon, D. I.; Keane, J.; Vita, J.; Singel, D.; Valeri, C. R.; Loscalzo, J. PNAS 1992, 89, 7674-7677. (2) Gaston, B.; Reilly, J.; Drazen, J. M.; Fackler, J.; Ramdev, P.; Arnelle, D.; Mullins, M. E.; Sugarbaker, D. J.; Chee, C.; Singel, D. J. Proc. Natl. Acad. Sci. 1993, 90, 10957-10961.

X-ray absorption spectroscopy characterization of Zn_{1-x}Co_xO thin films applied as ozone gas sensors

Presenter: Catto A. C.

Catto A. C.*, Zanatta A. R. and Mastelaro V. R.

Instituto de Física de São Carlos
ade.catto@gmail.com

Zinc oxide (ZnO) pure or doped are one of the most promising metal oxide semiconductors for gas sensing applications due the well-known high surface-to-volume area and surface conductivity. It was show that ZnO is an excellent gas-sensing material for different gases such as CO, O₂, NO₂ and ethanol. In this context, pure and doped ZnO exhibiting different morphologies and a high surface/volume ratio can be a good option regarding the limitations of the current commercial sensors. Different studies showed that the sensitivity of metal-doped ZnO (e.g. Co, Fe, Mn,) enhanced its gas sensing properties. Motivated by these considerations, the aim of this study consisted on the investigation of the role of Co ions on structural, morphological and the gas sensing properties of nanostructured ZnO samples. In this work, we will present the results concerning the short-range order study of the Zn_{1-x}Co_xO (0 < x < 5 wt%) thin films deposited by means RF-magnetron sputtering. Their gas sensing properties were investigated by exposing the samples to different ozone levels (0.06-2.5 ppm). Electrical measurements indicated that the Co addition into the nanocrystalline ZnO samples favors the ozone gas sensor performance of the Zn_{1-x}Co_xO thin films. The Zn and Co K-edge X-ray absorption spectra of Zn_{1-x}Co_xO thin films were collected at the XAFS2 LNLS beam line in order to investigate the electronic structure around Zn and Co atoms. In the as-prepared samples, Zn and Co K-edge XANES measurements pointed out the presence of metallic Zn and Co state. The annealing treatment in oxygen-rich atmosphere improved the thin film oxidation with XANES reveling the presence of Zn(II) and Co(III) ions. Acknowledgements: This work was supported by Brazilian financing agencies FAPESP and CNPq.

- T. Jiang; D. E. Ellis. X-ray absorption near edge structures in cobalt oxides. J. Mater. Res., Vol. 11, n. 9, p. 2242-2256, 1996. - H. S. Al-Salman, et al. Structural, optical, and electrical properties of Schottky diodes based on undoped and cobalt-do

Iron altered oxidation energy due to Yttrium doping in Fe₃O₄ spinel ferrites

Presenter: Coelho L. N.

Coelho L. N.; Silva A. F.; Parise M.; P. C. Morais

Instituto de Física - UnB

lcoelho@fis.unb.br

Doping of spinel ferrite nanoparticles (NPs) alters significantly their magnetic response and other characteristics REF. Furthermore magnetic fluids made with yttrium (Y) doped NPs show high stability, remaining years without settling or flocculating. The precise character of Y doping effects on the NPs is yet to be fully understood. EXAFS measurements showed that Y occupy the tetrahedral site, entering the crystalline structure without causing much structural damage, as can be readily verified by X-Ray diffraction data. One hypothesis for enhanced colloidal stability in these ferrites revolves around the fact that these systems, in particular, are ionic colloids, without any surfactant molecule on the particle surface. The stability, in these cases, comes from electrostatic repulsion between particles, coated with charge of equal sign that repel each other efficiently. The charge is highly influenced by the system pH. In this work we will present X-Ray Photoemission Electrons spectroscopy measurements which strongly indicates that the Y-doping of the NPs favors Fe²⁺ oxidation into Fe³⁺ ions, consequently increasing the particle surface charge. This is readily perceived by Zeta-potential measurements of doped and undoped particles at the same pH. The Y-doped NPs presented a Zeta potential about 38% higher than the undoped sample. Since the zeta potential is derived from surface charge which is directly associated with colloidal stability this different oxidation energy detected by XPS may be the main cause of low flocculation and virtually no sedimentation in Y-doped ferrites.

XAFS characterization of Sr_{1-x}Cu_xTiO₃ and SrTi_{1-x}Cu_xO₃ perovskites applied to water-gas shift reaction

Presenter: Coletta V. C.

Coletta V. C.; Marcos F. C. F.; Nogueira F. G. E.; Bernardi M. I. B.; Assaf E. M.; Gonçalves R. V.; Mastelaro V. R.

São Carlos Institute of Physics, University of São Paulo; São Carlos Institute of Chemistry, University of São Paulo
viktor.coletta@usp.br

Strontium titanate (SrTiO₃) has a wide range of possible applications, including catalysis, due to its high stability and the possibility of incorporation of active metals into the perovskite structure by the partial substitution of strontium or titanium sites. Copper-containing catalysts are a low-cost alternative to noble metals, such as gold and platinum for the water-gas shift (WGS) reaction. However, there are no reports of the Sr_{1-x}Cu_xTiO₃ and SrTi_{1-x}Cu_xO₃ systems as catalysts for the WGS reaction to our knowledge. Thus, our research work consists in the synthesis and characterization of nanoparticles of Sr_{1-x}Cu_xTiO₃ and SrTi_{1-x}Cu_xO₃ aiming for the application of these materials as catalysts for the water-gas shift reaction. The synthesis was carried out through a modified polymeric precursors method, with calcination in an inert atmosphere followed by a treatment in oxygen to remove carbon, which resulted in particles with large area in comparison to the conventional calcination in air. We performed in situ X-ray diffraction and absorption experiments at Cu and Ti K-edge and fitted the EXAFS spectra to study the reducibility of copper. Our results showed the specific reduction of copper from 2+ to metallic state after a reducing treatment until 350°C, which was kept during the WGS reaction. The presence of metallic copper is related to the activity, which reached 74% of CO conversion for SrTi_{0.80}Cu_{0.20}O₃.

RATNASAMY, C.; WAGNER, J. P. Water-gas shift catalysis. *Catalysis Reviews: Science and Engineering*, v. 51, n. 3, p. 325-440, 2009.
MALUF, S. S. et al. Study of La_{2-x}Cu_xO₄ perovskites for the low temperature water gas shift reaction. *Applied Catalysis A: General*, v. 413-414, p. 85-93, 2012. DOI: [dx.doi.org/10.1016/j.apcata.2011.10.047](https://doi.org/10.1016/j.apcata.2011.10.047)
DA SILVA, L. F. et al. An improved method for preparation of SrTiO₃ nanoparticles. *Materials Chemistry and Physics*, v. 125, n. 1-2, p. 168-173, 2011.

Structural characterization of kraft lignin under different pH

Presenter: Dias O. A. T.

Dias O. A. T., Negrão D. R., Gandin C. A., Leão A. L., Neto M. de O.

Sao Paulo State University (UNESP)
otaviotd@gmail.com

Lignin is a biopolymer with high molecular weight which can be totally solubilized on alkaline pH. After that, its molecular structure became very reactive occurring rearrangement till its stabilization. Because of this, is appropriate to wait a time for its molecular stability, approximately one week (Maziero et al., 2012). In this assay, lignin was recovered by acidification of the Kraft black liquor (LNK) at two pH 3.0 and 5.0. 5 mg of each type of Kraft lignin were transferred to 1.5 mL microtubes and daily was added 1 mL of NaOH solution (0.1M) in each tube. Samples were prepared to be diluted for 10 days in duplicate. SAXS analyses provided different patterns in fractal order of lignin due to its structural reorganization mainly till 6th d. After 7th d of dilution, it was observed an increase of fractal complex these molecules for both lignins obtained at pH 3.0 and 5.0, indicating molecular stabilization. Both lignins suffered an increase in the Rg according to the dilution days, stabilizing at 8th d; same behaviour was observed with polydispersity. The size of Rg from lignin recovered at pH 3.0 was lower than lignin recovered at pH 5.0. Based on the obtained data, SAXS analysis contributed to the structural characterization of lignin obtained at two pH regarding to the size, shape and polydispersity.

MAZIERO, P., OLIVEIRA NETO, M., MACHADO, D., BATISTA, T., CAVALHEIRO, C. C. S., NEUMANN, M. G., CRAIEVICH, A. F., ROCHA, G. J. M., POLIKARPOV, I., GONÇALVES, A.R. Structural features of lignin obtained at different alkaline oxidation conditions from sugarcane bagasse. *Industrial Crops and Production*, v. 35, 61-69, 2012.

Photoionization dynamic of O-methyl dithiocarbonate (dimethyl xanthate), $\text{CH}_3\text{OC}(\text{S})\text{SCH}_3$, on the sulfur 2p absorption edge

Erben M. F., Cánneva A., Pirani L. S. R., Cavasso-Filho R. L., Védova C. O. D.

Xanthates (from the Greek “golden”) are the esters of xanthic acid, with general formula $\text{ROC}(\text{S})\text{SR}'$. These are important organosulfur compounds used in the production of cellophane and as flotation agents for extraction of metals from many ores. As an example, sodium ethyl xanthate is added as a collector in the selective flotation of PbS (galena) to separate it from ZnS (sphalerite). A series of xanthate and xanthogen derivatives are being the subject of investigation in our group, including synthetic aspects together with the elucidation of structural, conformational and vibrational properties.¹ Following our general project aimed at elucidating the shallow and inner-shell core electronic properties and photoionization dynamics of sulfur-containing derivatives,^{2,3} we became now interested in the simplest xanthate compound, with $\text{R}=\text{R}'=\text{CH}_3$. Here we report a study of the photon impact excitation and dissociation dynamics of $\text{CH}_3\text{OC}(\text{S})\text{SCH}_3$ excited at the S 2p level by using synchrotron radiation. Interestingly, the photoelectron spectrum of $\text{CH}_3\text{OC}(\text{S})\text{SCH}_3$ in the valence region (7.5-13 eV energy range) was reported by Guimon et al. in 1974 and interpreted in terms of ionization of non-bonded orbital mostly localized on the sulfur atoms.⁴ The S 2p core XPS and KLL Auger spectra of $\text{CH}_3\text{OC}(\text{S})\text{SCH}_3$ were early reported by Suoninen et al.⁵ showing that the ionization energies of the =S and –S– atoms within the xanthate group differ from each other by 1.5 eV, this difference assigned to the initial-state charge distribution rather than to final-state relaxation. In this presentation, the TTY spectra of $\text{CH}_3\text{OC}(\text{S})\text{SCH}_3$ following S 2p excitations is reported and compared with the previous data. The dissociative photoionization is discussed in term of PEPICO and PEPIICO spectra and possible fragmentations mechanisms are deduced from the interpretation of the PEPIICO spectra. Thus, the advantage of energy tunability offered by synchrotron radiation allowed us for a clear understanding of the resonant electronic processes occurring after excitation of each of the sulfur atoms present in this molecule and how the ionic dissociation is affected.

Juncal, L. C.; Tobon, Y. A.; Piro, O. E.; Della Vedova, C. O.; Romano, R. M. *New J. Chem.* **2015**, *38*, 3708.

Berrueta Martínez, Y.; Bava, Y. B.; Erben, M. F.; Cavasso Filho, R. L.; Romano, R. M.; Della Védova, C. O. *The Journal of Physical Chemistry A* **2015**, *119*, 1894.

Bava, Y. B.; Berrueta Martínez, Y.; Moreno Betancourt, A.; Erben, M. F.; Cavasso Filho, R. L.; Della Védova, C. O.; Romano, R. M. *ChemPhysChem* **2015**, *16*, 322.

Guimon, C.; Gonbeau, D.; Pfister-Guillouzo, G.; Åsbrink, L.; Sandström, J. *J. Electron Spectrosc. Rel. Phenom.* **1974**, *4*, 49.

Suoninen, E. J.; Thomas, T. D.; Anderson, S. E.; Runyan, M. T.; Ungier, L. *J. Electron Spectrosc. Rel. Phenom.* **1985**, *35*, 259.

Core-shell aggregates formed by polyion-surfactant complex salts: study of the internal liquid crystalline structures and stability

Presenter: Ferreira G. A.

Ferreira G. A., Carneiro N. M., Vitorazi L., Loh W.

Institute of Chemistry, University of Campinas
guilherme.ferreira@iqm.unicamp.br

We have studied the self-assembly of complex salts, formed by ionic surfactants and polyions, in aqueous solution, to yield different liquid crystalline phases. Our group investigated the phase behavior of hexadecyl (C16TA+) and dodecyltrimethylammonium (C12TA+) surfactants counterbalanced by poly(acrylate) homopolymer in water and in the presence of different alcohols [1,2]. It was possible to achieve different liquid crystalline phases (cubic, hexagonal and lamellar), depending on the surfactant chain length and the cosolute used. Recently, we have reported colloidal dispersions of core-shell aggregates formed by complex salts of poly(acrylate-*b*-acrylamide), PAA-*b*-Pam, polymers in which the cores displayed liquid crystalline structure with the same geometry as the ones observed for complex salts of the poly(acrylate) homopolymer [3]. We are now using the same approach of employing a complex salt of the block copolymer PAA-*b*-Pam and cationic C12TA+ and C16TA+ surfactants to prepare systems with adequate compositions to reproduce the above-mentioned phase diagrams attempting to obtain stable core-shell dispersions with the cores reproducing the phase structure observed in the previous studies. Preliminary results showed the presence of different liquid crystalline cores by adding different amounts of *n*-alcohols, in agreement with our previous reports using the complex salts prepared with the homopolymer. The poly(acrylic acid-*b*-isopropylacrylamide) (PAA-*b*-PNIPAm) polymer is also being used to analyze the effect of temperature, since PNIPAm has $T_{LCST} \sim 32^\circ\text{C}$. This system holding PNIPAm shows similar crystalline phases at 25°C and 45°C , although there is a small contraction of the core size related to the increase in the hydrophobicity of the PNIPAm chains and segregation of a concentrated phase. Attempts to stabilize the dispersion in water using a second complex salt of PAA-*b*-PEO are promising, once PEO has more affinity to water and no further changes were observed.

1. Bernardes, J. S.; Normman, J.; Piculell, L.; Loh, W. *Journal of Physical Chemistry B*, v. 110, p. 23433-23442, 2006. 2. Bernardes, J. S.; Loh, W. *Journal of Colloid and Interface Science*, v. 318, p. 411-420, 2008. 3. Vitorazi, L.; Berret, J-F.; Loh. *Langmuir*, v. 29, p. 14024-14033, 2013.

Analysis of the concentration of heavy metals in the polychaete using the TXRF technique on sandy beaches of the coast of São Paulo

Presenter: Freitas M. C. S.

Freitas M. C. S.¹, Yokoyama L. Q.¹, Ignacio B. L.¹, De Jesus. F. O.², Mársico E. T.³, Ribeiro R. de O. R.³, Barbosa R. de F.¹

¹ Instituto Saúde e Sociedade, Departamento de Ciências do Mar, Universidade Federal de São Paulo; Laboratório de Instrumentação Nuclear, COPPE/UFRRJ, ²CLAN - Laboratório de Controle Físico-Químico, UFF.
michellefreitas01@hotmail.com

The sediment tends to embody and accumulate contaminants poured in the water, in which become available for associated organisms. In this regard, benthic invertebrates such as polychaetes, which often use the sediment to obtain food or to construct protective tubes, are susceptible to the contamination by elements present in this environment. Thus, the present study examined the concentration of heavy metals in the species of polychaete *Dispio remanei* Friedrich, 1956 found at the beaches of Itararé (São Vicente) and Boracéia (Bertioga) and *Orbinia cf. johnsoni* Moore, 1909 in Araçá bay and Guaecá beach, both located in São Sebastião. The Araçá and Itararé are located very close to port areas, characterized by high urbanization and industrialization, thus existing possibilities of coastal marine environment being contaminated by heavy metals, that can have negative impacts on the biological, social and economic aspects. During periods of low tide, on each site, was delimited a quadrat area of 100 m², in which three points were randomly selected to obtain individuals *D. remanei* and *O. cf. johnsoni*. The material collected was analyzed by using the X-Ray Fluorescence by Total Reflection (TXRF) technique; it is possible to perform the correlation between essential and toxic elements in the body, through the issue of spectrum with energies characteristics of each metal. From procurement of different metal concentrations, comparisons of the mean concentrations between the beaches were conducted. Significant differences were identified for concentrations of Zinc with a higher concentration of the beach Boraceia regarding to the Itararé beach. This result was different than expected, because the beach Boraceia lies far from the places where this metal is used. For species *O. cf. johnsoni*, we identified a significant difference to the Fe element in the Bay of Araçá, which had a higher concentration than Guaecá Beach. This result was expected, since the Bay of Araçá is a receiving area of effluent contents, and it is also very close to the port of São Sebastião, as well as to the industries of the region. Both beaches showed significant differences for the element Potassium.

Present and future developments for UV-VUV science at LNLS

Presenter: Galante D.

Galante D.; Ambrosio C.¹; Sobolewski S.^{1,2}; Teixeira V.¹; Araujo W.¹

¹Brazilian Synchrotron Light Laboratory; ²Federal University of Sao Carlos
douglas.galante@lnls.br

In this work, recent advancements and future perspectives for the science done at the UV-VUV range at LNLS will be discussed. Currently, the TGM beamline of LNLS can operate from 3 to 330 eV (ca. 400 to 4 nm), and it is coupled to LNLS D05 (4°) bending magnet, which is one of the two bending magnets providing photons with energies below 100 eV. Its design aims to provide photon fluxes of up to 1E10 photons per second per mm² with moderate resolving power. Three toroidal gratings are used to efficiently cover the large energy range with the following specifications: A Pt coated grating with 75 grooves/mm and two 200 and 1800 grooves/mm. Their optimal energies range are from 3-13 eV, 12-100 eV, 100-330 eV respectively. TGM was the first beamline of LNLS to be built and installed, and it has been upgraded on the last few years to ensure competitive characteristics on its energy range. In fact, it is currently the sole synchrotron beamline operating at the UV-VUV on the Americas. Recent upgrades have included the change on the control system, installation of a new grating for low energies, automation of its gas filter for harmonics' suppression and improvement of monitoring and stability, as ongoing projects. Near-future developments include the installation of a photoemission microscope (PEEM), and the development of new experimental stations for circular dichroism (SRCD), measurement of optical properties of materials (luminescence, fluorescence, absorption) and gas-phase reactions. These new stations are being developed in collaboration with the users' community. With Sirius being built, we will also discuss the perspective of the installation of a UV-VUV beamline at it, in order to ensure that the current and future needs for experiments at this energy range are fulfilled on the best possible way.

Degradation of carotenoid of poly-resistant bacterium *Deinococcus radiodurans* on simulated environments with applications in astrobiology

Presenter: Gallo T. M.

Gallo T. M.¹; Rodrigues F.²; Simões F. V.³; Galante D.⁴

LNLS¹; UNESP-Rio Claro²
tamires.gallo@lnls.br

From the moment that an organism dies and is buried the original organic material tends to be lost being transformed into disorganized forms of carbon or in some cases mineralized. Organic molecules derived from the buried body can also be fossilized sometimes being the only trace of their existence. These are known as chemofossils or biomolecules that after burial and changes imposed by different geological processes exhibit changes in their structure, but also bringing characteristics of the original molecule which in some cases may contribute for the identification of the organism that originated the molecular signature. Chemofossils are also of interest in astrobiology since the conditions of fossilization in extraterrestrial environments similar to what eventually happens on Earth may have not favored the preservation of the body but only of its molecules. We used different mineral substrates mixed with the poly-resistant bacterium *Deinococcus radiodurans* for the study of the interaction of one chosen biosignature (carotenoids, present on this bacteria) for the preservation process. We prepared pellets of substrate with bacterium and irradiated them in three different environmental conditions with different doses: with a solar simulator (UVA/UVB), in Martian simulation with a specially designed chamber (AstroCam), and with UV-VUV for space simulation at the TGM beamline of LNLS. After these different simulations we used Raman spectroscopy with 532 nm and 785 nm excitations to analyze the degradation of the carotenoid. It was observed there is a reduction of the carotenoid Raman signal as function of the dose and there are significant differences when the sample is irradiated with different wavelengths and in different substrates. These results can contribute for a better interpretation of future data from Mars explorations missions, such as ExoMars (2018, ESA) and Mars2020 (2020,NASA), which will carry Raman spectrometers for the search for signals of life.

Parnell, J. et al. (2007) "Searching for life on Mars: selection of molecular targets for ESA's Aurora ExoMars Mission *Astrobiology*,7(4),pp.578-604. Brocks, J.J; Logan, G.A.; Buick, R.; Summons, R.E. 1999. Archean molecular fossils and the Early rise of Eukaryotes. *Science*, 285: 1033-1036. Cady, S.L.; Farmer, J.D.; Grotzinger, J.P.; Schopf, J.W.; Steele, A. 2003. Morphological biosignatures and the search for life on Mars. *Astrobiology*, 3(2): 351-368. Chosson, P.; Lanau, C.; Connan, J.; Dessort, D. 1991. Biodegradation of refractory hydrocarbon biomarkers from petroleum under laboratory conditions. *Nature*, 351: 640-642. [5] DesMarais, D.J.; Nuth III, J.A.; Allamandola, L.J.; Boss, A.P.; Farmer, J.D.; Hoehler, T.M.; Jakovsky, B.M.; Meadows, V.S.; Pohorille, A.; Runnegar, B.; Spormann, A.M. 2008. The NASA Astrobiology Roadmap. *Astrobiology*, 8(4): 715-730. Farmer, J.D.; DesMarais, D.J. 1999. Exploring for a record of ancient Martian life. *Journal of Geophysical Research*, 104 (E11): 26977-26995. H.G.M. Edwards, I.B. Hutchinson, R. Ingle, *Int. J. Astrobiol.* 2012, 11, 269. [8] Klein, H.P.; Farmer, J.D. 1995. Status of the search for life on Mars. *Progress in the Search for Extraterrestrial Life*, ASP Conference Series, 74: 65-71. L.W. Beegle, R. Bhartia, L. DeFlores, M. Darrach, R.D. Kidd, W. Abbey, S. Asher, A. Burton, S. Clegg, P.G. Conrad, K. Edgett, B. Ehlmann, F. Langenhorst, M. Fries, W. Hug, K. Nealon, J. Popp, P. Sobron, A. Steele, R. Wiens, K. Williford, SHERLOC: Scanning Habitable Environments With Raman & Luminescence for Organics & Chemicals, an Investigation for 2020., in *GeoRaman XI*. 2014: St. Louis, Missouri, USA. Olcott, A.N.; Sessions, A.L.; Corsetti, F.A.; Kaufman, A.J.; Oliveira, T.F. 2005. Biomarker evidence for photosynthesis during Neoproterozoic glaciation. *Science*, 310: 471-474.

Grazing-incidence X-ray scattering studies of myelin membranes at air/water interface

Presenter: Gasperini A. A. M.

Gasperini A. A. M.*¹; Puentes-Martinez X. E.^{1,2}; Pusterla J. M.³; Oliveira R.³; Cavalcanti L. P.¹

¹Brazilian Synchrotron Light Laboratory, CNPEM, CP 6192, CEP 13083-970, Campinas, Brazil; ²Instituto de Ciência e Tecnologia, UNIFESP, CEP 12231-280, São José dos Campos, Brazil; ³Departamento de Química Biológica - CIQUIBIC (CONICET), Facultad de Ciencias Químicas, Universidad Nacional de Córdoba, Argentina
*agasperini@lnls.br

Thin and ultrathin films in liquid surfaces and interfaces have been intensively studied in different domains such as pharmaceuticals, electronics, and food industry. These materials represent a model case to study the dynamical and structural properties of 2D confined soft matter. A very interesting class of ultrathin films is given by the Langmuir monolayers, which are monomolecular layers of amphiphilic molecules spread on air/water interfaces, since they can represent a model for biological systems. Langmuir monolayers formed by myelin lipids or full myelin membranes offer advantageous features to approach the exploration of the surface properties of a complex lipid-protein interface since they contain all the components of natural membranes[1]. Surface-sensitive synchrotron-based X-ray scattering techniques such as grazing-incidence diffraction (GID) and scattering (GISAXS/GIXOS) are powerful tools for investigating the molecular structure of organic films on liquid surfaces due to the penetrating properties of the X-rays and the ability to couple structural and dynamical properties of interfaces with nanoscale resolution[2]. We present in this work the first results of a surface-sensitive X-ray scattering experiment performed at LNLS/XRD-2 beamline[3]. We used this technique to study Langmuir monolayers formed by myelin lipids and full myelin membranes as a function of the monolayer surface pressure. The new experiment opens new possibilities for the soft condensed matter community in Brazil. The structural study as a function of the change of preparation conditions and thermodynamical parameters make this kind of experiment ideal for many technological and industrial applications. AAMG, RGO and LCP acknowledge grants from FAPESP. XPM thanks to CNPq.

[1] Rosetti, C. et al. BBA - Biomemb.(2008) 1778, 1665; [2] Dai, Y. et al. J. Appl. Phys. (2011) 110, 102213; [3] Vieira, C. et al. J. Synch. Rad. (2015) 22, 859;

Magnetic moment of Fe₃O₄ films with thicknesses near the unit-cell size

Presenter: Gomes G. F. de M.

Gomes G. F. M.^{1,*}, Bueno T. E. P.¹, Parreiras D. E.¹, Abreu G. J. P.², De Siervo A.², Cezar J. C.³, Pfannes H.-D.¹ and Paniago R.¹

¹*Departamento de Física, ICEx, Universidade Federal de Minas Gerais, 31270-901 Belo Horizonte, MG, Brazil;* ²*Instituto de Física Gleb Wataghin, Universidade Estadual de Campinas, 13083-859 Campinas, SP, Brazil;* ³*Laboratório Nacional de Luz Síncrotron, C.P. 6192, 13083-970 Campinas, SP, Brazil*
gustavofmg@gmail.com

There is a large scientific and technological interest in magnetic materials in ultrathin film form due to the anisotropy created by the low dimensionality which can change physical properties. Magnetic and structural properties of ultrathin iron oxides composed of less than 10 atomic layers are poorly understood [1-4]. The magnetic spin moments for ultrathin magnetite as determined experimentally by various groups [1-3,5] present much lower values than the bulk spin moment, which is very intriguing. Another open question is what is the lowest thickness required to maintain the bulk ferrimagnetic order at room temperature. We have followed the evolution of the magnetic moment of ultrathin Fe₃O₄ as a function of the thickness (8–45 Å) in the [100] and [111] crystallographic directions. The stoichiometry and surface quality of the films have been attested by X-Ray absorption spectroscopy (XAS), X-Ray magnetic circular dichroism (XMCD), and low-energy electron diffraction (LEED). The XMCD study were performed at the PGM beam line at the Laboratório Nacional de Luz Síncrotron (LNLS). The results show that at low thicknesses, FeO has probably been formed and evolved to Fe₃O₄ above the thickness of 1 unit cell. For both the [100] and the [111] orientations we observe a characteristic dichroic signature of magnetite around the unit-cell thickness, however, with a lower spin moment that evolves to the bulk value for thicker films. A spin moment of 3.6 μB/f.u. was found at 35 Å thickness for Fe₃O₄ [111] [6]. These results are direct evidence that both the ferromagnetic order and the bulk moment value are preserved at room temperature around the thickness of 2 unit cells. We have also shown that even 10-Å-thick magnetite already presents a significant magnetic moment. We believe that the conclusions of this work are of great importance, especially if magnetite layers down to subnanoscale thickness are employed in spin electronics devices.

[1] J.Orna, P. A. Algarabel, L. Morellón, J. A. Pardo, J. M. de Teresa, R. López Antón, F. Bartolomé, L. M. García, J. Bartolomé, J. C. Cezar, and A. Wildes, *Phys. Rev. B* 81, 144420 (2010). [2] V. Hari Babu, R. K. Govind, K.-M. Schindler, M. Welke, and R. Denecke, *J. Appl. Phys.* 114, 113901 (2013). [3] J.-B. Moussy, S. Gota, A. Bataille, M.-J. Guittet, M. Gautier-Soyer, F. Delille, B. Dieny, F. Ott, T. D. Doan, P. Warin, P. Bayle-Guillemaud, C. Gatel, and E. Snoeck, *Phys. Rev. B* 70, 174448 (2004). [4] P. Morrall, F. Schedin, S. Langridge, J. Bland, M. F. Thomas, and G. Thornton, *J. Appl. Phys.* 93, 7960 (2003). [5] W. Q. Liu, Y. B. Xu, P. K. J. Wong, N. J. Maltby, S. P. Li, X. F. Wang, J. Du, B. You, J. Wu, P. Bencok, and R. Zhang, *Appl. Phys. Lett.* 104, 142407 (2014). [6] G. F. M. Gomes, T. E. P. Bueno, D. E. Parreiras, G. J. P. Abreu, A. de Siervo, J. C. Cezar, H.-D. Pfannes, and R. Paniago, *Phys. Rev. B* 90, 134422 (2014).

X-ray crystallographic structure of a transcriptional activator of virulence factor in enterococcus faecalis, ELRR.

Presenter: De Groot M. C. R.

De Groot, M. C. R.¹; Camargo, I.¹; Repoila, F.²; Serrão, P.²; Horjales, E.¹

¹Institute
horjales@ifsc.usp.br

RNPP family of transcriptional regulators is present exclusively in Gram positive bacteria and regulates factors involved in virulence, invasion, biofilm formation, etc. That family shares structure, functions and also the regulation by peptides. ElrR protein is a transcriptional regulator of Rgg family, that positively regulates ElrA, which is a virulence factor of *Enterococcus faecalis*. Rgg family was proposed to belong to RNPP family. Here we present the crystallographic structure of APO ElrR obtained at 2.15 Å resolution. We solved the phase problem using diffraction data at 2.55 Å resolution of Se-Met-ElrR crystals measured on the absorption edge ($\lambda=0.979096$ Å) of Selenium atoms, collected at LNLS Synchrotron, Brazil. We then improved the resolution using a dataset obtained at home ($\lambda=1.5418$ Å) which diffracted at 2.15 Å resolution. This structure was refined to Rwork 0,2024 e Rfree 0,258. Crystals presented space group P1 with crystallographic cell a 70.800 b 75.330 c 85.280 α 112.99 β 89.93 γ 103.88 which contains two homodimers. The crystallographic model has shown the same fold in ElrR as PgrX and RGG2sd structures, in spite of the low sequence identity (under 13% in all cases). The structure presents a helix-turn-helix XRE-type domain on the N-terminal, a 5-helix central domain and a C-terminal domain build of tetratricopeptides (TPR)-like repetitions. The interface between the Central and the C-terminal domains contains the allosteric site, like in distant homologous proteins of the RNPP family, but the cleft on the allosteric site in ElrR is wider. Then, ElrR ligand can be bigger than those found in these homologous structures.

1- Dumoulin R, et al: Enterococcal rgg-like regulator elrr activates expression of the elra operon. *Journal of Bacteriology* (2013) 195:(13):3073–3083. 2- Chaussee MS, et al: Rgg coordinates virulence factor synthesis and metabolism in *Streptococcus pyogenes*. *Journal of Bacteriology* (2003) 185(20):6016–6024. 3- Brinster S, et al: Enterococcal leucine-rich repeat-containing protein involved in virulence and host inflammatory response. *Infection and Immunity* (2007) 75(9):4463–4471.

Electronic Structure of $\text{SrTi}_{1-x}\text{Ru}_x\text{O}_3$

Presenter: Guedes E. B.

Guedes E. B.*; Abbate M.; Abud F.; Jardim R. F.; Mossaneck R. J. O.

Universidade Federal do Paraná; Universidade Federal do Paraná; Universidade de São Paulo; Universidade de São Paulo; Universidade Federal do Paraná
guedes@fisica.ufpr.br

Metal-insulator transition (MIT) is an intriguing phenomenon in transition metal oxides that can have different driving forces, such as electron correlation, disorder or percolation. The $\text{SrTi}_{1-x}\text{Ru}_x\text{O}_3$ (STRO) series undergoes a MIT for $x_c \sim 0.35$. The end members of the series show completely different physical properties: SrTiO_3 (STO) is a diamagnetic band insulator with cubic structure, whereas SrRuO_3 (SRO) is an itinerant ferromagnet with an orthorhombic structure. The electronic structure of the STRO series has been studied via electrical conductivity measurements [Phys. Rev. B **62**, 10785 (2000)], X-ray photoemission and x-ray absorption spectroscopies [Eur. Phys. J. B **25**, 203 (2002), Phys. Rev. B **73**, 235109 (2006)], band structure calculations [Phys. Rev. B **77**, 085118 (2008), Phys. Rev. B **77**, 212407 (2008)] and other techniques. Despite the efforts, the mechanism leading to the transition in this system is still under debate. Previously, a study on SRO where several spectroscopic measurements were interpreted via an extended cluster model [Phys. Rev. B **86**, 235127 (2012)] showed that the ground state of this material is dominated by configurations with holes in the ligand band. Now, in order to study the electronic structure of the STRO series, we developed and implemented a double cluster model, in which two octahedra are connected via an oxygen atom. The model includes correlation, covalence and multiplet effects, as well as charge fluctuations between the two octahedra. The results are compared with X-ray Photoemission Spectroscopy from the literature, and all the spectra were reproduced with a single set of parameters.

[1] R. F. Bianchi et al., Phys. Rev. B **62**, 10785 (2000). [2] M. Abbate et al., Eur. Phys. J. B **25**, 203 (2002). [3] J. Kim et al., Phys. Rev. B **73**, 235109 (2006). [4] K. Maiti, Phys. Rev. B **77**, 212407 (2008). [5] E. B. Guedes et al., Phys. Rev. B **86**, 235127 (2012).

Structure, activity and reaction mechanism of NahK and its complex with NahL

Presenter: Guimarães S. L.

Guimarães S. L., Coitinho J. B., Costa D. M. A., De Araújo S. S., Whitman C. P., Nagem R. A. P.
Universidade Federal de Minas Gerais, University of Texas
rapnagem@yahoo.com.br

Among all types of toxic Polycyclic Aromatic Hydrocarbons (PAHs), naphthalene is the most studied and a model compound. Its degradation by the bacteria *Pseudomonas putida* is the focus of numerous studies. In this organism, two consecutive pathways are able to convert naphthalene to pyruvate and acetyl-CoA. In the lower pathway, the enzymes NahK (4-oxalocrotonate decarboxylase) and NahL (vinylpyruvate hydratase) catalyze an interesting sequence of reactions that raise a number of mechanistic and structural questions. In this work we aim to characterize kinetically and structurally the NahK enzyme expressed without NahL, and also both enzymes co-expressed as a complex. The nahK gene was subcloned into pET28a-TEV vector for expression, and also along with nahL gene into pETDuet-1 vector for co-expression in *Escherichia coli* BL21(DE3) cells. The protein samples were analyzed by Dynamic light scattering, Circular dichroism, and the steady-state kinetic values for their natural substrates were obtained. The NahK/NahL complex was also analyzed by Small-angle X-ray scattering. NahK and NahK/NahL samples in their apo or ligated forms with different ligands were crystallized and X-Ray diffraction data were collected. NahK expressed alone and co-expressed with NahL was purified to homogeneity and both enzymes show k_{cat}/K_m values up to 10^7 M⁻¹ s⁻¹. The crystalline structures of NahK in apo and ligated forms with Mg²⁺ and substrate analogues allowed us to propose a dynamic reaction mechanism involving a lid domain. SAXS measurements suggested a particle of 240 kDa for NahK/NahL complex, and the crystalline structure of this complex confirmed a heterodecamer assembly. NahK and NahL face their active site cavities to each other into a large, elegant and functional quaternary structure. Our work provided a deep structural and functional understanding of this interesting protein complex.

[1] W.M. Baird, L.A. Hooven, B. Mahadevan, *Environ Mol Mutagen*, 45 (2005) 106-114. [2] M. Sota, et al., *J Bacteriol*, 188 (2006) 4057-4067. [3] S. Harayama, M. Rekik, K.L. Ngai, L.N. Ornston, *J Bacteriol*, 171 (1989) 6251-6258. [4] W.L. Collinsworth, P.J. Chapman, S. Dagley, *J Bacteriol*, 113 (1973) 922-931. [5] H. Lian, C.P. Whitman, *Journal of the American Chemical Society*, 116 (1994) 10403-10411. [6] S. Kim, O.K. Kweon, Y. Kim, C.K. Kim, K.S. Lee, Y.C. Kim, *Biochem Biophys Res Commun*, 238 (1997) 56-60. [7] E.A. Burks, W.H. Johnson, C.P. Whitman, *Journal of the American Chemical Society*, 120 (1998) 7665-7675. [8] T.M. Stanley, W.H. Johnson, Jr., E.A. Burks, C.P. Whitman, C.C. Hwang, P.F. Cook, *Biochemistry*, 39 (2000) 3514. [9] W.H. Johnson, Jr., S.C. Wang, T.M. Stanley, R.M. Czerwinski, J.J. Almrud, G.J. Poelarends, A.G. Murzin, C.P. Whitman, *Biochemistry*, 43 (2004) 10490-10501.

Au / Ag nanowires atomic distribution revealed by XAFS

Presenter: Herrera F. C.

Herrera, F. C.¹; Giovanetti L. J.¹; Gutiérrez-Wing, C.²; Requejo F. G.¹

¹Instituto de Investigaciones Fisicoquímicas Teóricas y Aplicadas, CONICET y Universidad Nacional de La Plata; ²Instituto Nacional de Investigaciones Nucleares, Carr. México-Toluca S/N La Marquesa, Ocoyoacac, Edo. de México C. P. 52750, México
herrera.facundo@gmail.com

Nanowires which were defined as having at least two dimensions between 1 and 100 nm, have received a great interest due to their unique optical, electrical, magnetic, and thermal properties with dimensionality and size confinement [1-4]. The intrinsic properties of nanowires are mainly determined by its size and composition. To study the size dependent properties, it is the crucial task to synthesize size-controlled nanowires. In order to investigate the local and electronic structure of Ag-Au(1-D) nanowires we perform a comprehensive study by XAFS in the Au-L3, Ag-L23 and Ag-K edges of isolated Ag-Au(1-D) nanowires with different Au:Ag molar ratio. Ag-Au(1-D) nanowires were synthesized by a method of colloid chemistry in a first stage (Ag), followed by a galvanic reaction to incorporate the second metal in the structure (Au). Au L3 EXAFS data shows that every Au atom, independently of the Au:Ag molar ratio, are incorporated in the Ag lattice surrounded by 8 and 4 Au and Ag atoms respectively. Ag K EXAFS data analysis shows that depending on the Au:Ag molar ratio the Ag atoms change their environment. This result is also supported by Ag L23 XANES data that shows different hole density in the Ag 4d level depending on the Ag-Au(1-D) nanowires stoichiometry.

1 - Y. Wu, J. Xiang, C. Yang, W. Lu, C. M. Lieber, Nature, 430 7000 704-704, 0028-0836, (2004) 2 - A. P. Alivisatos, P. F. Barbara, A. W. Castleman, J. Chang, D. A. Dixon, M. L. Klein, G. L. Mc Lendon, J. S. Miller, M. A. Ratner, P. J. Rossky. Advanced Materials, 10 16 1297-1336, 0935-9648, (1998). 3 - Z. L. Wang. Advanced Materials, 12 17 1295-1298, 0935-9648, (2000) 4 - Y. G. Sun, B. T. Mayers, Y. N. Xia. Nano Letters, 2 5 481-485, 0028-0836, (2002)

Python as a tool for analyze X ray small angle scattering data

Presenter: Huck-Iriart C.

Huck-Iriart C.*; Giovanetti L. J.

Instituto de Investigaciones Físicoquímicas Teóricas y Aplicadas, UNLP, La Plata, Argentina
chuck@inifta.unlp.edu.ar

Small angle x-ray scattering (SAXS) analysis requires several numerical steps to be done, starting from data reduction to data interpretation (physical models, invariants calculations, etc). All of these steps must be done in order to squeeze the information obtained by [1]. In the last decade they began to appear few user friendly programs available which allow doing a full data analysis [2]. Nevertheless, some of those software packages are useful to analyze simple systems or to perform a set of predetermined routines for SAXS data analysis. Other programs let users to write new functions or adding in-house written plug-ins. Those types of packages allow a complete and flexible analysis of the experimental data but at the expense of learning a specific programming language. Python is a general purpose, high level programming language with a coding syntax very easy to learn and is not restricted only to scientific computation. Language features and a small set of core packages includes: NumPy (mathematical arrays), SciPy (linear algebra, differential equations, signal processing and more), SymPy (symbolic mathematics), matplotlib (graph plotting), etc; turns Python into a very popular programming choice in the scientific community [3]. The main aim of this contribution is to introduce Python to the general user and to show some of its capabilities applied to the particular case of SAXS data analysis including a full pixel GISAXS image analysis and a few tricks to speed up computer calculations.

[1] Glatter, O.; Kratky, O. "Small Angle X-ray Scattering", Academy Press, 1982 [2] see for example <http://smallangle.org/content/software> [3] Perkel, J.M. Nature, 2015, 518, 125-126

Real Time Monitoring Nanoparticles Distance and Structure upon Different Variables.

Presenter: Ibañez F. J.

Ibañez F. J., Dalfovo M. C.¹, Stanic V.², Requejo F. G.¹, Giovanetti L. J.¹, Iriart C. H.¹

¹ Instituto de Investigaciones Fisicoquímicas, Teóricas y Aplicadas (INIFTA). Universidad Nacional de La Plata - CONICET. Sucursal 4 Casilla de Correo 16 (1900) La Plata, Argentina. ² Laboratório Nacional de Luz Síncrotron-LNLS. Centro Nacional de Pesquisa em Energia e Materiais – CNPEM. Rua Giuseppe Máximo Scolfaro, 10.000 - CP 6192 13083-970 - Campinas, SP – Brazil
fiban@inifta.unlp.edu.ar

The nanoparticles (NPs) separation, order, and structure play a crucial role not only in fundamental science but also, in the applied field such as in chemiresistors, localized surface plasmon resonance (LSPR), and surface-enhanced Raman scattering (SERS) for just mention a few. For instance, as long as a metal nanoparticle (Ag or Au) approaches another metallic center, electromagnetic waves are enhanced leading to an improved SERS or LSPR effect. We recently showed, via GISAXS experiments, that organic-coated NPs change their interparticle distance and film structure upon the exposure to volatile organic compounds (VOCs) and dithiols (nonanedithiol) place-exchange.[1] These results can be correlated with changes in current in chemiresistors. In this presentation I will show the importance of the film (NPs film) deposition method and type of organic coating needed for obtaining correlation. I will also discuss how inter-nanoparticles distance and film correlation changes upon different organic coatings (surrounding NPs), substrate type (graphene vs. silicon) increasing temperature, and addition of dithiols.[2]

[1] Dalfovo, et al, and Francisco J. Ibañez*. Real-time Monitoring Distance Changes in Surfactant-coated Au Nanoparticle Films upon Volatile Organic Compounds (VOCs). J. Phys. Chem. C 2015, 119, 5098–5106 [2] Proposal 17155-2014: Dithiols as molecular rulers: the importance of metal nanoparticles separation and graphene towards surface enhanced Raman scattering (SERS).

Spectroscopic Techniques on the Study of Biosignatures: Degradation of the Heme Group under Environmental Stress

Presenter: Junior J. C. S.

Junior J. C. S.^{1,2}; Rodrigues F.³; Puglieri T.³; Galante D.¹

¹Brazilian Synchrotron Light Laboratory; ²Unicamp; IQ-USP³
jose.salles@lnls.br / juniorsalles@msn.com

This study aims to examine preservation and degradation processes of biologically important molecules by spectroscopic techniques. The biomolecule model adopted as biosignature is the class of the porphyrins in their native as well degraded form (particularly the heme group), as this is an ubiquitous molecule on life as we know, and very resilient to degradation on the environment. The analysis of the degradation of heme group is mainly made by the study of the central metal ion behavior, through XANES, and neighboring chemical groups, by molecular spectroscopy techniques - Raman and Infrared. Our initial goal is to better understand the alterations suffered by the central metal ion after being exposed to simulated environmental stress, especially in which conditions the ion substitution happens. This may provide a diagnostic tool to infer the paleoenvironment from a measured substitution rate on fossil porphyrins. Simulations of extreme conditions (such as of the surface of Mars and extreme terrestrial environments), with varying pressure, temperature and incidence of electromagnetic radiation in different energy ranges are being performed in order to improve our understanding of the behavior of the molecules and to test their endurance. An interesting characteristic of porphyrins is the diversity of metal ions that can bind at its center, as in the heme (Fe) and chlorophyll (Mg), which can be replaced by geochemical processes. An example is the change of Fe by V in the heme group. The initial experiments were performed in aqueous media, in which the heme is not soluble, but some vanadium salts are, such as vanadium(III) chloride - VCl₃, which is soluble in hydrochloric acid, in which heme is not. Using X-ray Absorption Spectroscopy - XAS (in particular XANES), it was possible to assess the substitution grade, the oxidation state and chemical neighborhood of the central metal ion of heme in the native or degraded forms, as well as in contact with the vanadium solution. Within this scope, synchrotron based XAS is a powerful tool for the characterization of the results of the simulations, as well as for direct measurement of environmental samples containing preserved porphyrin groups. Practically without any need of special sample preparation or environmental simulations, in the first case due to the high brightness of the source and the second energy range and because of flow that can subjecting the sample.

X-ray back-diffraction pointing to a target soft inelastic X-ray scattering spectrometer

Presenter: Kakuno E. M.

Kakuno E. M.¹, Hönnicke M. G.², Conley R.³, Cusatis C.⁴, Zhou J.⁵, Bouet N.⁵, Marques J. B.⁶, Vicentin F. C.⁶

¹Universidade Federal do Pampa, ²Universidade Federal da Integração Latino-Americana, Advanced Photon Source, ³Argonne National Laboratory, ⁴Universidade Federal do Paraná, National Synchrotron Light Source II, ⁵Brookhaven National Laboratory, Laboratório Nacional de Luz Síncrotron, ⁶Centro Nacional de Pesquisa em Energia e Materiais
edsonmk2004@yahoo.com

Soft X-ray back-diffraction (SXBD), X-ray diffraction at angles near and exactly equal to 90° at low energies (~ 3.2 keV) was carried out at Soft X-rays Spectroscopy (SXS) beamline at Laboratório Nacional de Luz Síncrotron (LNLS) [1]. A high-resolution Si(220) multi-bounce back-diffraction monochromator was designed and constructed for this experiment. An ultra-thin Si(220) crystal (5 μm thick) was used as the sample. This ultra-thin crystal was characterized by profilometry, rocking-curve measurements and X-ray topography prior to the XBD measurements. It is shown that the measured forward-diffracted beam (o-beam) profiles, taken at different temperatures, are in close agreement with profiles predicted by the extended dynamical theory of X-ray diffraction (2-beam case), with the absence of multiple-beam diffraction (MBD). This is an important result for future studies on the basic properties of back-diffracted X-ray beams at energies slightly above the exact XBD condition (extreme condition where XBD is almost extinguished). Also, the results presented here indicate that stressed crystals behave like ideal strain-free crystals when used for low-energy XBD. This is mainly due to the large widths of SXBD profiles, which lead to a low strain sensitivity in the detection of defects. This result opens up new possibilities for mounting spherical analyzer crystals without degrading the energy resolution, at least for low energies. With these results we aspire to build a soft inelastic X-ray scattering spectrometer, where experiments such as element-specific magnetic imaging tools [2] could be explored.

[1] Hönnicke M.G., Conley, R., Cusatis, C., Kakuno, E. M., Zhou, J., Bouet, N., Marques, J. B., Vicentin, F. C. J. Appl. Cryst. 47 16581665, 2014. [2] Mentès, T. O., Sanchez-Hanke, C. & Kao, C. C. J. Synchrotron Rad. 9, 90–95, 2002.

Influence of the nanoparticle concentration on the magnetic and structural properties in Fe₃O₄-PVA nanocomposites

Presenter: Londoño O. M.

Moscoso-Londoño O.¹; Tancredi P.¹; Muraca D.; Knobel M.²; Wolff U.³; Damm C.⁴; Neu V.³; Rellinghaus B.⁴; Socolovsky L. M.¹

Laboratorio de Sólidos Amorfos (LSA), INTECIN, Facultad de Ingeniería, Universidad de Buenos Aires - CONICET, C1063ACV Buenos Aires, Argentina; Laboratorio de Materiais e Baixas Temperaturas (LMBT), Instituto de Física Gleb Wataghin, Universidade Estadual de Campinas, Cep 13083-859 Campinas-Sp, Brasil; Department of Magnetic Microstructures, Leibniz Institute for Solid State and Materials Research Dresden, Helmholtzstraße 20, 01069 Dresden, Germany; IFW Dresden, Institute for Metallic Materials, Dresden, Germany
omoscoso@fi.uba.ar

Our aim is to design magnetic nanocomposites in which the dipolar inter-nanoparticles interactions can be tuned. To achieve this, a set of magnetic gels were synthesized, with different nanoparticle concentrations. Polyvinyl alcohol (PVA) was chosen as a containing non-magnetic matrix due to its biocompatible properties. To ensure a correct dispersion of the fine particles within the PVA matrix, these were coated with citric acid (CA), thus the hydrogen bonds formed between the carboxylic (CA) and hydroxyl (PVA) groups promotes a better dispersion and prevent percolation of the nanoparticles [1]. Magnetic results indicated that when the nanoparticles concentration rises, a shift in the blocking temperature (TB) towards higher values is observed. According to the superparamagnetic theory, such behavior is related to an increase in the magnetic anisotropy of the system [2] or an increase in dipolar magnetic interaction between nanoparticles [3]. To discard any structural distortion in the internal structure of the nanoparticles, which could lead to changes in the magnetic anisotropy of the studied systems, we decided to carry out measures of X-ray absorption fine structure (EXAFS and XANES). XAFS results are indicating that the internal structure of the NPs is not affected by the increase in nanoparticle concentration (or inter-nanoparticles interactions). Changes in TB, and in magnetic properties in general are associated with the increase in magnetic interactions, possibly due to the formation of non-compact aggregates. In order to confirm this hypothesis, were performed measures of small angle X-ray scattering (SAXS). SAXS experimental data were fitted using the expression postulated in fractal aggregate model [4]. Fitting results suggest that the increase in the nanoparticle concentration promotes the formation of denser and compact aggregates. We acknowledge the support of CONICET and ANCPyT (Argentina); LNLS, FAPESP and UNICAMP (Brasil); and IFW (Germany).

[1]. O. Moscoso-Londoño, J. S. Gonzalez, D. Muraca, C. E. Hoppe, V. A. Alvarez, A. López-Quintela, L. M. Socolovsky, and K. R. Pirota. Structural and magnetic behavior of ferrogels obtained by freezing thawing of polyvinyl alcohol / poly (acrylic acid) (PAA) – coated iron oxide nanoparticles. *European Polymer Journal*, 49, (2013), 279–289. [2]. M. Knobel, W. C. Nunes, L. M. Socolovsky, E. De Biasi, J. M. Vargas, and J. C. Denardin. Superparamagnetism and other magnetic features in granular materials: a review on ideal and real systems. *Journal of Nanoscience and Nanotechnology*, 8, 2008, 2836–2857. [3]. J. M. Vargas, W. C. Nunes, L. M. Socolovsky, M. Knobel, and D. Zanchet, Effect of dipolar interaction observed in iron-based nanoparticles. *Physical Review B*, 72, (2005), 184428. [4]. Sow-Hsin Chen and Jose Teixeira. Structure and Fractal Dimension of Protein-Detergent Complexes. *Physical Review Letters*, 57, 20, 1986.

Solving the structure of bimetallic particles with EXAFS

Presenter: López J. M. R.

Ramallo-López J. M.; Mizrahi M.; Giovanetti L. G.; Krylova G.; Béron F.; Pirota K.; Shevchenko E.; Requejo F. G.

Instituto de Investigaciones Fisicoquímicas, Teóricas y Aplicadas (INIFTA), Universidad Nacional de La Plata - CONICET, Suc. 4 C. C. 16 (1900) La Plata, Argentina; Center for Nanoscale Materials, Argonne National Laboratory 9700 South Cass Avenue, Building 440 Argonne, IL 60439 USA; Laboratório de Materiais e Baixas Temperaturas, Universidade Estadual de Campinas (UNICAMP), São Paulo, Brasil
ramallolopez@gmail.com

We resolved the structure of core-shell bimetallic Co-Pt nanoparticles using Extended X-ray Absorption Fine Structure (EXAFS) spectroscopy at the Co-K and Pt-L3 edges. Using the results of the EXAFS fits at both edges and theoretical models we could determine the core and shell composition as well as the inner and outer radius of two different bimetallic nanoparticles obtained varying the synthesis conditions. The only compatible structure with our results is a CoPt₃@Pt core-shell nanoparticle. Our models are supported by X-ray fluorescence, Transmission Electron Microscopy and Small Angle X-ray Scattering results.

XANES and micro-XRF spectroscopies for chemical characterization of fossil samples

Presenter: Maldanis L.

Maldanis L.*; Perez C. A.; Lima F. A.; Rodrigues F.; Galante D.; Xavier-Neto J.

Brazilian Synchrotron Light Laboratory; Brazilian Biosciences National Laboratory; Chemistry Institute, University of São Paulo.
lara.maldanis@lnls.br

The application of novel analytical techniques to study fossils is enabling new and more sophisticated scientific problems to be attacked in paleobiology, both in morphology and chemical composition of the specimens and of the surrounding rock matrix, with none or minimum damage to the sample. Particularly, micro-X-Ray Fluorescence spectroscopy can be applied onto chemical mapping of paleontological specimens, allowing the correlation of chemical findings with morphological features, which can provide a range of information about biochemical preservation of the specimen structures and also about the fossilization process. We applied micro-X-Ray Fluorescence in fossil fishes from the Cretaceous Santana Formation of North-East Brazil and in fixed and resin-included Zebrafish samples, to analyze and correlate the distribution of the elements, that could be associated with biological or diagenetic origin. We also applied XANES spectroscopy to better characterize the iron minerals of the fossil and its matrix, besides look for possible remains of hemoglobin preservation. Our results show the association of elements as iron and zinc with specific structures as bones, gastrointestinal tract and scales, both in the fossil and Zebrafish samples. Other elements, as manganese, appears as a diagenetic marker, distributed nonspecifically in the fossil. We can also observe rare-earth elements as neodymium associated to geochemically modified apatite. XANES spectroscopy of iron showed a clear contribution of pyrite in the matrix and some regions of the fossil sample, but could not identify hemoglobin traces in the fossil sample, probably because of the very low (if present) concentration of this kind of iron among the iron minerals of the sample.

Trace elements alterations in mammary cells exposed to doses used in mammograms – an investigation using TXRF

Presenter: Mantuano A.

Mantuano A.^{1*}; Mota C. L.²; Pickler A.²; Machado S. C. F.³; Salata C.³; De Almeida C. E.³; Braz D.²; Barroso R. C.¹

¹LabFisMed - Physics Institute (University of State of Rio de Janeiro) – RIO DE JANEIRO – BRAZIL;

²Nuclear Instrumentation Laboratory (COPPE/Federal University of Rio de Janeiro) – RIO DE JANEIRO – BRAZIL; ³Laboratory of Radiological Sciences (State University of Rio de Janeiro) – RIO DE JANEIRO – BRAZIL

mantuanoandrea@gmail.com

The developments in the diagnosis, and treatment techniques for the breast cancer (BC), which include chemotherapy and/or radiotherapy, increased the patients survival rates for this type of cancer, increasing the chances of late effects due to the treatment. A mammogram is an exam that uses ionizing radiation and aims to obtain radiographic images of the breast for the detection of early stages breast cancer. Considering that during interaction of the radiation with the mammary tissue, important biomolecules ionization and subsequent destabilization may occur, the use of ionizing radiation in health care must be justified (1-5). Most studies concerning the effects using low dose radiation focus, mainly, the alterations in the DNA molecule (6-8). Elemental alterations may be associated with changes in the enzymatic activities of the cell. Our purpose was to quantify the trace elements in the two different cell lines: human breast tumor cells MCF-7 and non-tumor cells MCF-10 after the exposure of doses used for mammograms, considering low breast density (9 mGy) and high breast density (18 Gy), subjected to doses used in mammography and compare the results between those groups. Our study indicated some changes in the concentration of certain elements such as Ca, Fe, Cr and Zn in different tumor cell lines, after different treatments, using the TXRF method. We are trying to identify the potential mechanism of how ionizing radiation can activate cellular targets associated with tumor progression (9-12). MCF-7 and MCF-10 cells were irradiated with doses of 17 mGy and 2Gy in a conventional mammography equipment (Siemens). From the resulting solutions, 5 μ L were pipetted on the quartz reflectors used for TXRF analysis. These results can help us to better understand the mechanisms involved in the neoplastic transformations, enzymatic alterations, and biomolecules destabilization that may occur after a breast screening.

(1) Olive PL. *Mutat Res.* 2009;681(1):13-23. (2) Young KC, Faulkner K, Wall B, Muirhead C. Sheffield, UK: National Health Service Cancer Screening Programmes, (2003). (3) Heyes, G. J., Mill, A. J., Charles, M. W. *The British Journal of Radiology*, 79, 195–200, (2006). (4) J D. Boice, Jr., D. Preston, F. G. Davis and R. R. Monson. *Radiat. Res.* 125, 214–222, (1991). (5) E. Pukkala, A. Auvinen and G. Wahlberg. 1967–92. *Br. Med. J.* 311, 649–652, (1995). (6) International Commission on Radiological Protection (1991) 1990 Recommendations of the International Commission on Radiological Protection (Pergamon, Oxford). (7) Pochin, E. E. *Health Phys.* 31, 148–151, (1976). (8) Brand M, Sommer M, Achenbach S, Anders K, Lell M, Löbrich M, Uder M, Kuefner MA. *Eur J Radiol.* 2012 Mar;81(3). (9) Stankevicius L, Almeida da Silva AP, Ventura Dos Passos F, Dos Santos Ferreira E, Menks Ribeiro MC, G David M, J Pires E, Ferreira-Machado SC, Vassetzky Y, de Almeida CE, de Moura Gallo CV. *Radiat Oncol.* 2013 Oct 5;8(1):231. (10) Sofia Vala I, Martins LR, Imaizumi N, Nunes RJ, Rino J, Kuonen F, Carvalho LM, Rüegg C, Grillo IM, Barata JT, Mareel M, Santos SC. *PLoS One.* 2010 Jun 21;5(6). (11) Polgári Z1, Ajtony Z, Kregesamer P, Strelci C, Mihucz VG, Réti A, Budai B, Kralovánszky J, Szoboszlai N, Záray G. *Talanta.* 2011 Sep 30;85(4):1959-65. (12) Arredondo M, Cambiazo V, Tapia L, González-Agüero M, Núñez MT, Uauy R, González M. *Am J Physiol Gastrointest Liver Physiol.* 2004 Jul;287(1):G27-32.

Core level and valence band electronic structure of Sr₂FeMoO₆

Presenter: Martins H. P.

Martins H. P.; Prado F.; Caneiro A.; Mossaneck R. J. O.; Abbate M.

*Universidade Federal do Paraná; Universidad Nacional del Sur; Centro Atómico Bariloche; Universidade Federal do Paraná;
Universidade Federal do Paraná*
henrique@fisica.ufpr.br

The Sr₂FeMoO₆ material is a half-metallic ferromagnet with $\mu \approx 4.0\mu_B$, and presents a low-field and high-temperature tunneling magnetoresistance (TMR) effect. Despite extensive studies, there are still open questions about the electronic structure of this compound. The electronic structure of Sr₂FeMoO₆ was studied using X-ray photoemission spectroscopy (XPS) at the SXS beamline in the LNLS (Campinas, Brazil). The sample was confirmed to be in a pure single state phase and the concentration of antisites was less than 3%. The sample was promptly measured to prevent aging effects and repeatedly scraped with a diamond file to remove surface contamination. The valence band spectrum was taken with a photon energy of 1840 eV. Measurements of the Fe 2p and Mo 3p core levels were also taken. The experimental results were interpreted using cluster model calculations. This model expands the ground state beyond the ionic approximation Fe 3d⁵ - Mo 4d¹ [1], treating the correlation on the Fe and Mo sites in a better suited way, as well as the hybridization between the metal ions and the ligand. The Fe 2p and Mo 3p core level XPS spectra were used to determine the parameter set of the cluster model, which were then fine tuned to describe the valence band spectrum. These results help to better understand the electric and magnetic properties of this compound.

[1] H. P. Martins, F. Prado, A. Caneiro, F. C. Vicentín, D. S. Chaves, R. Mossaneck, and M. Abbate, *J. Alloys Compd.* 640, 511 (2015).

Study of a highly crystalline Y₂O₃ sample by Rietveld and Pair Distribution Function Analysis

Presenter: Martinez, L. G.
Martinez, L. G.; Ichikawa, R. U.; Turrillas, X.

Instituto de Pesquisas Energéticas e Nucleares - IPEN
lgallego@ipen.br

An Y₂O₃ highly crystalline sample, used as standard reference material for X-ray diffraction experiments, was studied by Rietveld and Pair Distribution Function analysis. The structural parameters obtained using Rietveld refinement, such as cell parameters, atomic positions and isotropic atomic displacement factors were compared previous studies and literature data. Besides that, the high-energy x-rays scattering data, collected at the LNLS-XDS beamline, allowed perform pair distribution function (PDF) analysis. The data was collected in Bragg-Brentano geometry and using a scintillation punctual detector, with 20 keV energy radiation, reaching a Q_{max} resolution of 20.05 Å⁻¹. The PDF analysis showed that the SRM exhibits a very large structural coherence length, no structural disorder and can be considered perfectly ordered over very large interatomic distances, as expected from a standard reference material.

Temperature and high-pressure dependent X-ray absorption of SmNiO₃ at the Ni K- and Sm-L3 edges

Presenter: Massa N. E.

Massa N. E.^{1*}, Ramos A. Y.², Tolentino H. C. N.², Neto N. S.³, Junior J. F.³, Martínez-Lope M. J.⁴ and Alonso J. A.⁴

¹LANAIS EFO-CEQUINOR, UNLP, La Plata, Argentina, ²Inst. Néel-CNRS, F-38042 Grenoble. France, ³LNLS, 13084-971, Campinas, São Paulo, Brazil, ⁴ICMM-CSIC, Madrid, Spain.
neemassa@gmail.com

The primary consequence of applying quasihydrostatic pressure P is the reduction of interatomic distances, the progressive bond shortening, and the modification of superexchange M-O-M angles. Pressure change as thermodynamic external dynamical variable is a unique tool for probing the relationship between structural sublattice distortions and electronic properties by triggering increments in band hybridization and the eventual emerging into a metallic state by valence and conduction band superposition. SmNiO₃ is a member of the family of undoped compounds RNiO₃ (R=Rare Earth) in which a sharp temperature driven insulator to metal phase transition takes place. The transition from high temperature orthorhombic metallic to an insulating charge disproportionate ($2\text{Ni}^{3+} \rightarrow \text{Ni}^{3+\delta} + \text{Ni}^{3-\delta}$) monoclinic distorted phase is consequence of the Ni-O bond length increase and a simultaneous decrease of the Ni-O-Ni angle. SmNiO₃, TIM = 400 K, also has a paramagnetic insulating phase, and orders magnetically below $T_N \sim 205$ K. A negative slope, $-T_{MI}/dP$, is shared by all RNiO₃ (R=Rare Earth \neq La.). We report XANES and EXAFS measurements of SmNiO₃ from 20 K to 600 K and up to 38 GPa at the Ni K- and Sm L3-edges. They were performed at the LNLS in the DXAS energy dispersive beamline. Increasing pressure induces Ni-O-Ni angle increments toward more symmetric Ni³⁺ octahedra of the rhombohedral $R\bar{3}c$ space group (metallic LaNiO₃). A multiple component pre-edge tail accounts for 1s transitions to 3d-4p states while a post-edge shoulder raises distinctively smoother due to the reduction of electron-phonon interactions as Ni 3d and O 2p orbitals overlap. Pressure dependent room temperature Ni white line peak energies show an abrupt 2.4 GPa valence discontinuity due to non-equivalent Ni sites with Ni^{3+\delta} + Ni^{3-\delta} charge disproportionate in the monoclinic distortion turning at TMI into Ni³⁺ of the perovskite distorted orthorhombic Pbnm metal oxide phase. At 20 K, still distinctive, this turns smoother.

Short-range order study around Iron atoms: Crystallization Process in glassy samples followed by X-ray absorption spectroscopy

Presenter: Mastelaro V.

Mastelaro V. R.^{1*}; Bayer P. S.^{1,2}; Zanutto E. D.³

¹Instituto de Física de São Carlos, USP São Carlos; ²Instituto Federal de Educação, Ciência e Tecnologia de Santa Catarina, Joinville - SC, Brasil.; ³DEMa-Universidade Federal de São Carlos, São Carlos, S.P.
valmor@ifsc.usp.br

Transition metals (TM) and metallic particles are widely incorporated within glass-ceramics (GC) due to two distinct roles: they can affect the nucleation rate dramatically, acting as nucleating agents, or give specific properties to the GC, acting as “active” agents [1-3]. The nucleating agents can be used together or separately to promote simultaneous and related phenomena such as bulk nucleation, decrease in crystallization temperatures and increase in nucleation kinetics, either by accelerating phase separation or by lowering the energy barrier of nucleation. To understand the processes governing the amorphous- to-crystal transformation at the atomic scale, we need to follow the first stages of the nucleation and to identify the structural rearrangements that occur around the nucleating agents. These two aspects can be measured simultaneously by recording the X-ray absorption spectra (XANES, EXAFS) and the X-ray diffraction pattern. However, when the amount of nucleating agent is lower, only the measurement of the XANES and EXAFS spectra is possible. XAS technique was applied to study the nucleating process in a CaMgSi₂O₆ (diopside) glassy sample which contain iron as nucleating agent [4-5]. The purpose of this study is to better understand the potential of iron as nucleating agent for this particular glass using XAS technique. Samples with 2, 4, 7 and 9% Fe₂O₃ were nucleated for 8 h and crystallized at T_c (crystallization peak onset) for 10, 20, 30 and 40 min. XANES and EXAFS spectra were collected ex-situ and in-situ conditions. The ex-situ experiment was done with samples previously submitted to a controlled heat-treatment. The in-situ experiment was done with the 7% and 9% samples submitted to a heat treatment at the beam line. The analysis of XANES and EXAFS spectra confirms the role of iron in the nucleating process. In-situ experiments allowed to determine the temperature where the crystallization around iron takes place.

1) Y. J. Eoh and E. S. Kim, Jpn. J. Appl. Phys. 53, 08NB01 (2014). 2) T. Nonami and S. Tsutsumi, J. Biomed. Mater. Res. 50 8 (2000). 3) A. Goel, A. M. Ferrari, I. Kansal, M. J. Pascual, L. Barbieri, F. Bondioli, I. Lancellotti, M. J. Ribeiro, J. M. F. Ferreira, J. Appl. Phys. 106 093502 (2009). 4) E. D. Zanutto, J. Non-Cryst. Sol. 130 217 (1991). 5) N. Karpukhina and R. G. Hill, R. V. Law, Chem. Soc. Rev. 43 2174 (2014).

In situ XPD study of structural changes in iron-cerium mixed oxides under reducing conditions

Presenter: Mazan M. O.

Mazan M.; Martins T.; Prado R.; Larrondo S.

Facultad de Ingeniería - UBA; UNIFESP - Universidade Federal de São Paulo; UFMT - Universidade Federal de Mato Grosso; CINSO - Centro de Investigaciones en Sólidos*
marianomazan@gmail.com

Although cerium oxide presents good oxygen storage capacity (OSC) and good redox properties, these properties could be improved by doping ceria with trivalent ions like Fe. Doping with aliovalent cations potentially increases the number of anion vacancies improving the oxygen mobility and the reducibility of the material. The resultant solid would be a better material for catalytic applications. Samples with different iron content (Fe:[Ce+Fe] molar ratios= 0, 0.05, 0.1, 0.15, 0.20, 0.30 and 1) were synthesized by Citrates and Liquid-mix methods and calcined at 623K for 2h. The samples were named 0Fe, 5Fe, 10Fe, 15Fe, 20Fe, 30Fe and 100Fe, respectively. The structural changes during the reduction of the CeCeFeO_{δ} system was studied by “in situ” X-ray powder diffraction (XPD), at the D10B-XPD beamline of the Brazilian Synchrotron Light Laboratory, at different temperatures, in an atmosphere containing 5% H_2 , using a high-intensity and low-resolution configuration. The diffraction patterns were well resolved with high intensity thus allowing the use of Rietveld refinement method. At room temperature all cerium containing samples showed only the peaks corresponding to the fluorite structure of CeO_2 . However, sample 30Fe presented asymmetric peaks indicating that some kind of inhomogeneity could exist. Sample 100Fe presented two phases with hematite-like and magnetite-like structures. At 623K sample 100Fe reduced to pure magnetite while no changes were observed for cerium containing samples. At 923K, all samples excepting pure cerium oxide (0Fe) showed the presence of FeO (wustite). At 1073K, sample 100Fe showed only peaks associated to wustite phase while the mixed oxides presented the peaks corresponding to CeFeO_3 superimposed with those corresponding to the fluorite structure and very small peaks associated to wustite. No other cerium containing phases were observed during the experiments.

In situ SR μ XRF analysis of Pb in plants used for phytoextraction of soil pollutants

Presenter: Mera M. F.

Mera M. F.¹, Rubio M.^{1,2,3}, Pérez C. A.⁴, Germanier A.¹, Cazón S.¹, Carranza L.¹

¹CEPROCOR. Álvarez de Arenales 230 B° Junios (5000). Córdoba, Argentina; ²FAMAF. Ciudad Universitaria (5000). Córdoba, Argentina; ³CONICET. Rivadavia 1917 (1033). Buenos Aires, Argentina. ⁴LNLS, Laboratorio Nacional de Luz Sincrotron. Campinas. SP, Brazil.

mariafernanda.mera@gmail.com

The phytoextraction technology uses plants to extract toxic metals from contaminated soils and accumulate them in the harvestable parts of the plants, which can then be removed from site. SR μ XRF technique offers a powerful approach for probing and mapping the *in situ* distribution of a wide range of elements in plant tissues. In order to understand how Pb and other elements are incorporated into the plant from the soil, we consider essential to use SR-mXRF analysis to investigate the spatial distribution of these elements in selected sections of the studied plant. The measurements were carried out at the D09B XRF Fluorescence beamline of the LNLS. The experiments were conducted in *Lolium perenne sp.* plants, grown in soil contaminated with Pb, and in hydroponics crops exposed to lead at industrial and basal levels. SR μ XRF measurements were performed *in situ* on different parts of the plant (roots and leaves) and in living conditions. Plants specimen were sandwiched between two Ultralene thin films to prevent sample drying or oxidation. The capability for Pb phytoextraction in hydroponics crops versus lead-contaminated soil was compared. The results showed the hydroponics crops of *L. perenne sp.* can extract and translocate Pb from the ground to the leaves more effectively than plants grown in contaminated soil, where lead mainly stayed in the root. In addition, a spatial correlation between Pb, S and P distributions was observed. The results suggest that further investigations should be done in order to show whether other plants species can offer better efficacy for Pb phytoextraction than the *L. perenne sp.*

This work was developed at Brazilian National Synchrotron Light Laboratory under the proposal XAFS1-16907. The authors would like to thank the LNLS staff for its technical support.

[1] Scheckel K. and col., In Vivo Synchrotron Study of Thallium Speciation and Compartmentation in *Iberis intermedia*, Environ. Sci. Technol. 2004, 38, 5095-5100.

[2] Donner E and col, Mapping Element Distributions in Plant Tissues Using Synchrotron XRF Techniques. Chapter 9, 2012.

[3] Lombi E and col, In situ analysis of metal(loid)s in plants: State of the art and artefacts. Environmental and Experimental Botany, 72, 2011, 3-17.

[4] EPA Phytoremediation resource guide, United States Environmental Protection Agency, EPA 542-B-99-003, June 1999.

[5] Sarret G and col., Use of Synchrotron-Based Techniques to Elucidate Metal Uptake and Metabolism in Plants, Chapter 1, Advances in Agronomy, 119, 2013, 1-82.

Application of XANES spectroscopy to investigate Sb species in corroded bullets crust material oriented to evaluate the potential toxic effects in the environment

Presenter: Mera M. F.

Mera M. F.¹, Rubio M.^{1,2,3}, Pérez C. A.⁴, Vicentin F. C.⁴, Germanier A.¹

¹ CEPROCOR. Álvarez de Arenales 230 B° Junios (5000). Córdoba, Argentina; ² FAMAF. Ciudad Universitaria (5000). Córdoba, Argentina; ³ CONICET. Rivadavia 1917 (1033). Buenos Aires, Argentina. ⁴ LNLS, Laboratorio Nacional de Luz Sincrotron. Campinas. SP, Brazil.
mariafernanda.mera@gmail.com

Pb, Sb and others toxic metals from pellets alloy are disperse in the soil of the shooting fields. As long as the corroding bullets are present in soil, secondary Pb and Sb phases in the weathering crusts appears being an important source of bioavailable Pb and Sb. Knowledge on the corrosion mechanism of Sb from the bullet is limited and reports on Sb speciation in soils are still scarce. Preliminary studies by SR- μ XRF were performed at the D09B XRF Fluorescence beamline of the LNLS (proposal *XAFSI-15234*). A positive correlation between Sb and Fe was detected in crust material measured in the outer rim of the weathered bullets due to Sb adsorption to Fe oxyhydroxides of soil. It was also observed a spatial correlation between Sb and Cu and between Sb and Zn in crust. Considering that Sb species have different toxicological properties on the environment, our survey continued performing XANES measurements at the Sb *L*-edges in order to identify its oxidation states in crust (Sb^0 , Sb^{3+} or Sb^{5+}). The measurements were carried out at the D04A SXS Soft X-ray Spectroscopy beamline of the LNLS. Samples consisted of dust crust taken from physically deformed and strongly corroded metallic bullets retained in soil samples sieving from shooting fields of North and East region of Córdoba, Argentina. The results showed that the main species found in all samples was Sb^{5+} (Sb_2O_5) followed by Sb^0 (metallic). Sb^{3+} was not detected, and it is known that Sb^{3+} is more toxic than Sb^{5+} . The results suggested that in these environmental conditions, pentavalent Sb was the predominant species after weathering of metallic Sb from the corroding bullets.

Acknowledgements: This work was developed at Brazilian National Synchrotron Light Laboratory under the proposal SXS-16953. The authors would like to thank the LNLS staff for its technical support.

References

- [1] Ackermann S. et al., Antimony sinks in the weathering crust of bullets from Swiss shooting ranges, *Sci. Total Environ.* 2009, 407, 1669-1682.
- [2] Mera M. F., Rubio M., Pérez C. A., Galván V., Germanier A., SR μ XRF and XRD study of the spatial distribution and mineralogical composition of Pb and Sb species in weathering crust of corroded bullets of hunting fields, *Microchemical Journal* 119 (2015) 114–122.
- [3] Scheinost A. et al., Quantitative antimony speciation in shooting-range soils by EXAFS spectroscopy, *Geochimica et Cosmochimica Acta* 70 (2006) 3299–3312

Amine-alcohol-silicate hybrid matrix as efficient adsorbents for water cleaning

Presenter: Molina E. F.

Moura A. L. A., De Oliveira L. K., Ciuffi K. J. and Molina E. F.

UNIFRAN

molina_ferreira@yahoo.com.br

Pollution from dye wastewater is becoming a major environmental problem[1-3]. For the removal of anionic dyes, here we employed epoxy-silicate hybrid matrix which are based on polyethers chains covalently linked to silica framework via an amino-alcohol bridge. To prepare the hybrid matrices from 3-glycidoxypropyl-trimethoxysilane and PEO ((O,O'-bis(2-aminopropyl)-poly(ethylene oxide)) of molecular weight 500 and 1900 g mol⁻¹, we used the one-pot sol-gel route. The diameter of the xerogels augmented, because the free volume increased as a result of the swollen network. Next, we immersed the PEO xerogels in a solution containing the cationic dye Methylene Blue (MB). However, PEO remained transparent after contact with the MB solution, showing that the xerogels did not adsorb MB. The xerogel efficiently removed the anionic RB dye from the starting solution within a contact time of 120 min; in contrast, the MB concentration in this same solution remained constant throughout this period. The kinetic experiment reveal that equilibrium was reached after 2h with RB dye removal efficiency of 97%). These matrices were able to easily and rapidly separate anionic dyes from a mixture containing anionic along with cationic dyes. The active site of the RB dye and the site groups present in the PEO hybrid matrices played an important role in the capacity of the xerogel to adsorb anionic species. The synthesis of the PEO hybrid is easy to reproduce in any industrial or academic lab. This matrices is potentially applicable as an efficient, fast, selective, and convenient device in water treatment for removal of dyes and metal ions. Financial support: Fapesp (2013/20455-2).

1. V. K. Gupta, I. Ali, V. K. Saini, Environ. Sci. Technol., 2004, 38, 4012-4018. 2. Y. Chen, M. He, C. Wang, Y. Wei, J. Mater. Chem. A, 2014, 2, 10444-10453. 3. K. Mukherjee, A. Kedia, R. K. Jagajjani, S. Dhir, S. Paria, RSC. Adv., 2015, 5, 30654-30659.

Spectroscopic characterization of the interface semiconductor/active layer in sensors based on DNA

Presenter: De Moraes M. O. S.

Silva-Moraes M. O.*^{1,2}, Brito W. R.¹, Mota A. J.³, Assis I. M.^{1,2}, Wilson D.⁴, Passos R. R.¹, Galante D.⁵, Garcia-Basabe Y.⁶, Rocco M. L. M.⁷, Casarini J. R.²

¹ Chemistry Department, Federal University of Amazonas (UFAM), Manaus (AM), Brazil ² Senai Institute of Innovation (ISI), Manaus (AM), Brazil ³ Postgraduate Program of Biotechnology, Federal University of Amazonas (UFAM), Manaus (AM), Brazil ⁴ Physic Department, Federal University of Amazonas (UFAM), Manaus (AM), Brazil ⁵ Brazilian Synchrotron Light Laboratory LNLS / CNPEM, Campinas (SP), Brazil ⁶ Physical Department, Federal University of Paraná (UFPR), Curitiba (PR), Brazil ⁷ Physical Chemistry Department, Federal University of Rio de Janeiro (UFRJ), Rio de Janeiro (RJ), Brazil
oneide.moraes@gmail.com

The biosensors based on ion-sensitive field-effect transistor (ISFET), as well as the implementation of biosensors based on nanoparticles of TiO₂, carbon nanotubes, or graphene occupying a large part of contemporary scientific production(1) having a particular interest for the study of antioxidants compounds(2,5). Sensors based on DNA molecule are high sensitivity and selectivity for the detection of pathogenic and genetic diseases. NEXAFS and XPS techniques were used for the determination which of three kinds of DNA molecules, this is genomic, plasmid and PCR, is more suitable as active layer in biosensors devices. NEXAFS experiments were carried out in the SGM beam line (250-1000 eV) by measuring TEY and the photon flux by Au grid monitor at the LNLS, Campinas-SP. The XPS spectra were obtained at the LaQuiS-IQ, UFRJ. Spectra were obtained in the edges at 1sC, 1sN, 1sO, 2pTi and 2sP before and after the anchorage of the active layer for each type of DNA. For genomic DNA/TiO₂, all NEXAFS spectra showed a low intensities and a slight chemical shifts for low energies in relation to others samples. The plasmid DNA/TiO₂ and PCR/TiO₂ are very similar showing slight differences. In the XPS spectra, genomic DNA presented an opposite behavior, high intensities and shifts to higher energies in relation to others samples. These results indicate a resistive character in charge mobility in the sample genomic DNA/TiO₂. Were attributed this resistive characteristics to the presence of histone proteins in structure of genomic DNA even after the removal treatment. A comparative study between the different kinds of anchored DNA was performed to deepen in to the mechanisms of anchoring of the biologically active layers on semiconductor substrate through the NEXAFS and XPS. It's possible to conclude that the genomic DNA is not suitable for the use as the biologically active layer in electrochemical sensors if compared with the anchored mechanism of the plasmid and the PCR DNA molecule.

[1] Fernandes, J., Transistor de Efeito de Campo (FET) para Detecção Química e Bioquímica utilizando Dielétrico de Porta constituído de Camada Empilhada SiNx/SiOxNy. Tese Mestrado (2009). [2] J. Liu, C. Roussel, G. Lager, P. Tacchini, H. H. Girault. Antioxidant Sensors Based on DNA-Modified Electrodes. *Analytical Chemistry A.* 77, 23, 2005. [3] EunKyung Cho, A. B. T. F. K., Chemical Characterization of DNA-Immobilized InAs Surfaces Using X ray Photoelectron Spectroscopy and Near-Edge X ray Absorption Fine Structure. *Langmuir* 2012, 28, 11890–11898.

In-situ and in-operando studies of cobalt doped titanates by XRD, XAS and electrochemical impedance spectroscopy simulating working conditions as SOFC anodes and cathodes

Presenter: Napolitano F. R.

Napolitano F.; Soldati A.; Geck J.; Giebeler L.; Fernández-Zúvich A.; Saleta M.; Caneiro A.; Serquis A.; Moggi L.

CONICET; CONICET; IFW-Dresden; IFW-Dresden; CNEA; UNICAMP; CNEA; CONICET; CONICET
napolitf@gmail.com

Perovskites with Ti on their B-site has recently been subject of study on the Solid Oxide Fuel Cell (SOFC) field since these materials presents good properties that enables their use as a possible anode materials[1]. At the SOFC cathode side, the (La,Sr)CoO₃ is one the most studied cathode material [2]. In this work we present the study of the La_{0.4}Sr_{0.6}(Ti,Co)O₃ family (LSTC) for their use as electrode material for new devices with symmetric designs (S-SOFC)[3,4]. In a first step, we completely characterized, for first time, their crystal and electronic structures at room temperature through X-ray diffraction and X-ray Absorption Spectroscopy. This study was followed by non-ambient experiments, simulating in-situ conditions as S-SOFC electrode (oxidizing and reducing atmospheres up to 750°C)[5-7]. We found that cobalt doping increases the electrical conductivity by 5 to 8 orders of magnitude under an oxidizing condition respect to the undoped sample (La_{0.4}Sr_{0.6}TiO₃-d), making these materials suitable to be used as cathodes but higher Co doping levels ($x \leq 0.7$) decrease the material stability as anode under reducing atmospheres. Besides, Co doping induces a slight rhombohedral distortion in the crystal symmetry at room temperature, favoring a transformation to a cubic phase at higher temperatures (100-500°C, depending of the Co/Ti ratio). On the other hand, recent advances on materials characterization techniques have provided new platforms that enable the in-situ study of crystallographic, mechanical, electronic, and electrochemical properties under a wide range of environmental conditions, not only for fundamental research but also in order to recreate a more realistic environment in the case of applied research [8,11]. Here, we also present preliminary results on LSTC S-SOFC from our recently commissioned characterization device, capable to perform simultaneous XRD and Electrochemical Impedance Spectroscopy measurements.

[1] X. Zhou, N. Yan, K. T. Chuang, J. Luo, RSC Advances 4 (1) (2014) 118-131. [2] S. B. Adler, Chemical Reviews 104 (10) (2004) 4791-4843. [3] J.C. Ruiz-Morales, Nature 439 (2006) 568. [4] J.C. Ruiz-Morales, J. Canales-Vázquez, J. Peña-Martínez, D.M. López, P. Nuñez, Electrochimica Acta 52 (2006) 278-284. [5] F. Napolitano, D. Lamas, A. Soldati, A. Serquis, International Journal of Hydrogen Energy 37 (2012) 18302-18309. [6] F. Napolitano, A. Soldati, J. Geck, D. Lamas, A. Serquis, International Journal of Hydrogen Energy 38 (2013) 8965-8973. [7] F. Napolitano, A. Soldati, J. Geck, L. Suescun, A. Acuña, A.F. Zúvich, D.G. Lamas, A. Serquis ECS Transactions 58(3) (2013) 185-193. [8] M. Liu, M.E. Lynch, K. Blinn, F.M. Alamgir, Y.-M. Choi, Materials Today 14(11) (2011) 534-546. [9] P.R. Shearing, R.S. Bradley, J. Gelb, S.N. Lee, A. Atkinson, P.J. Withers, N.P. Brandon, Electrochemical and Solid State Letters, 14(10) (2011) B117-B120. [10] S. Wolf, N.A. Cañas, K.A. Friedrich, Fuel Cells, 13(3) (2013) 404-409. [11] D.N. Mueller, M.L. Machala, H. Bluhm, W.C. Chueh, Nature Communications, 6 (2015), 6097

Structural characterization of fragmented kraft lignin by biological processes by SAXS

Presenter: Negrão D. R.

Negrão D. R.¹, Brenelli L. B.², Gandin C. A.³, Dias. A. T.⁴, Leão A. L.⁵, Neto M. de O.⁶, Squina F. M.⁷, Monteiro R. T. R.⁸

CENA/USP^{1,8}; CNPEM/CTBE^{2,7}; IBB/UNESP, Botucatu^{3,6}; FCA/UNESP, Botucatu^{4,5}
djanegrão@hotmail.com

The enzymatic fragmentation of lignin was investigated by direct cultivation of basidiomycetes fungus in 10% (v/v) Kraft black liquor (KBL) containing 10 g L⁻¹ dextrose. Four fungi isolates (BT-10, BT-21, BT-40, JAU-3) were grown in KBL, kept under stirring for 15 d at 30 °C. The lignin fractions (LF) were recovered after KBL acidification at pH 3.0 and drying at 60 °C. Prior to SAXS analysis, LF were purified on a gel filtration column Superdex 30 pepgrade (70 cm x 0.6 cm) in an AKTA@ system equipped with UV detector in order to separate the LF from proteins. The LF were eluted and diluted in NaOH solution (0.1 M/pH 11.0). 1 mL was injected into the column at the rate of 0.3 mL.min⁻¹ and detected at 280 nm. The LF analysed by SAXS were selected based on the first and third absorption peaks detected at 280 nm and collected in microtubes by AKTA@ system. SAXS analysis indicated that the profile of the LF obtained after cultivation of BT-10 and BT-40 in KBL were similar, with identical radius gyration values (R_g) (1:58) and very close polydispersity. The profile of the LF biodegraded by JAU-3 and BT-10 (first and second peaks respec.) also were similar to R_g and σ values, however differing in the sizes of fractals (D). Based on the obtained data, SAXS analysis contributed to the structural characterization of LF fragmented by biological processes, regarding to the size, shape and polydispersity.

References: NEGRÃO, D. R., SAIN, M., LEÃO, A. L., SAMENI, J., JENG, R., JESUS, J. P. F., MONTEIRO, R. T. R. Fragmentation of lignin from organosolv black liquor by white rot fungi. *Bioresources* (Raleigh, N.C)., v.10, p.1553 - 1573, 2015. MAZIERO, P., OLIVEIRA NETO, M., MACHADO, D., BATISTA, T., CAVALHEIRO, C. C. S., NEUMANN, M. G., CRAIEVICH, A. F., ROCHA, G. J. M., POLIKARPOV, I., GONÇALVES, A.R. Structural features of lignin obtained at different alkaline oxidation conditions from sugarcane bagasse. *Industrial Crops and Production*, v. 35, 61-69, 2012.

Iterative Reconstruction of Tomographic Images Using Accelerated Projection/Backprojection Techniques

Presenter: Neto E. S. H.

Neto E. S. H.

ICMC / USP

elias@icmc.usp.br

We will present techniques to speed up iterative reconstruction techniques for tomographic imaging. We will apply the techniques in several sub-optimal acquisition settings. Applications include sparse-view reconstruction and interior-exterior tomographic acquisition with mixed resolution.

Small angle X-ray scattering applied to Glycoside hydrolases from families GH5 and GH6

Presenter: Neto M. de O.

Neto M. de O.¹; Gandin C. A.¹; Gonçalves T.²; Pimentel A. C.²; Alvarez T. M.²; Squina F. M.²

¹Departamento de Física e Biofísica, Instituto de Biociências, UNESP Univ Estadual Paulista; ²Laboratório Nacional de Ciência e Tecnologia do Bioetanol, Centro Nacional de Pesquisa em Energia e Materiais
mario.neto@ibb.unesp.br

Glycoside hydrolases (GHs) are a group of enzymes of great importance for carbohydrate metabolism (HENRISSAT, 1991), and therefore are key enzymes for biotechnological processes, such as the production of biofuels from plant feedstocks (LI et al, 2009). GH5 and GH6 are formerly known as cellulase families A and B, respectively. The cellobiohydrolases of these families are widely believed to act processively from the non-reducing ends of cellulose chains to generate cellobiose. The encoding genes for the cellulases GH5 and GH6 were identified through functional screening of a metagenomics library derived from the soil. Both genes were cloned in a vector of expression pET28a, submitted to heterologous expression on *Escherichia coli* and purified by affinity chromatography and gel filtration chromatography. New theoretical and computational approaches were developed for the treatment and interpretation of the small angle X-ray scattering (SAXS) data, allowing a detailed analysis of the global structure of proteins in solution (SVERGUN et al, 1996), prediction of quaternary structures (SVERGUN et al, 1998) (OLIVEIRA NETO et al, 2008), among others. In this study we utilize SAXS to characterize two glycoside hydrolases from families GH5 and GH6 of metagenomics origin. Using SAXSMoW (FISCHER et al, 2008), we determine that both enzymes are monomers in solution. Pair distance distribution function $p(r)$ and shape analysis were done using ATSAS package (KONAREV et al, 2006). The maximum diameter (D_{max}) of the GH5 enzyme presented a significant decrease in the presence of calcium, suggesting that calcium ions provide a higher stability to the enzyme. GH5 in the presence of calcium ions had a radius of gyration (R_g) of approximately 27 Å and a D_{max} of 90 Å and in the absence, respectively, 41.8 Å and 120 Å.

FISCHER, H.; OLIVEIRA NETO, M.; NAPOLITANO, H. B.; CRAIEVICH, A. F.; POLIKARPOV, I. The molecular weight of proteins in solution can be determined from a single SAXS measurement on a relative scale. *J. Appl. Cryst.* 43, 101-109, 2009. HENRISSAT, B. A classification of glycosyl hydrolases based on amino acid sequence similarities. *Biochemical Journal*, 1991, Vol. 280(Pt 2), pp. 309-316. P. V. KONAREV; M. V. PETOUKHOV; VOLKOV, V. V.; D. I. SVERGUN. ATSAS 2.1, a program package for small-angle scattering data analysis. *Journal of Applied Crystallography*, v. 39, n. 2, p. 277-286, 2006. LI, LL, MCCORKLE, SR, MONCHY, S, TAGHAVI, S. AND VAN DER LELIE, D. Bioprospecting metagenomes: glycosyl hydrolases for converting biomass. *Biotechnology for Biofuels*, 2:10, 2009. OLIVEIRA NETO, M.; ALONSO, R.L.; LEITE, F.L.; OLIVEIRA JR, O.N., POLIKARPOV I.; MASCARENHAS, Y.P. Simulated Annealing of Two Electron Density Solution Systems. I-Tech Education and Publishing KG.(Org.). *Global Optimization: Focus on Simulated Annealing*. Kirchengasse 43/3: I-Tech Education and Publishing KG, 2008. SVERGUN, D.I.; VOLKOV, V.V.; KOZIN, M.B.; STUHRMANN, H.B. New Developments in Direct Shape Determination from Small-Angle Scattering. 2. Uniqueness *Acta Cryst. A*, v. 52, p. 419-426, 1996. SVERGUN, D.I.; ALDAG, I.; SIECK, T.; ALTENDORF, K.; KOCH, M. H. J.; KANE, D.J.; KOZIN, M.B.; GRUBER G. A Model of the Quaternary Structure of the *Escherichia coli* F1 ATPase from X-Ray Solution Scattering and Evidence for Structural Changes in the Delta Subunit during ATP Hydrolysis. *Biophysical Journal*, v. 75, p. 2212-2219, 1998

In situ study of austenite decomposition during thermal cycles and under application of stress in ferrous alloys

Presenter: Nishikawa A. S.

Nishikawa A. S.*; Echeverri E. A. A.; Centeno D. M. A.; Huallpa E. A.; Tschiptschin A. P.; Goldenstein H.

Department of Metallurgical and Materials Engineering of the Polytechnic School of the University of São Paulo
arthur.nishikawa@usp.br

In this work, the kinetics of austenite decomposition during the application of the novels thermomechanical treatments of Quenching and Partitioning (Q&P) and Hot Stamping + Quenching and Partitioning (HSQP) on a ductile cast iron and a TRIP steel, and also during the application of tensile stress in a metastable austenitic steel were studied by means of in situ synchrotron X-ray diffraction. Both experiments were performed at the XTMS experimental station facilities at LNLS/LNNano using a Gleeble thermomechanical simulator integrated to the XRD1 beamline. Real time information about kinetics of competitive reactions was obtained by following the lattice parameter and phase fractions changes. The results were validated by global and local measurements techniques, e.g., high resolution dilatometry and electron microscopy, and also confronted with information on literature. The results demonstrated to be in fairly agreement with the expected from previous experiments and also provided complimentary information about the bainite and martensite reactions occurring in the studied samples.

Synchrotron small angle X-ray scattering Investigation of niobium oxyhydroxide nanostructured

Presenter: Pereira I. M.

Pereira I. M.¹, De Souza S. D.², Oliveira L. C. A.³, De Souza A. R.², Rodrigues A. P. H.³, Boaventura T. P.⁴, Oréface R. L.⁴, Patrício P. S. O.²

¹Centro Tecnológico do Exército; ²Centro Federal de Educação Tecnológica de Minas Gerais; ³Universidade Federal de Minas Gerais. iacipere@yahoo.com.br

Our research group has developed an material based on niobium. They are: (i) hydroxide niobium (NbO₂OH), (ii) niobium oxyhydroxide (NbO₂OH/H₂O₂) and (iii) amphiphilic niobium oxyhydroxide (NbO₂OH/amp). In this work SAXS was employed to explore the niobium nanoparticle form. The symmetric maxima observed at NbO₂OH, NbO₂OH/H₂O₂ curve suggests the existence of small spheroid like particles. Results suggests that the O–H surface groups increase nanoparticle size without altering significantly the particle size. The asymmetric maximum presented on NbO₂OH/amp curve and the second-order peak presented as a ‘bump’ at larger q-values suggests elongated lamellar structure. The niobium compound plots shows: a well defined bump around 2.9 nm⁻¹, attributed to NbO₂OH particles, an overlaid bump around 4.0 nm⁻¹, attributed to O–H surface groups and, observed at NbO₂OH/amp, a defined peak at 1.658 nm⁻¹ attributed to the surfactant molecule. The Porod’s Law negative deviation is not observed at NbO₂OH/H₂O₂, apparently, the compact boundary is the result of the hydrogen bonds between the hydrogen atoms of the hydroxyl groups and oxygen atoms. On the other hand, the Porod’s plot of NbO₂OH/amp showed more complex information, suggesting that the hybrid system has significantly different surface composition. The strong negative deviation is due to the diffuse-boundary and due the electrostatic interaction between the surfactant organic molecular chains and Nb=O, Nb–O or Nb(O–O) groups which leads the interfaces to stimulate the negative deviation. The interphase thickness, σ , of NbO₂OH is 0.06. On the other hand, NbO₂OH/amp σ is 0.23.

1. Oliveira LCA, Costa NT, Pliego Jr JR, Silva AC, de Souza PP, et al. (2014) Amphiphilic niobium oxyhydroxide as a hybrid catalyst for sulfur removal from fuel in a biphasic system. *Applied Catalysis B: Environmental* 147: 43-48. 2. di Stasio S, Mitchell JBA, LeGarrec JL, Biennier L, Wulff M (2006) Synchrotron SAXS (in situ) identification of three different size modes for soot nanoparticles in a diffusion flame. *Carbon* 44: 1267-1279. 3. Pereira IM, Oréface RL (2010) The morphology and phase mixing studies on poly(ester-urethane) during shape memory cycle. *Journal of Materials Science* 45: 511-522. 4. Bolze JP, D; Ballauff, M; Narayanan, T; Cölfen H. (2004) Time-resolved SAXS study of the effect of a double hydrophilic block-copolymer on the formation of CaCO₃ from a supersaturated salt solution. *Journal of Colloid and Interface Science* 277: 84-94. 5. Luo J, Liang Y, Yang J, Niu H, Dong J-Y, et al. (2011) Mechanisms of nucleation and crystal growth in a nascent isotactic polypropylene/poly (ethylene-co-octene) in-reactor alloy investigated by temperature-resolved synchrotron SAXS and DSC methods. *Polymer* 52: 4590-4599. 6. Vainio U, Lauten RA, Serimaa R (2008) Small-Angle X-ray Scattering and Rheological Characterization of Aqueous Lignosulfonate Solutions. *Langmuir* 24: 7735-7743. 7. Xiao-Xu L, Jing-Hua Y, Dao-Bin S, Wen-Bin B, Wei-Dong C, et al. (2010) Small-Angle X-Ray Scattering Study on Nanostructures of Polyimide Films. *Chinese Physics Letters* 27: 096103. 8. Xu Y, Li Z, Fan W, Wu D, Sun Y, et al. (2004) Density fluctuation in silica-PVA hybrid gels determined by small-angle X-ray scattering. *Applied Surface Science* 225: 116-123. 9. Perrin P, Prud'homme RE (1994) SAXS Measurements of Interfacial Thickness in Amorphous Polymer Blends Containing a Diblock Copolymer. *Macromolecules* 27: 1852-1860. 24. Norton DR, Keller A (1985) The spherulitic and lamellar morphology of melt-crystallized isotactic polypropylene. *Polymer* 26: 704-716.

Investigation of the Morphology Exhibited by Multilayered Films of Collagen and Cellulose Nanowhiskers by Small-angle X-ray Scattering

Presenter: Pereira I. M.

Pereira I. M.¹, De Souza S. D.², Patricio P. S. de O.²

¹Brazilian Army Technological Center, ²Federal Center of Technological Education of Minas Gerais
iacipere@yahoo.com.br

Collagen (COL)/glycerol (GLI)/cellulose nanocrystal (CNC) nanocomposites were prepared by solution blend. The blends were obtained by integrating the COL solution with GLI/CNC solution and varying the CNC. Films were produced by casting the dispersions in a PVC mold and allowing them to dry at 40°C. Synchrotron small angle X-ray scattering (SAXS) was employed: (i) to investigate the macromolecular structure of neat COL/GLI and COL/GLI/CNC nanocomposites, (ii) to explore, in water solution, the CNC form and dispersion and (iii) to investigate the lyophilized cellulose whiskers surface. SAXS results indicated that CNC in concentrations up to 1 wt. % present an intermediate shape between a rod and a plane with 9.34 nm radius of gyration (R_g). Apparently, when dispersed in water, the CNC rod-like particle expands to a planar shape with a very smooth particle surface. SAXS patterns of lyophilized CNC present anisotropic feature typically observed for rod like particles. Lyophilized CNC scattering curve shows only one power-law regime, $\alpha = -3.7$, which describe a surface fractal structure formed by CNC clusters with irregular surface. The COL/GLI/CNC nanocomposites present two different structural levels with two types of particles with very different R_g . At the intermediate power-law regime, it is observed a large-scale mass fractal aggregate. In the high power-law regime, it is observed scattering from primary particles smaller than 1 nm. Besides, the primary particle of neat COL/GLI is a rod where the shrunken CNC rods attach. As the CNC concentration increases the original particle distorts from a rod to a plate. As expected, the CNC concentration controls the particle radius because while the CNC is introduced into the system it attaches to the original primary particle which raises the particle radius. From the TEM data, it is not possible determine the dimensions of the isolated particles. However, the smaller cluster would have less than 3 nm in radius.

1. Lodha, P. & Netravali, A. N. Thermal and mechanical properties of environment-friendly “green” plastics from stearic acid modified-soy protein isolate. *Ind. Crops Prod.* 21, 49–64 (2005). 2. Fortunati, E. et al. Cellulose nanocrystals extracted from okra fibers in PVA nanocomposites. *J. Appl. Polym. Sci.* 128, 3220–3230 (2013). 3. Ram, G. Preparation of a Partially Calcified Gelatin Membrane as a Model for a Soft-to-Hard Tissue Interface. (2013). 4. Pereira, I. M. & Oréfice, R. L. Study of the Morphology Exhibited by Linear Segmented Polyurethanes. *Macromol. Symp.* 299-300, 190–198 (2011). 5. Pereira, I. M. & Oréfice, R. L. In situ evaluation of structural changes in poly (ester-urethanes) during shape-memory cycles. 51, 1744–1751 (2010). 6. Pajot-augy, E., Axelos, M. A. V, Recherche, U. De, Concert, D. & Physico-chimique, I. D. B. The effect of organic crysolvents on actin structure : studies by small angle X-ray scattering. 179–184 (1992). 7. Hyeon-lee, J., Beaucage, G. & Pratsinis, S. E. Fractal Analysis of Flame-Synthesized Nanostructured Silica and Titania Powders Using Small-Angle X-ray Scattering. 7463, 5751–5756 (2000). 8. Ramachandran, R. et al. Persistence Length of Short-Chain Branched Polyethylene. *Macromolecules* 41, 9802–9806 (2008). 9. Singh, M., Sinha, I., Singh, a. K. & Mandal, R. K. Formation of fractal aggregates during green synthesis of silver nanoparticles. *J. Nanoparticle Res.* 13, 69–76 (2010). 10. Caetano, B. L. et al. In Situ and Simultaneous UV - vis / SAXS and UV - vis / XAFS Time-Resolved Monitoring of ZnO Quantum Dots Formation and Growth. 4404–4412 (2011). 11. Rämänen, P., Penttilä, P. a., Svedström, K., Maunu, S. L. & Serimaa, R. The effect of drying method on the properties and nanoscale structure of cellulose whiskers. *Cellulose* 19, 901–912 (2012). 12. S. de O. Patricio, P. et al. Increasing the elongation at break of polyhydroxybutyrate biopolymer: Effect of cellulose nanowhiskers on mechanical and thermal properties.

Use of oyster *Crassostrea rhizophorae* as biomonitor in analysis of heavy metals pollution in the marine environment under influence of the ports of Santos and São Sebastião.

Presenter: Pezzatti R. R.

Pezzatti R. R.¹, Yokoyama L. Q.¹, Ignacio B. L.¹, De Jesus E. F. O.², Mársico E. T.³, Ribeiro R. de O. R.³, Barbosa R. de F.¹

¹ Instituto Saúde e Sociedade, Departamento de Ciências do Mar, Universidade Federal de São Paulo; Laboratório de Instrumentação Nuclear, COPPE/UFRJ, ³ CLAN - Laboratório de Controle Físico-Químico, UFF.
clamire@hotmail.com

All living organisms change the environment in which they are inserted. However, the human is changing the environment with higher intensity compared with other living beings. The coastal region is, due to the high population concentration and polluting industrial activities, the subject of considerable emission of heavy metals, suggesting potential effects on their populations, the marine environment as a whole and to the human population that consumes (whether or not routinely) organisms in this ecosystem. Thus, this study had the objective to examine the concentrations of Ca, Cr, Cu, Fe, K, Mn e Zn in two different tissues of *Crassostrea rhizophorae*, the adductor muscle of the shells and the edges of the mantle. These organisms were collected from four areas between the ports of Santos and São Sebastião, Millionaires Beach, Boracéia Beach, Guaecá Beach and Araçá Bay. The metal concentrations were determined by the technique of X-ray fluorescence by Total Reflection (TXRF). Through the obtained concentrations, we observed elevated concentrations of metals compared with other studies conducted by the scientific community, so that such sites are admittedly influenced by polluting activities of these two ports. Moreover, compared to the maximum allowable limits for human ingestion, such sites had higher concentrations of metals, which can pose risks to human health, since several people have the habit of consuming oysters as food.

Refinement of single crystal structures by X-ray multiple diffraction.

Presenter: Remédios C. M. R.

Remédios C. M. R.¹; Morelhão S. L.²

¹Universidade federal do Pará; ²Instituto de Física da Universidade de São Paulo (IF/USP)
rocha@fisica.ufc.br

The methods of X-ray, neutron and electron diffraction are of fundamental importance in crystallography where resolution in determining crystal structures relies primarily on refinement procedures. The collection of large data sets of diffracted intensities and adjustment of parameters in model structures to simulate the experimental intensities are the very basic steps common to all refinement procedures. Apart from these procedures, there are also validation tools necessary in structural biology to avoid serious errors when resolving macromolecular crystals from electron-density maps (Read et al., 2011). Structural resolution in crystallography in the 21st century is therefore limited to structural details producing an unambiguous set of diffracted intensities in atomic models presenting physical and chemical consistency. In this work A pair of enantiomer crystals is used to demonstrate how X-ray phase measurements provide reliable information for absolute identification and improvement of atomic model structures. Reliable phase measurements are possible thanks to the existence of intervals of phase values that are clearly distinguishable beyond instrumental effects. Because of the high susceptibility of phase values to structural details, accurate model structures were necessary for succeeding with this demonstration. It shows a route for exploiting physical phase measurements in the crystallography of more complex crystals.

Read, R.J. et al (2011) Structure, 19, 1395-1412

Thermal transformations metakaolin – spinel type aluminosilicate: Al and Si k-xanes characterization

Presenter: Requejo F. G.

Requejo F. G.; Andrini L.; Rendtorff N.

IFTA (FCE-UNLP, CONICET); INIFTA (FCE-UNLP, CONICET); CETMIC (FCE-UNLP, CIC, CONICET)
andrini@inifta.unlp.edu.ar

Since the pioneering work of G.W. Brindley and M. Nakahira it is known that one of the open problems concerning the metakaolin phase, the manner in which it transforms into a spinel-type phase and mullite, and the relation of this spinel-type phase to mullite, because the series of reactions by which kaolinite transforms to mullite is perhaps the most important in the entire field of ceramic technology [1]. The thermal transformations of kaolinite (K) in metakaolin (MK) and the metakaolin in a spinel type aluminosilicate (SAS) were studied by Al and Si K-XANES to correlate the information obtained with this technique with that obtained by conventional X-ray Diffraction, and clarify and assign the structural changes. Simultaneously with XANES technique is possible to observe changes in the electronic structure of the system. For K à MK transformation, by Al K-XANES it was obtained results consistently with reported Aluminium coordination changes occurred in the kaolinite dehydroxylation process [2]. In general, Al K-XANES spectra of aluminum-containing oxides showed three distinguishable peaks: one at 1566.0 eV assignable to tetrahedral AlO₄ and two assigned to AlO₆ characteristic at 1568.0 and 1572.0 eV [3]. In the case of SAS there are several features, particularly there is a shoulder at 1566 eV and two AlO₆-peaks one at 1567.8 and other at 1571.4 eV. No major changes in the Si K-XANES were observed, i.e. the environments of Si it is not primarily affected for thermal transformations, except for a slight variation in the 3p-holes density. This leads to the conclusion that the structural changes are attributable to changes in the Al environment.

[1] G.W. Brindley and M. Nakahira, *J. Am. Ceram. Soc.*, 42, 311-314 (1959). [2] C.E. White, L.M. Perander, J.L. Provis, J.S.J. van Deventer. *J. Mater. Chem.*, 21, 7007-7010 (2011). [3] Y. Kato, K.-I. Shimizu, N. Matsushita, T. Yoshida, H. Yoshida, A. Satsuma, T. Hattori. *Phys. Chem. Chem. Phys.*, 3, 1925-1929 (2001).

Study of Eu³⁺! Eu²⁺ reduction in BaAl₂O₄: Eu prepared in different gas atmospheres

Presenter: Rezende M. V. dos S.

Rezende M. V. dos S. a^{1*}, Valerio M. E.G.², Jackson R. A.

¹Departamento de Física, Universidade Federal de Sergipe, Campus Universitário, 49100-000 Itabaiana-SE, Brazil; ²Departamento de Física, Universidade Federal de Sergipe, Campus Universitário, 49100-000 São Cristovão-SE, Brazil; ³School of Physical and Geographical Sciences, Keele University, Keele, Staffordshire ST5 5BG, UK
mvsrezende@gmail.com

The effect of different gas atmospheres such as H₂(g), synthetic air, carbon monoxide (CO) and nitrogen (N₂) on the Eu³⁺! Eu²⁺ reduction process during the synthesis of Eu-doped BaAl₂O₄ was studied using synchrotron radiation. The Eu³⁺! Eu²⁺ reduction was monitored analyzing XANES region when the sample are excited at the Eu LIII-edge. The results show that the hydrogen reducing agent are the most appropriate gas for Eu²⁺ stabilization in BaAl₂O₄ and that only a part of the Eu ions can be stabilized in the divalent state. A model of Eu reduction process, based on the incorporation of charge compensation defects, is proposed.

[1] M. Peng, G. Hong, J. Lumin. 127 (2007) 735. [2] S.H.M. Poort, W.P. Blokpoel, G. Blasse, Chem. Mater. 7 (1995) 1547. [3] X. Lü, W. Shu, Q. Yu, Q. Fang, X. Xiong, Glass Phys. Chem. 33 (2007) 62. [4] T.-P. Tang, C.-M. Lee, F.-C. Yen, Ceram. Int. 32 (2006) 665. [5] R. Sakai, T. Katsumata, S. Komuro, T. Morikawa, J. Lumin. 85 (1999) 149. [6] Z. Qiu, Y. Zhou, M. Lu, A. Zhang, Q. Ma, Acta Mater. 55 (2007) 2615. [7] T. Takeyama, T. Nakamura, N. Takahashi, M. Ohta, Solid State Sci. 6 (2004) 345. [8] P.J.R. Montes, M.E.G. Valerio, J. Lumin. 130 (2010) 1525. [9] P. Dorenbos, Chem. Mater. 17 (2005) 6452. [10] P. Dorenbos, J. Electrochem. Soc. 152 (2005) h107

Ionization and fragmentation of the acetaldehyde (CH₃CHO) molecule by 20-330 eV photons

Presenter: Ribeiro L. C.

Ribeiro L. C.; Santos M. de J.; Dos Santos A. M.; Arruda M. S.; Mendes L. A. V.; Dos Santos A. C. F.; Marinho R. dos R. T.; Prudente F. V.

Universidade Federal da Bahia; Universidade Federal da Bahia; Universidade Federal da Bahia; Universidade Federal do Recôncavo da Bahia; Universidade Federal da Bahia; Universidade Federal do Rio de Janeiro; Universidade Federal da Bahia; Universidade Federal da Bahia;
leofisicafederal@yahoo.com.br

The aim of this proposal is to perform a study of the ionization and fragmentation of the acetaldehyde molecule (CH₃CHO) in the gas phase after interaction with 20-330 eV photons. The acetaldehyde is a prebiotic molecule. From the physical and chemical point of view, the study of the origin of life is related to the formation of biomolecules, as the nucleic acids (DNA and RNA) and the proteins. A hypothesis to explain the origin of life suggests that the biomolecules were created in space by the recombination of simpler organic molecules subjected to radiation and collisions with the solar wind particles, such as protons, electrons and ions, and then brought to Earth by meteors and comets. Therefore, the study of simple prebiotic molecules is of fundamental importance to understand the formation of complex organic molecules. The experimental set up includes the time-of-flight mass spectrometer assembled at the rotating chamber. The chamber needs to be in ultra high vacuum and liquid nitrogen traps were used for the mechanical pumps. The molecule were inserted into the chamber through the gas inlet system. To take into account the influence of the higher harmonics orders we measured the photoionization for a known gas, the N₂. We have determined the branching ratios for fragmentation products as a function of the energy of the projectiles. We have measured the total (TIY) and partial (PIY) ion yields, as well as the single (PEPICO) and double (PEPIPICO) mass spectra, for interactions with photons between 20 eV and 330 eV. Our group had previously measured some prebiotic molecules in the low (TGM beamline) and high (SGM beamline) energy range (for example, see reference [1]). Besides comparing the results of the interaction with different projectiles, with this work we could also provide information about the photofragmentation process with energies from opening channels until core excitation.

[1] Manuela S. Arruda, Ricardo R. T. Marinho, Angelo M. Maniero, Maria Suely P. Múndin, Alexandra Mocellin, Sergio Pilling, Arnaldo N. de Brito, Frederico V. Prudente, J. Phys. Chem. A 116, 6693 (2012).

Heavy metals measurement in sandy beaches: influence of the benthic fauna associated

Presenter: Ribeiro R. M. M.

Ribeiro R. M. M.¹, Yokoyama L. Q.¹, Jesus E. F. O.², Ribeiro R. O. R.³, Mársico E. T.³, Gennari R. F.⁴, Barbosa R. F.¹

*1*Department of Marine Sciences, Federal University of São Paulo, Santos - SP, Brazil. *2*Nuclear Instrumentation Laboratory, Federal University of Rio de Janeiro, Rio de Janeiro - RJ, Brazil. *3*Laboratory of Chemical Control, Fluminense Federal University, Niterói - RJ, Brazil. *4*Physics Institute, São Paulo University, São Paulo - SP, Brazil
rodholforibeiro@gmail.com

Heavy metals in trace amounts are naturally found in the environment some of them are essentials to life, however, they cause toxicity at high concentrations¹. The absorption of heavy metals on intertidal sandy beaches sediment is related to the contamination of its inherent biota². It may affect not only on the metal concentration on body tissues but also on the diversity and distribution of these organisms. The scientific literature did not present results that consider the influence of benthic fauna at concentrations of trace metals in the sediment. Based on the literature about heavy metals contamination at sediment from sandy beaches, this work aims to analyze the influence of the benthic fauna (macro- and meiofauna) in the quantification of trace metal contents of sandy beaches. Sediment from the intertidal regions of Itararé, located at the São Paulo State coast (southeast Brazil), will be sampled and analysed for heavy metal contents and granulometric composition. The collected sediment will get through different processes for comparison: the first will not be processed; the second one will be sieved to macrofauna's separation. Macrofauna will be sorted out by sieving the sediment through a 0.5 mm mesh. Heavy metals concentrations will be analyzed using TXRF technique. Among the metals found this work Ag, Ca, Cr, Cu, Fe, K, Mn P, S Si, Ti e Zn and some of these have a possible contributions in concentrations of metals in benthic macrofauna and coarse and very coarse sediment were found. The metals were analyzed to find out the main contribution of each element in each fraction of the sediment and organisms. Keywords: TXRF. Sediment. Macrofauna. Metals.

Exploratory Methodology for Retrieving Oxidation State Information from X-ray Resonant Raman Scattering Spectrometry

Presenter: Robledo J. I.

Robledo J. I.; Sánchez H. J.; Leani J. J.; Pérez C. A.

FaMAF-UNC; IFEG-CONICET
jorobledo2@gmail.com

It has been observed recently that the resonant Raman scattering (RRS) peak of an X-ray spectrum contains information about the chemical environment of the irradiated matter [1]. This information is extracted with complex processing of the spectrum data. Principal component analysis (PCA) [2] is a statistical multivariate technique that allows exploring the variance-covariance structure of a set of data. This methodology can be applied to obtain information from any kind of spectra (In particular RRS spectra). To analyze its potentiality, several measurements of different oxides in surface nanolayers were measured in total reflection conditions using synchrotron radiation from the LNLS, in Campinas, Brazil. PCA was used to obtain the information encrypted in the RRS peak, and to establish a new methodology [3]. The results show that multivariate analysis techniques are suitable for the analysis of this kind of spectra, foreseeing its application in future research.

Leani, J. J.; Sánchez, H. J.; Valentinuzzi, M.; Pérez, C., *J. Anal. At.Spectrom.* 2011, 16, 378–382.

Johnson, R. A.; Wichern, D. W. *Applied Multivariate Statistical Analysis*; Prentice Hall, Inc.: Upper Saddle River, NJ, 1992.

Robledo, J. I.; Sánchez, H. J.; Leani, J. J.; Pérez, C. A., *Anal. Chem.* 2015, 87, 3639–3645.

The effect of annealing on the electronic structure, morphology and charge transport in polymer: fullerene blends for photovoltaics

Presenter: Rocco M. L.

Rocco M. L. M.^{1,*}, Garcia-Basabe Y.¹, Marchiori C. F. N.², De Moura C. E. V.¹, Rocha A. B.¹, Roman L. S.²

¹Institute of Chemistry, Federal University of Rio de Janeiro, Rio de Janeiro, 21941-909, Brazil ²Department of Physics, Federal University of Paraná, Curitiba, 81531-990, Brazil
luiza@iq.ufjf.br

In the last decade internal donor-acceptor copolymers emerged as the most promising polymers for organic solar cell applications. Photovoltaic devices with power conversion efficiency (PCE) higher than 10% have been achieved using these polymers as active layer. Several reports show good photovoltaic device characteristics especially after thermal annealing. Therefore, it is highly important to investigate the effect of thermal annealing on the electronic structure, morphology and charge transfer dynamics in these polymers and their blends. For that we applied Near-edge X-ray Absorption Fine Structure (NEXAFS), X-ray Photoelectron Spectroscopy (XPS) and Resonant Auger Spectroscopy (RAS) in the context of the core-hole approach for the poly[2,7-(9,9-bis(2-ethylhexyl)-dibenzosilole)-alt-4,7-bis(thiophen-2-yl)benzo-2,1,3-thiadiazole] (PSiF-DBT) polymer and its blend with fullerene. The effect of the thermal annealing treatment at 100 and 200 °C on the electronic structure, charge transfer delocalization times and molecular orientation were probed. Edge-on and plane-on molecular orientations with respect to the substrate surface were measured for the thiophene and benzothiadiazole units, respectively, using angular dependent NEXAFS spectra at the S K-absorption edge. Molecular orientation of the silafluorene unit was also probed by NEXAFS at the Si K-edge. The improvement of the polymer ordering with annealing was evaluated by NEXAFS. Femtosecond charge transfer times were measured. Differences in charge transfer times at Si and S K-edges may be related to the localized-delocalized character of the molecular orbitals involved in these excitation processes, which was corroborated by theoretical calculations, with explicit relaxation of molecular orbitals due to the core-hole. The authors would like to acknowledge CNPq, CAPES, LNILS and FAPERJ.

Iron oxide nanoparticles coated with different Silica thicknesses: SAXS analysis of size, shape and agglomeration and its relationship with magnetic properties.

Presenter: Rojas P. C. R.

Rivas P.; Tancredi P.; Moscoso-Londoño O.; Socolovsky L. M.

Laboratorio de Sólidos Amorfos (LSA), INTECIN, Facultad de Ingeniería, Universidad de Buenos Aires – CONICET, C1063ACV 6 Buenos Aires, Argentina
privas@fi.uba.ar

Iron oxide nanoparticles were synthesized via high temperature decomposition of organic precursors, and the obtained nanoparticles were then coated with SiO₂ via the reverse microemulsion method, attempting to regulate the coating thickness by varying the amount of tetraethyl orthosilicate (TEOS) and the reaction time. As a result five core-shell systems of single magnetic core (of fixed composition, structure, shape and diameter) with different silica shell thicknesses are presented here. TEM images corroborate the formation of such structures, with nearly-uniform spherical cores of mean diameter of 7.2nm and standard deviation of 0.2nm. The shell thicknesses increase with the amount of TEOS, reaching average values near 18nm for the highest TEOS amount. These values are in good agreement with those obtained by SAXS after analyzing the patterns with a core-shell model. The magnetic dipolar interaction strength dependence with the shell thickness was studied with static magnetic measurements, where the blocking temperature estimated from the temperature dependence of magnetization (FC/ZFC curves) decreases as the shell thickness increase, as expected for progressively less interacting systems. And the magnetization as a function of applied field curves show in all cases the behavior of a superparamagnetic system with interactions above the blocking temperature, according to the Interacting Superparamagnetic model formulated by Allia. The relationship between the size and morphological information provided by SAXS and the magnetic properties is exhaustively analyzed. Acknowledgements: authors would like to acknowledge CONICET (Argentina) for financial support and CNPEM (Brasil) for the use of synchrotron light (SAXS line, LNLS) and TEM facilities (LNNano).

J. Park, K. An, Y. Hwang, J.-G. Park, H.-J. Noh, J.-Y. Kim, J.-H. Park, N.-M. Hwang, and T. Hyeon, "Ultra-large-scale syntheses of monodisperse nanocrystals," *Nat. Mater.*, vol. 3, no. 12, pp. 891–5, Dec. 2004. H. L. Ding, Y. X. Zhang, S. Wang, J. M. Xu, S. C. Xu, and G. H. Li, "Fe₃O₄@SiO₂ Core / Shell Nanoparticles : The Silica Coating Regulations with a Single Core for Different Core Sizes and Shell Thicknesses," 2012. Svergun, D. I. & Koch, M. H. J. Small-angle scattering studies of biological macromolecules in solution. *Reports Prog. Phys.* 66, 1735–1782 (2003) Allia, P.; Coisson, M.; Tiberto, P.; Vinai, F.; Knobel, M.; Novak, M. A.; Nunes, W. C. Granular Cu-Co Alloys as Interacting Superparamagnets. *Phys. Rev. B* 2001, 64, 144420.

Electronic Studies on Coordination Metal Complexes with Xanthates Ligands: S, Ni and Mn K-edge XANES

Presenter: Romano R. M.

Juncal L. C.; Condori E. A. O.; Védova C. O. D.; Romano R. M.

CEQUINOR (UNLP-CONICET), Departamento de Química, Facultad de Ciencias Exactas, Universidad Nacional de La Plata
romano@quimica.unlp.edu.ar

In this work, and as part of a general project aimed to the preparation and study of coordination complexes with potential pharmacological applications, we present the results of sulfur, nickel and manganese K-edge XANES study on a series of Ni and Mn coordination complexes with xanthate ligands and their potassium salts. Twenty three samples, with general formula $(\text{ROC}(\text{S})\text{S}-\text{K}^+)$, $(\text{M}(\text{ROC}(\text{S})\text{S})_2)$ and $(\text{M}(\text{ROC}(\text{S})\text{S})_2(\text{N-donor})_{1\text{ or }2})$, with $\text{M} = \text{Ni, Mn}$; $\text{R} = \text{Me, Et, nPr, iPr, nBu, CF}_3\text{CH}_2-$ and $\text{N-donor} = \text{py, bipy, phen}$, were prepared by our group in La Plata and characterized using vibrational (IR and Raman) and UV-visible spectroscopy, and also by single-crystal X-Ray diffraction analysis. The sulfur K-edge Total Ion Yield (TIY) spectra were investigated in the SXS beam-line under the proposal 16063 while the Ni and Mn K-edge XANES spectra were measured in the XAFS-1 beam-line under the proposal 17950. The XANES spectra of potassium xanthate salts $(\text{ROC}(\text{S})\text{SK})$ present three resonances below the ionization energy of the 1s electrons of the sulfur atom, at 2468.3 ± 0.1 , 2469.0 ± 0.1 y 2470.6 ± 0.2 eV, which were assigned to $\text{S}1\text{s} \rightarrow \pi^*\text{C}=\text{S}$ and $\text{S}1\text{s} \rightarrow \sigma^*\text{C}-\text{S}$ transitions. In the nickel complexes, besides transitions to antibonding orbitals of the ligands, a new band around 2469.6 eV, assigned to a $\text{S}1\text{s} \rightarrow \sigma^*\text{S}-\text{Ni}$ transition, was observed. The Ni K-edge spectra of the studied complexes present several resonances. The pre-edge peak around 8330 eV corresponds to the transition of the nickel 1s electron to its empty 3d orbitals. The low-intensity of this resonance is in agreement with its essentially forbidden character by the dipole selection rule. The most-intense peak, assigned to a $\text{Ni}1\text{s} \rightarrow \text{Ni}4\text{p}$ transition, appears in the region of 8340 to 8350 eV and shows the most significant difference in both its intensity and the chemical shift, in dependence on the ligand alkyl substituent. The Mn K-edge spectra present two peaks, the pre-edge resonance around 6540 eV and the main feature close to 6550 eV.

1. E. I. Solomon, D. W. Randall, T. Glaser, *Coord. Chem. Rev.*, 2000, 200-202, 595. 2. J. E. Penner-Hahn. *Coord. Chem. Rev.*, 1999, 190-192, 1101. 3. E. R. T. Tiekink, I. Haiduc. *Prog. Inorg. Chem.*, 2005, 54, 3, 127. Acknowledgments This work has been largely supported by LNLS under Proposals SXS-16063 and XAFS1-17950. We thank the beamlines staff for their assistance throughout the experiments, and also Facultad de Ciencias Exactas, Universidad Nacional de La Plata, CONICET and ANPCyT for financial support.

Atomic Pair Distribution Function at LNLS: A New Tool for Material Science

Presenter: Saleta M. E.

Saleta M. E. ^{1*}; Mastelaro V. R. ²; Granado E. ¹

¹ Instituto de Física “Gleb Wataghin”, Universidade de Campinas, Campinas (SP), Brazil, ² Instituto de Física de São Carlos, Universidade de São Paulo, São Carlos (SP), Brazil.
msaleta@ifi.unicamp.br

The atomic pair distribution function (PDF) method is an attractive alternative to the X-ray absorption and diffraction methods for studying the local and medium-range atomic arrangements in material science. [1,2] In the PDF method, Bragg diffraction and diffuse scattering intensities are measured and the structural information is obtained by a Fourier transformation to real space. This technique can identify local atomic order much beyond the nearest neighbor atoms. With this powerful technique we can detect small local distortions that conventional X-ray diffraction studies miss, since the sharp Bragg peaks only reflect the information about the average structure.[1,2] The XDS beamline of the LNLS, was designed to take advantage of the 4T superconducting multipole wiggler inserted in the storage ring. This multipurpose beam line is employed for X-ray diffraction and X-ray absorption spectroscopy in the energy range between 5 and 30 keV. The X-ray total scattering experiment can be performed in two different arrangements: a) Bragg-Brentano configuration, using a scintillation detector with an analyzer and b) Debye-Scherrer configuration, where the sample is mounted into capillaries and the diffraction pattern is acquired with an arrangement of 6 Mythen detectors or a scintillator. The sample can be measured at different atmospheres and temperatures. To study the viability of the beamline for this kind of experiment were acquired data of two standard materials at LNLS and then we validated our experiment measuring the same material at a dedicated PDF beamline of the Advanced Photon Source (APS). Our results are very promising. With our configuration we can study both the local order and the meso-scale (r up to 300Å). In this work we summarize our first results on the standards, ferroelectrics and superconductor materials

[1] T. Egami & S.J.L. Billinge, “Underneath the Bragg Peaks, Volume 16, Second Edition: Structural Analysis of Complex Materials”, Pergamon Materials Series 7 (2003) [2] V. Petkov, Characterization of Materials, Pair Distribution Functions Analysis, (2012) 1361–1372.

Multivariate SAXS Profiles Analysis Applied to Synthesis of Heterogeneous Titania Photocatalysts by Sol-Gel Method

Presenter: Dos Santos J. H. Z.

Dos Santos J.H.Z.¹, Moreno Y.P.²

UFRGS

jhzds@iq.ufrgs.br

The Persistent Organic Pollutants (POPs) that result from some industrial processes are a major source of water pollution, and they may create health problems for humans. In recent years, Advanced Oxidation Processes (AOPs) have been presented as an alternative to conventional methods. Among all of the AOPs, the degradation of organic pollutants by heterogeneous photocatalysis based on titania is one of the most successful applications that uses this technology for recalcitrant pollutant degradation in waste water at ambient conditions [1]. In parallel, silica-based catalyst supports can be produced by sol-gel technology and have been widely used for catalysis applications [2, 3]. Nevertheless, to our knowledge, silica nanoparticles have not been employed as supports to remove POPs in water. In the present investigation, microporous nanoparticles and mixed-structured silicas were employed as supports for photocatalysts. TiCl_4 was used as the titanium precursor in the preparation of the nano- and mixed heterogeneous supported titania photocatalysts. For comparative reasons, photocatalytic tests were carried out with commercial titania (P25). The systems were evaluated in the photodegradation of Rhodamine B (RhB). The solids were characterized by nitrogen porosimetry, small-angle X-ray scattering (SAXS), zeta potential (ZP), dynamic light scattering (DLS) and diffuse reflectance spectroscopy in the ultraviolet (DRS-UV). All intensity profiles of X-ray scattering were treated by multivariate analysis tools [4], using the Hierarchical Cluster Analysis (HCA) and the Principal Components Analysis (PCA) in the modulus of scattering vector (q) region from 0.04 to 4.0 nm^{-1} . The supported nanometric photocatalyst prepared with silica nanoparticles achieved the highest percentage of RhB degradation under the ultraviolet (68.0%) and visible (45.1%) radiation. The photocatalyst activity of nanometric catalyst was better than the commercial P25 (12.3% under visible radiation).

[1] S. Harrad, Persistent organic pollutants. 2010: Wiley Online Library. [2] A. G. Fisch, N. S. M. Cardozo, A. R. Secchi, F. C. Stedile, N. P. d. Silveira, and J. H. Z. d. Santos, *Journal of Non-Crystalline Solids*, 354 (2008) 3973-3979. [3] F. A. Harraz, O. E. Abdel-Salam, A. A. Mostafa, R. M. Mohamed, and M. Hanafy, *Journal of Alloys and Compounds*, 551 (2013) 1-7. [4]. Brereton, R.G., *Chemometrics: data analysis for the laboratory and chemical plant*. 2003: John Wiley & Sons.

The importance of the active site molecular interactions to the oligomerization and reactivity of the typical 2-Cys Prx

Presenter: Dos Santos M. C.

Dos Santos M. C.^{*1}; Junior C. A. T.²; Netto L. E. S.³; De Oliveira M. A.⁴

Universidade de São Paulo^{1,2,3}; Universidade Estadual Paulista "Julio de Mesquita Filho"⁴
santos_mc@usp.br

Typical 2-Cys Peroxiredoxins (Prx) are antioxidant proteins able to decompose hydroperoxides with second-order rate constants of 10^6 - 10^8 /Ms. To decompose hydroperoxides, typical 2-Cys Prx use a Cys residue (peroxidatic cysteine - CP) and, during catalysis, it is oxidized to sulfenic acid (CP-SOH), which condenses with a second Cys residue (resolving cysteine - CR) to form a disulfide. These enzymes are obligate dimers which can associate in (α 2)₅ decamers in response to several factors, as the redox state. In reduced form, these enzymes are decamers and oxidation to disulfide results in their dissociation in dimers. The high reactivity of Prx is related to the activation of CP by two neighboring residues: Thr/Ser and Arg, the so-called catalytic triad, that allow the establishment of a transition state. The analysis of Tsa1 crystallographic structure, a typical 2-Cys Prx from yeast, revealed that the active site lies in the dimers boundaries in the decamer. Thereby, a hydrogen bond (CH- π) between Tyr77 residue and Thr44 from catalytic triad of adjacent dimer, very conserved among the Prx, apparently positions the Thr favorably to perform the interactions involved in the transition state establishment. To shed a light in this hypothesis, we generated mutant enzymes carrying the replacement of Thr44 by Val (Tsa1T44V) or the Tyr77 by Ala (Tsa1Y77A). Analysis by size exclusion chromatography revealed that both substitutions resulted in decamer destabilization and the evaluation of the catalytic activity of by steady state kinetics and fluorometric approaches showed a high decrease of the catalytic efficiency to both mutants. Together, our results evince the importance of molecular interactions between Tyr77 and Thr44 in the 2-Cys Prx oligomerization and the full catalytic activity. To gain insights of the substitution effects over Tsa1 active site environment, crystallization trials were performed and the refinement of promising initial conditions are in progress.

1. Halliwell, B., and Gutteridge, J. M. C. (2010) Free Radicals in Biology and Medicine 4th ed., p 851. Oxford University Press; 2. Hall, A., Karplus, P. A., and Poole, L. B. (2009) Typical 2-Cys Peroxiredoxins: Structures, mechanisms and functions. FEBS Lett. 276, 2469–2477. 3. Tairum, C. a, de Oliveira, M. a, Horta, B. B., Zara, F. J., and Netto, L. E. S. (2012) Disulfide biochemistry in 2-cys peroxiredoxin: requirement of Glu50 and Arg146 for the reduction of yeast Tsa1 by thioredoxin. J. Mol. Biol. 424, 28–41. 4. Hall, A., Parsonage, D., Poole, L. B., and Karplus, P. A. (2010) Structural evidence that peroxiredoxin catalytic power is based on transition-state stabilization. J. Mol. Biol. 402, 194–209. 5. Ferrer-Sueta, G., Manta, B., Botti, H., Radi, R., Trujillo, M., and Denicola, A. (2011) Factors affecting protein thiol reactivity and specificity in peroxide reduction. Chem. Res. Toxicol. 24, 434–50.

Microemulsions for application as corrosion inhibition: a SAXS approach

Presenter: Sarmiento V. H. V.

Sarmiento V. H. V.¹; Gonçalves H. B.¹; Huck-Iriart C.²; Costa E. V.¹

UFS¹; INIFTA²

vhsarmiento.ufs@gmail.com

Microemulsions (ME) are clear, stable and isotropic mixtures of oil, water and surfactant, frequently in combination with a cosurfactant. Microemulsions are a class of microheterogeneous systems having unique features of stability, solubilization capacity, structural morphology, physical property and applicability. They have found numerous applications in different fields from drug delivery vehicles up to corrosion inhibitors [1,2,3]. In the latter, microemulsions have generated considerable interest over the years. Advantages associated with their thermodynamic stability, optical clarity and ease of preparation enable corrosive agents to be solubilized, surfactants to be adsorbed on metal surface and hence the corrosion is reduced. Depending on the types of oil and surfactant and environmental conditions, microemulsified systems of varied categories, consistence and internal structures may result. This study aims to obtain microemulsified systems using vegetable inhibitors based on *A. muricata* L. (Am) and *A. squamosa* L. (As) extracts, (Annonaceae) as oil phases (FO). Tween80 and ethanol were used, respectively, as surfactant and cosurfactant and saline NaCl 3.5% (corrosive environment) and aqueous phase (AP). The formation of ME were analyzed and verified by SAXS and rheology allowing such systems are promising corrosion inhibitors. The results shows a broad peak typical of microemulsion systems with a maximum at approximately $q = 1\text{nm}^{-1}$ for all samples. Quantitative structural information was obtained from the ellipsoidal "core-shell" model. The adjustment of the model provided information about the maximum radius (R_{max}) and minimum (R_{min}) and therefore the size of the ME.

[1] M. J. Lawrence, G. D. Rees, *Advanced Drug Delivery Reviews* 64, 175–193(2012) [2] R. Shlomovitz, L. Maibaum, M. Schick, *Biophysical Journal* 106, 1979-1985 (2014) [3] A. O. Wanderley Neto, E. F. Moura, H. S. Júnior, T. N. C. Dantas, A. A. Dantas Neto, A. Gurgel, *Colloids and Surfaces A: Physicochem. Eng. Aspects* 398, 76– 83(2012)

Phase Contrast X-ray Imaging of Human Peripheral Nerves

Presenter: Scopel J. F.

Scopel J. F.^{1*}; Queiroz L. S.²; O'Down F. P.³; Junior M. C. F.⁴; Nucci A.⁵; Hönnicke M. G.⁶

¹UFG; ²Unicamp; ³LNLS; ⁴Unicamp; ⁵Unicamp; ⁶Unila
jonasscopel@hotmail.com

Diagnostic imaging techniques play an important role in assessing the exact location, cause, and extent of a nerve lesion, thus allowing clinicians to diagnose and manage more effectively a variety of pathological conditions such as entrapment syndromes, traumatic injuries, and space-occupying lesions. Ultrasound and nuclear magnetic resonance imaging are becoming useful methods for this purpose, but they still lack spatial resolution. In this regard, recent phase contrast x-ray imaging experiments of peripheral nerve allowed the visualization of each nerve fiber surrounded by its myelin sheath as clearly as optical microscopy. In the present study, we attempted to produce high-resolution x-ray phase contrast images of a human sciatic nerve by using synchrotron radiation propagation-based imaging. The images showed high contrast and high spatial resolution, allowing clear identification of each fascicle structure and surrounding connective tissue. The outstanding result is the detection of such structures by phase contrast x-ray tomography of a thick human sciatic nerve section. This may further enable the identification of diverse pathological patterns, such as Wallerian degeneration, hypertrophic neuropathy, inflammatory infiltration, leprosy neuropathy and amyloid deposits. To the best of our knowledge, this is the first successful phase contrast x-ray imaging experiment of a human peripheral nerve sample. Our long-term goal is to develop peripheral nerve imaging methods that could supersede biopsy procedures.

Martinoli C (2010) Imaging of the peripheral nerves. *Semin Musculoskelet Radiol* 14: 461–462. Kermarrec E, Demondion X, Khalil C, Le Thuc V, Boutry N, et al. (2010) Ultrasound and magnetic resonance imaging of the peripheral nerves: current techniques, promising directions, and open issues. *Semin Musculoskelet Radiol* 14: 463–472. Lewis RA (2004) Medical phase contrast x-ray imaging: current status and future prospects. *Phys Med Biol* 49: 3573–3583. Kim B-I, Kim K-H, Youn H-S, Jheon S, Kim J-K, et al. (2008) High resolution X-ray phase contrast synchrotron imaging of normal and ligation damaged rat sciatic nerves. *Microsc Res Tech* 71: 443–447. Beckmann F, Heise K, Kölsch B, Bonse U, Rajewsky MF, et al. (1999) Three-dimensional imaging of nerve tissue by x-ray phase-contrast microtomography. *Biophys J* 76: 98–102. Lareida a, Beckmann F, Schrott-Fischer a, Glueckert R, Freysinger W, et al. (2009) High-resolution X-ray tomography of the human inner ear: synchrotron radiation-based study of nerve fibre bundles, membranes and ganglion cells. *J Microsc* 234: 95–102. Kelly ME, Coupal DJ, Cole Beavis R, Schultke E, Romanchuk K, et al. (2007) Diffraction-enhanced imaging of a porcine eye. *Can J Ophthalmol / J Can d'Ophtalmologie* 42: 731–733. Giles C, Hönnicke MG, Lopes RT, Rocha HS, Gonçalves OD, et al. (2003) First experiments on diffraction-enhanced imaging at LNLS. Zhou S-A, Brahma A (2008) Development of phase-contrast X-ray imaging techniques and potential medical applications. *Phys Med* 24: 129–148.

Structural 3D Characterization of Silica, Zirconia and Titania Monoliths and Columns for Capillary Liquid Chromatography

Presenter: Da Silva C. G. A.

Da Silva C. G. A., Archilha N. L., Collins C. H., Bottoli C. B. G.

¹ IQ/UNICAMP, CAMPINAS - SP - BRASIL; ² LNLS/CNPEM, CAMPINAS - SP - BRASIL.
carlag@live.com

Keywords: 3D Characterization; inorganic monoliths; tomography

The morphology and the pore structure of a monolithic chromatographic bed are very important features in the design of stationary phases since these aspects directly influence the hydrodynamic properties (e.g., flow properties), thermodynamic properties (e.g., loadability) and the mass transfer kinetics (e.g., efficiency) [1]. Imaging techniques like scanning (SEM) and transmission (TEM) electron microscopy rapidly provide direct information about monolith morphology from bulk or cross sectional capillary images. However, SEM images offer no reliable depth information and thus lack the required morphological details [2]. In this way, a 3D micro tomography images of silica (SiO₂), zirconia (ZrO₂) and titania (TiO₂) monoliths prepared by the sol-gel process (SGP) using different experimental conditions and their columns were obtained. The 3D imaging information obtained by acquiring projection images of the sample along a number of different directions greatly improved our knowledge about the morphology of monoliths inside the capillaries and in the bulk and helped to understand and optimize the synthesis of the materials as well as improved the understanding the chromatographic performance of the columns.

D. Lubda, W. Lindner, M. Quaglia, C. du F. von Hoheneschec, K. Unge, J. Chromatogr. A1083 (2005) 14.

S. Bruns, T. Mullner, M. Kollmann, J. Schachtner, A. Holzel, U. Tallarek, Anal. Chem. 82 (2010) 6569.

The authors would like to thank LNLS-Campinas, Brazil (Proposal IMX-17042) and FAPESP (Project No. 2012/23518-2) for financial support.

Near edge structure at the lithium K-edge in LiH by inelastic X-ray scattering

Presenter: Stutz G. E.

Stutz G. E. ^{*1,2}, Mellone O.A. P.¹, Ceppi S.A.^{1,2}, Larochette PP. A.³

¹ Facultad de Matemática, Astronomía y Física. Universidad Nacional de Córdoba (UNC). Córdoba, Argentina. ² Instituto de Física Enrique Gaviola. CONICET - UNC. Córdoba, Argentina. ³ Centro Atómico Bariloche. CNEA. San Carlos de Bariloche, Argentina.
stutz@famaf.unc.edu.ar

The excitation of core electrons of Li in LiH was studied by means of inelastic x-ray scattering spectroscopy (IXSS) at low and high momentum transfer. Measurements were carried out at the XDS beamline of LNLS. A Johann type spectrometer based on a spherical analyzer crystal [1] was used. The core electron contribution was extracted from the whole electronic excitation spectrum. At low momentum transfer the near edge fine structure of the spectrum is interpreted in terms of dipole allowed transitions to empty states. At higher momenta an additional structure was observed, which was assigned to the opening of excitation channels other than dipolar. A chemical shift of the Li K-edge of 2.2 eV to higher energies relative to Li metal was measured. Calculation of the density of states and simulations of the excitation spectrum were made using the FEFF code [2]. Core-hole effects were found to be appreciable and need to be taken into account in the simulations in order to reproduce the observed spectral features. The present experiment demonstrates the feasibility of investigating near edge structures of light elements by means of IXSS with high energy resolution at the XDS beamline.

[1] G. Tirao, G. Stutz, C. Cusatis, J. Synchrotron Rad. 11, 335 (2004). [2] J.J Rehr, J.J. Kas, F.D. Vila., M.P. Prange, K. Jorissen, Phys. Chem. Chem. Phys., 12, 5503-5513 (2010).

Characterization of nanostructured $A_{1-x}Sr_xFe_{0.8}Cu_{0.2}O_{3-d}$ perovskites (A=La, Ba) as IT-SOFC cathodes.

Presenter: Suescun L.

Suescun L.¹; Vázquez S.¹; Davyt S.¹; Faccio R.¹; Basbus J.²; Napolitano F.²; Soldati A. L.²; Serquis A.²

¹*Crysmat-Lab/Cátedra de Física/DETEMA, Facultad de Química, Universidad de la República, Montevideo, Uruguay; Grupo de Caracterización de Materiales, CAB/CNEA, Bustillo 9500, 8400 Bariloche, Argentina*
leopoldo@fq.edu.uy

Solid Oxide Fuel Cells operating in the 500-800 °C temperature range (IT-SOFCs) require the development of new cathode materials with high mixed ionic-electronic conductivity and good catalytic activity of the oxygen reduction reaction (ORR).[1] Traditional $La_{1-x}Sr_xMnO_{3-d}$ perovskite material does not operate well at low temperatures due to the absence of oxygen conductivity and strong reduction of ORR activity. Cobaltites $Sm_{0.5}Sr_{0.5}CoO_{3-d}$ and related compounds show excellent conducting properties and are good ORR catalysts, but they show a large thermal expansion coefficient (TEC) and high reactivity towards common electrolyte materials which prevents their efficient application as IT-SOFC cathodes.[2] In recent years our group has been exploring the preparation of cobalt-free, nanostructured cathode materials, with good ORR activity based on Fe-Cu perovskites. We have designed a novel gel-combustion technique that allowed the preparation of $Ba_{0.5}Sr_{0.5}Fe_{0.8}Cu_{0.2}O_{3-d}$ (BSFCu) and $La_{0.6}Sr_{0.4}Fe_{0.8}Cu_{0.2}O_{3-d}$ (LSFCu) materials, compatible with standard $Ce_{0.9}Gd_{0.1}O_{1.95}$ (CGO) electrolyte and characterized its phase evolution with temperature, TEC, microstructure and electrochemical performance in the 500 - 700 °C temperature range of symmetrical cells with the configuration cathode/CGO/cathode prepared at different temperatures. Both LSFCu and BSFCu materials show very promising ASR values of 0.035 and 0.15 $\text{ohm}\cdot\text{cm}^2$ at 700 °C. Structural and microstructural characterization of the materials show that BSFCu shows a very isotropic and homogeneous arrangement of nanoparticles 18nm wide and a cubic $Pm\bar{3}m$ structure at all studied temperatures while LSFCu shows larger particles with average size of 41 nm (as determined by TEM) with rhombohedral $R\bar{3}c$ space group symmetry at RT, that transforms to cubic $Pm\bar{3}m$ above 375 °C. This phase transition is accompanied by a significant change in the TEC that suggests BSFCu is a better candidate material for IT-SOFC cathodes [3,4].

[1] Adler S.B.; Chemical Reviews 104 (2004) 4791-4873. [2] Ling Y.; Zhao L.; Lin B.; Dong Y.; Zhang X.; Meng G.; International Journal of Hydrogen Energy 35(13) (2010) 6905-6910. [3] Vázquez S.; Basbus J.; Napolitano F.; Soldati A.L.; Serquis A.; Suescun L.; Journal of Power Sources 275 (2015) 318-323. [4] Vázquez S.; Davyt S.; Basbus J.; Soldati A.L.; Amaya A.; Serquis A.; Faccio R.; Suescun L.; Journal of Solid State Chemistry 228 (2015) 208-213.

Study of Ag@Fe₃O₄ nano-heterostructures by synchrotron radiation techniques

Presenter: Tancredi P.

Tancredi P.¹; Moscoso-Londoño O.¹; Muraca D.²; Pirota K.²; Knobel M.²; Wolff U.³; Damm C.⁴; Neu V.³; Rellinghaus B.⁴; Socolovsky L.M.¹

¹ Laboratorio de Sólidos Amorfos (LSA), INTECIN, Facultad de Ingeniería, Universidad de Buenos Aires - CONICET, C1063ACV Buenos Aires, Argentina. ² Laboratorio de Materiais e Baixas Temperaturas (LMBT), Instituto de Física Gleb Wataghin, Universidade Estadual de Campinas, Cep 13083-859 Campinas-Sp, Brasil. ³ Department of Magnetic Microstructures, Leibniz Institute for Solid State and Materials Research Dresden, Helmholtzstraße 20-01069 Dresden, Germany. ⁴ IFW Dresden, Institute for Metallic Materials, Dresden, Germany
pablotancredi@gmail.com

Nanostructured samples of Ag@Fe₃O₄ with controlled morphology were prepared by chemical synthesis. The bi-phase nanoparticles were obtained by decomposition and epitaxial growth of Fe₃O₄ over previously prepared Ag seeds. By this reaction pathway, the morphology of the samples can be tuned as a consequence of the electron-donor capacity of the employed solvent, either 1-octadecene, phenyl ether or a mixture of both. In this way, two kinds of nanoparticles were prepared and observed by microscopy techniques: dimer-like or flower-like. Further structural characterization was performed by synchrotron radiation-related techniques in order to study the morphology of the nanoparticles (SAXS) and possible structural distortions at the interface caused by the distinct coupling of Fe₃O₄ at the Ag seeds in flowers and dimers (XANES and EXAFS). Also, Fe₃O₄ nanoparticles prepared without the Ag seeds were studied and characterized to compare the single phase material properties with the Ag@Fe₃O₄ coupled product properties. In previous works, we have studied how the nanostructure final shape influences the magnetic properties of the sample, and we found significant differences in the magnetic behavior between flower-like and dimer-like Ag@Fe₃O₄, and isolated Fe₃O₄ nanoparticles[1]. In this sense, complementary analysis derived from synchrotron radiation-related techniques provides helpful evidence to try to understand and relate structural features with the observed magnetic behavior. Acknowledgements: Argentinian agency CONICET and LNLS-CNPEM.

[1] O. Moscoso-Londoño, D. Muraca, P. Tancredi, C. Cosío-Castañeda, Kleber R. Pirota, L. M. Socolovsky; Physicochemical Studies of Complex Silver–Magnetite Nanoheterodimers with Controlled Morphology; J. Phys. Chem. C (2014), 118, 13168–13176

Investigation of band structure of insulators using vacuum ultraviolet spectroscopy

Presenter: Teixeira V. de C.

Teixeira V. de C.¹; Valerio M. E. G.²

¹Laboratório Nacional de Luz Síncrotron, ²Universidade Federal de Sergipe
veronica.teixeira@lnls.br

Vacuum ultraviolet spectroscopy is a powerful tool to investigate the band structure of semiconductors and insulators. At this work some studies were performed to investigate the optical band gap of calcium aluminosilicates (CAS) used as matrix to prepare luminescent materials. For this, it was used a special geometry for optical measurements the TGM (Toroidal Grating Monochromator) beamline at the LNLS (Synchrotron Light National Laboratory). The main aim of this work is to better understand the band structure of CAS and propose luminescent mechanism for them when they are exposed to the ionizing radiation. It was recorded both the photoluminescence yield and the emission spectra for all samples. The samples studied were from the family of Ca₂Al₂SiO₇ (CAS) doped with transition metals as rare earths. They were prepared using a hybrid methodology that combines sol-gel and solid state reaction and are potential to be used as scintillators for ultraviolet and soft x-rays [1]. Results carried out in photoluminescence yield indicated a strong absorption around 6 eV in all samples suggesting CAS optical band gap is around this value. The emission spectra indicated typical transitions from dopants and large band emissions from near ultraviolet to visible range from pure samples were also observed suggesting this emission are associated to the exciton. With this set of results it was possible to observe CAS optical band gap is around 6 eV, which is good agreement with previous result [1] and the behavior of emission when the samples are excited immediately above the optical band gap. It was also possible describing the excitation from fundamental levels, that is an important key to know the whole luminescence process when the material is exposed to the ionizing radiation.

TEIXEIRA, V.C., MONTES, P.J.R., VALERIO, M.E.G., "Structural and optical characterizations of Ca₂Al₂SiO₇: Ce³⁺, Mn²⁺ nanoparticles produced via a hybrid route", Opt Mater, 36, pp. 1580-1590 (2014)

XANES study of the oxidation state of Cu, Ni and Ce cations in the Cu-Ni/ $\text{Ce}_{0.9}\text{Zr}_{0.1}\text{O}_2$ cermet in reducing atmospheres

Presenter: Toscani. M.

Toscani L. M.; Zimicz M. G.; Martins T.; Lamas D. G.; Larrondo S. A.

UNIDEF-CONICET, Buenos Aires, Pcia. de Buenos Aires, Argentina; IFISUR-CONICET, Bahía Blanca, Pcia. de Buenos Aires, Argentina; LMH-ICAQF-UNIFESP, Diadema, São Paulo, Brazil; CONICET y UNCOMA, Neuquén Capital, Pcia. de Neuquén, Argentina; UNIDEF-CONICET, Buenos Aires, Pcia. de Buenos Aires, Argentina
luciatoscani@gmail.com

Solid Oxide Fuel Cells stand as a promising technology for efficient and sustainable energy production. In this context, $\text{Ni/Zr}_{0.1}\text{O}_2$ (Ni/ZDC) cermets are an excellent alternative to Ni/YSZ commercial anodes. The aim of this work is to study the effect of partial substitution of Ni by Cu in that cermet and to evaluate its performance in redox and catalytic conditions. In situ XANES experiments using synchrotron radiation were performed at the Ce-LIII, Cu-K and Ni-K edges. Temperature programmed reduction (TPR) experiments were carried out in 5 mol.% H_2 /He atmospheres. Ce-LIII edge results showed Ni/ZDC and CuNi/ZDC almost identical profiles up to 670°C, while the bimetallic sample presented higher reduction percentages up to 800°C. Both samples concluded the experiment with a total 40% of Ce reduction. In the Ni-K edge, the bimetallic sample presented a lower reduction onset temperature and a higher proportion of Ni surface species exhibited in the larger area under first peak of TPR profile, with 100% Ni reduction in both cases. Cu-K edge results showed a two step Cu reduction for the bimetallic sample. When the cermets are exposed to $\text{CH}_4:\text{O}_2=2.6$ ratio atmosphere, they exhibited low catalyst reduction percentages: 8% Ni reduction for both cermets, 4% and 2% Ce reduction for cermets containing Ni and CuNi, respectively. The mass spectrometer signals of the exhaust gases during the experiments showed the production of both H_2 and CO for temperatures above 650°C. Acknowledgements: To LNLS (proposal XAFS1-15329), PIDDEF N°011/11 and ANPCyT (PICT 2013-1587).

Photofragmentation of a perfluorocarboxylic acid using synchrotron radiation: Study of CF₃CF₂C(O)OH

Presenter: Védova. O. D.

Védova C. O. D.; Martínez Y. B.; Bava Y. B.; Filho R. C.; Romano R. M.

CEQUINOR (UNLP-CONICET), Departamento de Química, Facultad de Ciencias Exactas, Universidad Nacional de La Plata, La Plata, Argentina; Universidade Federal do ABC, Rua Catequese, 242 CEP: 09090-400 Santo Andre SP, Brasil
carlosdv@quimica.unlp.edu.ar

Perfluorinated compounds have been extensively used in industrial applications during the last years. Recently, some perfluorinated species were detected in tissues of animals, in environmental waters, and in the atmosphere.[1,2] Different processes may be responsible for the presence of these compounds in the environment. For example, the thermolysis of fluoropolymers and the degradation of fluorotelomer alcohols result in the emission of perfluorocarboxylic species to the atmosphere. In this work, and as part of a general project aimed to the elucidation of the photofragmentation mechanisms of compounds relevant for atmospheric chemistry, we present the study of perfluoropropionic acid using synchrotron radiation with energies between 7.3 and 300eV. The photoexcitation and photofragmentation of this species was studied in the TGM beamline at LNLS. Above 11.7 eV different ions can be observed in the PEPICO spectra. At exactly 11.7 eV, COH⁺, C₂F₄⁺, and M⁺ were detected. This result shows that the cleavage of two covalent bonds is carried out at energies barely higher than the first ionization potential. The peak corresponding to C(O)OH⁺ was detected at 11.8 eV, and CF₃CF₂⁺ appeared in the spectra from 15 eV. The parent ion was only detected below 16 eV. From that energy, the heaviest ion observed in the PEPICO spectra was the M-OH⁺ fragment. Unlike the fragments observed in the previously studied analogous molecule CF₃CF₂CF₂C(O)Cl,[3] CF⁺, CF₂⁺, and CF₃⁺ ions were not the most abundant peaks in the spectra.

[1] Hurley, M. D.; Ball, J. C.; Wallington, T. J.; Anderson, M. P. S.; Ellis, D.A.; Martin, J.W.; Mabury, S. A. *J. Phys. Chem. A*, 2004, 108, 5635-5642. [2] Shine, K.P.; Gohar, L.K.; Hurley, M. D.; Marston, G.; Martin, D.; Simmonds, P. G.; Wallington, T. J.; Watkins, M. *Atmos. Environ.*, 2005, 39, 1759-1763. [3] BerruetaMartínez, Y.; Bava, Y. B.; Erben, M. F.; Cavasso Filho, R. L.; Romano, R. M.; Della Védova, C. O.J. *Phys. Chem. A*, 2015, 119, 1894-1905. Acknowledgements: This work has been largely supported by LNLS under Proposal TGM-17872. We thank Arnaldo Naves de Brito and TGM beamline staff for their assistance throughout the experiments, and Facultad de Ciencias Exactas, Universidad Nacional de La Plata, CONICET and ANPCyT for financial support.

Phosphorus speciation during the production of phosphate fertilizers using a metallurgical acid residue

Presenter: Vergütz L.

Vergütz L.; Santos W. O.; Filho L. F. S. S.; Hesterberg D. R. L.; Mattiello E. M.

Departamento de Solos - Universidade Federal de Viçosa; Departamento de Solos - Universidade Federal de Viçosa; Departamento de Solos - Universidade Federal de Viçosa; Department of Soil Science - North Carolina State University; Departamento de Solos - Universidade Federal de Viçosa
leonardusvergutz@gmail.com

Soluble phosphate fertilizers are produced in the fertilizer industry by the acidification of rock phosphates (RP) using pure acids. Therefore, the use of acid residues (AR) to solubilize RP is a potential way of reusing any sort of AR. This way, the objective of this work was to evaluate the use of a metallurgical AR to produce phosphate fertilizer from three contrasting RP commonly found in Brazil. This AR comes from the leaching of pegmatite by a mixture of three acids (H₂SO₄/HF/HCl) in order to extract Ta and Nb. The work was carried out in a 3x5 factorial design: three RP (Araxá, Patos, and Bayóvar) and five RA concentrations (0,0; 12,5; 25,0; 50,0; and 75,0 % v/v in water). The changes occurring in the original RP and the P solubility of the products following the addition of AR were evaluated by X-ray diffraction (XRD), P K-edge XANES, and water soluble P (P_{water}) and neutral ammonium citrate soluble P (PNAC). In terms of P solubility, the reactivity of the RP increased with increasing AR concentration. It means that the concentrations of P_{water} and PNAC increased the higher the AR concentration. This increase in RP reactivity was also accompanied by the disappearing of apatite (P-Ca) peaks in the XRD, which is the main P species in the RP and not readily bioavailable. Phosphorus K-edge XANES spectrum of P-Ca species is characterized by the absence of pre-edge structures and the presence of strong post-edge shoulders. As AR concentration increased, these features disappeared in the products, agreeing with the XRD. What XRD could not show was the formation of non-crystalline P-Ca and P-Fe species. As AR concentration increased, an important feature arose, which was the pre-edge structure, characteristic of amorphous P-Fe species. At the end, linear combination fitting showed that as the AR concentration increased, P-Ca species present in the RP changed to more soluble species of P-Ca, with the formation of great amounts of amorphous P-Fe.

Identification of the substrate binding sites in Actinobacteria sulfotransferase Cpz8

Presenter: Vieira B. D.

Vieira B. D.¹; Fernandes A. Z. N.¹; Kaysser L.²; Gust B.²; Trivella D. B. B.^{1*}

¹Chemistry and Natural Products Laboratory, Brazilian Biosciences National Laboratory, CNPEM, Campinas, Brazil; ²Pharmaceutical Institute, University of Tübingen, Tübingen, Germany
daniela.trivella@lnbio.cnpem.br

The understanding of natural product biosynthetic pathways has received increased interest of the modern scientific community. Recently, our collaborators at the University of Tübingen (Germany) identified steps in the biosynthesis of the antibiotic caprazamicin (CPZ) in *Streptomyces* sp.. The CPZ sulfation pathway is catalyzed by a PAPS dependent sulfotransferase, Cpz8. Cpz8 uses PAPS as sulfate donor and a presuficidins as sulfate acceptors. Interestingly, Cpz8 doesn't display a typical sequence for PAPS binding domain. Low similarity is displayed by Cpz8 when compared to known sulfotransferases (19 and 29% similarity for human and *S. mansoni* respectively). Therefore, we attempted to determine the crystal structure of Cpz8 to elucidate its mechanism of catalysis and substrate binding. For this, the enzyme was heterologously expressed, purified and subjected to crystallization at RoboLab (LNBio-CNPEM). Diffraction data sets were collected at the MX-2 beam line (LNLS-CNPEM) with resolution better than 2 Å. It wasn't possible to determine the crystal structure of Cpz8 by molecular replacement. Therefore, SAD experiments were carried out also at the MX-2, using quick cryo-soaking with NaI, CsCl and GdCl₃. After data processing, the phases were recovered using SAD data sets with iodine. The calculated electron density map allowed for the determination of the crystal structure of Cpz8. The atomic model was refined and analyzed. It was found that - despite the poor similarity with known PAPS binding motives in the primary sequence - the Cpz8 3D-structure presents a large cavity compatible with the PAPS binding site. The important chemical groups to interact with PAPS and sulfate transfer are preserved in this putative binding site. A second cavity is also found and predicted to bind the sulfate acceptors. The crystallization of Cpz8 in complex with PAPS and the sulfate acceptor (presuficidin A-D) are in progress.

Surface nanomodification of polypropylene

Presenter: Waldman W. R.

Waldman W. R.¹, Galante D.², Fitaroni L. B.³, Cruz S. A.¹

¹UFSCar, ²LNLS, ³UFABC

walter@ufscar.br

Surface modification of polymeric materials by exposure to light occurs by absorption of luminous radiation and the subsequent excitation and reaction of specific chemical groups with each other or with the atmosphere. The modification advantage is the production of a highly reactive surface. The aim of this work is to study the polypropylene surface modification as a function of exposure time to extreme UV under vacuum, in order to verify the kinetics and the nature of the modification. Polypropylene was exposed to extreme UV, generated in Toroidal Grating Monochromator beamline (TGM) during different times, from 10 to 60 minutes. The obtained results showed that the modified region presented an evolution as a function of time of the surface modification pattern, as followed by scanning electron microscopy (SEM). The observed modification was a corrugated morphology, with dimensions ranging from 200 to 300 nm without any evidence of cracking or crazing, which is the opposite of the expected in photodegradation under vacuum or in presence of atmosphere.

Daniel E. Weibel, Polymer Surface Functionalization Using Plasma, Ultraviolet and Synchrotron Radiation. *Composite Interfaces* 17 (2010) 127-136

Masaki Ono and Eizi Morikawa. Ultraviolet Photoelectron Spectroscopy Study of Synchrotron Radiation-Degraded Polyethylene Ultrathin Films. *J. Phys. Chem. B* (2004), 1894-1897

Extreme UV and Selective Inner-Shell Fragmentation Studies of Novel Polymeric Resist Materials

Presenter: Weibel D. E.

Chagas G.¹; Satyanarayana V. S. V.²; Kessler F.³; Belmonte G. K.¹; Gonsalves K. E.²; Weibel D. E.¹

Department of Chemical Physics, Chemical Institute, UFRGS, Porto Alegre, RS, Brazil¹; School of Basic Sciences, Indian Institute of Technology Mandi, Mandi – 175001, Himachal Pradesh, India²; School of Chemistry and Food, Federal University of Rio Grande, Av. Itália, RS, Brazil³ danielw@iq.ufrgs.br

Two key concepts are important in extreme ultraviolet lithography (EUVL) to be the candidate for mass production of future integrated circuits: the polymer formulation and the photo-fragmentation process. We present here a detailed study of EUV and carbon inner-shell excitation of homopolymers and copolymers that have in their structures sulfonium and triflate groups as EUV absorption-enhancing units. The goal is to achieve sub-20 nm line patterns having low line edge roughness (LER) of < 2.0 nm and high sensitivity. The present work demonstrates the lithographic performance of several photoresists, MAPDST homopolymer and MAPDST-MMA copolymer, and the correlation with the photodynamic fragmentation processes. The dependence of the photodynamic processes on the excitation energy was studied by scanning the synchrotron energy. Particular excitations were selected which finally led to selective fragmentation of the polymers. The unique properties of the synchrotron radiation, highly monochromatic and intense, allowed to obtain detailed information about the photodegradation process in the new resists. The SGM (spherical grating monochromator) and the Planar Grating Monochromator (PGM) beamlines for VUV and soft X-ray spectroscopy were used in the present study. NEXAFS, XPS and QMS techniques were employed as analytical tools. The polymers were found to be sensitive to EUV irradiation at 103.5 eV showing that the triflate and the ester group were the weakest part of the MAPDST homopolymer with important desorption of SO_2^+ , SO^+ and CF_3^+ fragments during irradiation. The presence of a metacrylate group (MMA) led to a lower gas desorption rate and higher resistant to irradiation than the homopolymer. When a new MANTMS homopolymer and co-polymer (having a biphenyl group) were irradiated at selected carbon inner-shell excitation energies it was found a highly selective process of bond breaking mainly under the $\pi^*_{\text{C}=\text{C}}$ excitation of the phenyl functional groups. The defluorination and loss of sulfonated groups with the increase in the irradiation time for the MANTMS homopolymer was evident when the excitation energy was tuned to excite the $\pi^*_{\text{C}=\text{C}}$ transition. On the contrary, $\text{C1s} \rightarrow \pi^*_{\text{C}=\text{O}}$ and $\text{C1s} \rightarrow \sigma^*_{\text{C}-\text{F}}$ excitations did not produce important changes in the polymer surface region. This methodical investigation will provide guidance in designing new resist materials with improved efficiency for EUVL through polymer microstructure engineering.

1. Singh, V.; Satyanarayana, V. S. V.; Batina, N.; Reyes, I. M.; Sharma, S. K.; Kessler, F.; Scheffer, F. R.; Weibel, D. E.; Ghosh, S.; Gonsalves, K. E., Performance evaluation of nonchemically amplified negative tone photoresists for e-beam and EUV lithography. *J. Micro. Nanolith. Mem.* 2014, 13 (4), 043002-043002.
2. Satyanarayana, V. S. V.; Kessler, F.; Singh, V.; Scheffer, F. R.; Weibel, D. E.; Ghosh, S.; Gonsalves, K. E., Radiation-Sensitive Novel Polymeric Resist Materials: Iterative Synthesis and Their EUV Fragmentation Studies. *Appl. Mater. Interfaces* 2014, 6, 4223–4232.
3. Selective Fragmentation of Radiation-Sensitive Novel Polymeric Resist Materials by Inner-Shell Monochromatic Irradiation Gabriela Chagas, Vardhineedi Sri Venkata Satyanarayana, Felipe Kessler, Guilherme Kretzmann Belmonte, Kenneth E Gonsalves and Daniel Eduardo Weibel. *ACS Appl. Mater. Interfaces*, Submitted April 2015.

Purification, Crystallization and Preliminary Analysis of the X-Ray Diffraction Data from an Epoxide Hydrolase identified in *Streptomyces* sp.

Presenter: Wilson C.

Wilson, C.^{1, 2}; Santos, J. C.²; González, G. D. T.³; Oliveira, L. G.³; Dias, M. V. B.^{1, 2}

¹Instituto de Ciências Biomédicas, ICB-USP, SP; ²Programa de Pós Graduação em Microbiologia, IBILCE-Unesp, SP; ³Instituto de Química, IQ-UNICAMP, SP, Brazil
carol87.wilson@gmail.com

Epoxide hydrolases (EHs) are co-factors independent enzymes which catalyse the conversion of epoxides to transdihydrodiols. They exhibit different biological roles such as metabolism of mutagenic and/or carcinogenic epoxides. In microorganisms, EHs are also responsible for hydrolysing specific carbon sources such as tartaric acid, limonene and epichlorohydrin. Epoxide hydrolases from *Streptomyces* sp. in addition to metabolic functions, exhibit biocatalytic activity properties using a limited range of substrates. They have biotechnological interest to discover new processes for enzymatic separation of enantiomeric mixtures of epoxides and region specific hydrolysis. The objective of this work was to perform the purification, crystallization and obtain data of X-ray diffraction for B1EPH2, an EH identified in *Streptomyces* sp. Initially, B1EPH2 gene was cloned into pET28b (+) and transformed into *E. coli* BL21(DE3). The enzyme was expressed in 2YT medium with induction by IPTG. Purification was carried out using affinity and size exclusion chromatography. Crystals grown using the vapour diffusion methods. The diffraction screening and data collection of crystals was performed at the MX2 line of LNLS, Campinas, Brazil. The X-ray diffraction data were processed using the CCP4 program package. B1EPH2 was purified by affinity chromatography using a buffer containing 50 mM Tris-HCl pH 7.0; 100mM NaCl and 10% (v / v) glycerol and a gradient of imidazole from 0-500 mM. The pure protein was concentrated up to 12.5 mg/ml and co-crystallized with 10 mM of valpromide, an inhibitor of epoxide hydrolases, at 18°C. Crystallization occurred in different conditions. The crystals were diffracted up to 2.5 Å and belong to space group P412121. The protein B1EPH2 was crystallized in different conditions and the crystals were diffracted up to 2.5Å. The next step of this work is to perform the resolution of the structure and compare it to other epoxide hydrolases from different organisms.

Jacobs, M. H.; Van den Wijngaard, A. J.; Pentenga, M.; Janssen, D. B. Characterization of the epoxide hydrolase from an epichlorohydrin-degrading *Pseudomonas* sp, *Eur J Biochem*, v. 202, p. 1217-1222, 1991. Rink, R.; Fennema, M.; Smids, M. et al. Primary structure and catalytic mechanism of the epoxide hydrolase from *Agrobacterium radiobacter*, *AD1 J Biol Chem*, v. 272, p. 14650-14657, 1997. van der Werf, M. J.; Swarts, H. J.; de Bont, J. A. *Rhodococcus erythropolis* DCL14 contains a novel degradation pathway for limonene, *Appl Environ Microbiol*, v. 65, p. 2092-2102, 1999. van Loo, B.; Lutje Spelberg, J. H.; Kingma, J. et al. Directed evolution of epoxide hydrolase from *A. radiobacter* toward higher enantioselectivity by error-prone PCR and DNA shuffling, *Chem Biol*, v. 11, p. 981-990, 2004. Amano, Y.; Yamaguchi, T.; Tanabe, E. Structural insights into binding of inhibitors to soluble epoxide hydrolase gained by fragment screening and X-ray crystallography, *Bioorg Med Chem*, v. 8; p. 2427-2434, 2014.

Physical Simulation and Advanced Characterization of Structural Materials

Presenter: Wu L.

Wu L.

LNNano
leonardo.wu@lnnano.cnpem.br

The X-ray Scattering and Thermo-Mechanical Simulation (XTMS) experimental station has been co-developed by the Materials Characterization and Processing group of the Brazilian Nanotechnology National Laboratory (LNNano) and the Brazilian Synchrotron Light Laboratory (LNLS) Engineering and Technical staff. Such installation, which is located at LNLS XRD1 beamline, is operated by LNNano with LNLS support. It consists of a diffraction beamline built around an advanced thermo-mechanical simulator, the Gleeble® Synchrotron system, which allows the material of interest to be submitted to a wide range of thermo-mechanical conditions with high accuracy and reproducibility. Linear or area X-ray detectors are mounted in a high-resolution goniometer for fast data acquisition, which allows time resolved measurements.

Micelle and mesoporous silica formation with different cethylammonium surfactants

Presenter: Zapelini I. W.

Zapelini I. W., Campos A. F. P., Modesto P. P., Ferreira A. R. O., Alkimim I. P., Araujo J. A., Silva L. L., Cardoso D.

Laboratório de Catálise, Universidade Federal de São Carlos, SP, Brasil
iagozapelini@gmail.com

MCM-41 hexagonal mesoporous silica is of high interest by the scientific community because its easy preparation, pore diameter adjustment (between 1.5 and 10 nm), high superficial area, porosity and short range of pore diameter distribution. These characteristics allow this material to be used as catalysts, supports, adsorbents and membrane in many processes. This material is formed by the combination between polyanionic silica species and the micelles of the cationic surfactant. The way that this combination performs has high influence on the mesoporous phase obtained. Therefore, the objective of this study is evaluate the influence of surfactants with different hydrophilic head sizes on micelles formation and then on the MCM-41 hybrid silica. The studies were performed by small angle x-ray scattering curves of aqueous solutions of cethylammonium surfactants. The results showed a decrease of the micellar organization and of the bromide anion layer thickness around the micelles when the size of surfactant head increases (C16TMABr < C16TEABr < C16TPABr). It is believed that the high size of the surfactant head provides a decrease on the condensation of bromide anions around the micelles [1] and larger steric hindrance between heads, interfering on the mesoporous silica formation. According to the SAXS results, the x-ray patterns of the mesoporous silicas prepared by C16TEABr and C16TPABr showed the formation of structures with less organization and with only the (100) diffraction peak, compared to the MCM-41 prepared by C16TMABr surfactant which has, additionally, the (110), (200) and (210) peaks.

[1] N. V. Sastry, N.M. Vaghela, V.K. Aswal. Fluid Phase Equilibria 327 (2012) 22-29.

Fragment based drug discovery targeting proteins associated with virulence and resistance to antibiotics in *Mycobacterium tuberculosis*

Presenter: Zuniga G. A. L.

Libreros-Zuniga G.A; Dias M.V.B

¹: *Laboratório de Biologia Estrutural Aplicada - Unidade de Desenvolvimento de Fármacos. Instituto de Ciências Biomédicas, Universidade de São Paulo. SP. Brasil;* ²: *IBILCE. Universidade Estadual Paulista. São Jose do Rio Preto. SP. Brasil;* ³: *Departamento de Microbiologia. Universidad del Valle. Cali-Colombia*
mvdias@usp.br

The emergence of multidrug resistant *Mycobacterium tuberculosis* has led to the development of new anti tuberculosis drugs. L, D-transpeptidases (LdtMt) catalyzes 3-3 transpeptide linkages and usually are not inhibited by β -lactams. Its association with an intrinsic β -lactamase prevents the use of these antibiotics to treat tuberculosis. LdtMt1 and LdtMt2 are essential for Mt and their disruption results in severe morphological and functional alterations. Another M. tuberculosis protein named Eis, Enhance the survive of M. tuberculosis within of macrophages phagosomes by negatively modulating multiple signal that conduce to bacterial death, and also induces intrinsic resistance to aminoglycosides by acetylation and prevent its binding to the bacterial ribosome. Both, L,D transpeptidases and Eis proteins are interesting targets for Drug discovery. This work aim to identify simple molecules that maybe chemically modified for the generation of potent inhibitors against L,D transpeptidases and Eis protein from *Mycobacterium tuberculosis*. The genes for LdtMt1 LdtMt2 and Eis proteins were cloned from M. tuberculosis genomic DNA (Strain H37Rv) in pET28a, superexpressed in E. coli BL21(DE3), and the products were purified by immobilized-metal affinity (IMAC) and size-exclusion chromatography (SEC). We are performing a screening using thermal shift against a library of about 400 compounds to identify hits which have low affinity to these targets. The proteins have already been crystallized in different condition using hanging drop and the crystals are being used for in soaking experiments with compounds identified by the first trial. We will also further apply a variety of biophysical and crystallographic techniques to validate the candidate molecules. In collaboration with research groups of organic chemistry, molecules with higher affinity to the targets will be synthesised and promising inhibitors might be tested against M. tuberculosis cultures.

1. Croft SL, Public-private partnership: from there to here. *Trans. R. Soc. Trop Med Hyg.* 2005. 99. Suppl 1. S9-S14. 2. Duncan, Progress in TB drug development and what is still needed. *Tuberculosis.* 2003, 83 (1-3). 201. 3. Vollmer W. et al. The architecture of murein (peptidoglycan) in Gram negative bacteria: vertical scaffold or horizontal layer(s)? *J. of Bacteriol.* 2004. 186. 5978 4. Lavollay M. et al. The peptidoglycan of stationary- phase *Mycobacterium tuberculosis* predominantly contains cross-links generated by L,D transpeptidation. *J. of Bacteriol.* 2008. 190 (12). 4360 5. Gupta R. et al. The *Mycobacterium tuberculosis* protein LdtMt2 is a nonclassical transpeptidase required for virulence and resistance to amoxicillin. *Nature Medicine.* 2010. 16 (4). 466. 6. Schoonmaker M. et al. Non classical transpeptidases of *Mycobacterium tuberculosis* alter size, morphology, the cytosolic matrix, protein localization, virulence and resistance to β lactams. *J. of Bacteriol.* 2014. 196 (7).1394 7. Correale S. et al. Structures of free and inhibited forms of the L,D transpeptidase LdtMt1 from *Mycobacterium tuberculosis*. *Acta. Cryst.* 2013. D69.1967 8. Erdemli S et al. Targeting the cell wall of *Mycobacterium tuberculosis*: Structure and mechanism of L,D transpeptidase 2. *Structure.* 2012. 20 (12). 2103 9. Kim, H et al. Structural basis for the inhibition of *Mycobacterium tuberculosis* L,D transpeptidase by meropenem, a drug effective against extensive drug resistant strains. *Acta. Cryst.* 2013. D69. 420 10. Hugonnet, JE. et al. Meropenem- clavulanate is effective against extensively drug resistant *Mycobacterium tuberculosis*. *Science.* 2009. 323. 215

An investigation of the Morphology exhibited by HDPE composites after being subjected at very high rates of loading

Presenter: Zylberberg M. P.

Zylberberg M. P.¹; Saldanha A. L. M.²; Patricio P. S. de O.²; Pereira I. M.¹

¹Brazilian Army Technological Center; ²Federal Center of Technological Education of Minas Gerais
marcelzylberberg@gmail.com

Due to the low weight allied with high mechanical resistance, high-density polyethylene (HDPE) composites are the current state-of-the-art body armor system. In ballistic systems, HDPE is the matrix of the ballistic panel. Because material properties might be enhanced controlling process conditions and introducing fillers, we aim to be effective in improving the ballistic properties of the ballistic panel matrix by the dispersion and orientation of a second phase. In the present study, the filler, vermiculite particles modified by carbon nanofibers, V900 and VTRITFe800, was synthesized by chemical vapor deposition (CVD) method. The V900 particle were synthesized at 900oC and the VTRITFe800 were impregnated with iron chloride and synthesized at 800oC. Due to their amphiphilic character, hydrophobicity from the nanofibers and hydrophilicity from Si and Si-Al oxide surface, the particle were used in the production of polymeric composites using HDPE as matrix. In order to study the material behavior and it's mechanical properties, the specimen were subjected to high strain rates, 104 s⁻¹, using a split Hopkinson pressure bar. At this article, using SAXS technique, we investigated the composite nanomorphology before and after deformation. Before deformation, the presence of the non-polar chains on the vermiculite surface favored the dispersion in the polyolefin. HDPE lamellar structure originated a peak at 0.246 nm⁻¹. The peak position of HDPE composites slightly shifts to lower 0.234 nm⁻¹ values, suggesting an increase of the spacing of the periodical lamellar structure and smaller degree of order. The lamellae thickness was controlled by the filler. After deformation, results showed that composites containing particles presented the optimal results for energy absorption. The after deformation morphology varies due the particle composition and concentration. HDPE lamellar peak did not change after deformation, indicating its lamellar structure is less susceptible.

1- Ellwood, S.H. Dynamic Mechanical Properties of Austenitic Stainless Steels. Doctoral Thesis : Loughborough University, 1983. Kolsky, H. Stress Waves in Solids. 1a. New York : Drover Publications, Inc., 1963. 2- Yan Ping Bai and Ying Jie Lei, 'The Model of Impact Waves in a Circular Elastic Bar and Application in Measuring Dynamic Characteristic of Microstructure', Appl. Math. Comput., 173 (2006), 1350–1356. 3- Ana Paula C Teixeira and others, 'Amphiphilic Magnetic Composites Based on Layered Vermiculite and Fibrous Chrysotile with Carbon Nanostructures: Application in Catalysis', Catalysis Today, 190 (2012), 133–143. 4- Aluir D. Purceno and others, 'Carbon Nanostructures-Modified Expanded Vermiculites Produced by Chemical Vapor Deposition from Ethanol', Applied Clay Science, 54 (2011), 15–19. 5- Jorge Manuel C F Justo, 'Estudo Do Comportamento Ao Impacto de Alta Velocidade de Estruturas Em Materiais Compósitos', 2005. 6- Tao Xu and Richard J Farris, 'Comparative Studies of Ultra High Molecular Weight Polyethylene Fiber Reinforced Composites', 2007. 7- Advait R Bhat, 'Finite Element Modeling and Dynamic Impact Response Evaluation for Ballistic Applications' (Mumbai University, 2009). 8- Jan Golebiewski and others, 'Low Density Polyethylene–montmorillonite Nanocomposites for Film Blowing', Eur. Polym. J., 44 (2008), 270–286.